

---

# **Impact of Liver-derived Complement Component C5 on Atherosclerosis in ApoE-deficient Mice**

**Zhe Ma**

---



München 2019

Aus dem Institut für Prophylaxe und Epidemiologie der Kreislaufkrankheiten

Kliniker Ludwig-Maximilians-Universität München

Direktor: Univ.-Prof. Dr. med. Christian Weber

# **Impact of Liver-derived Complement Component C5 on Atherosclerosis in ApoE-deficient Mice**



Dissertation  
zum Erwerb des Doktorgrades der Naturwissenschaften  
an der Medizinischen Fakultät der  
Ludwig-Maximilians-Universität zu München

vorgelegt von  
Zhe Ma

aus  
Henan, China

2019

Mit Genehmigung der Medizinischen Fakultät  
der Universität München

**Betreuerin: Univ.-Prof. Dr. rer. nat. Sabine Steffens**

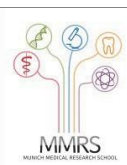
**Zweitgutachter: PD Dr. rer. nat. Andreas Herbst**

**Dekan: Prof. Dr. med. dent. Reinhard Hickel**

**Tag der mündlichen Prüfung: 23. 07. 2020**



Dean's Office  
Faculty of Medicine



## Affidavit

Ma, Zhe

Surname, first name

Street

Munich

Zip code, town

Germany

Country

I hereby declare, that the submitted thesis entitled *Impact of Liver-derived Complement Component C5 on Atherosclerosis in ApoE-deficient Mice* is my own work. I have only used the sources indicated and have not made unauthorised use of services of a third party. Where the work of others has been quoted or reproduced, the source is always given.

I further declare that the submitted thesis or parts thereof have not been presented as part of an examination degree to any other university.

Munich, 07 04 2020

Place, date

Zhe Ma

Signature doctoral candidate

**Impact of Liver-derived Complement  
Component C5 on Atherosclerosis  
in ApoE-deficient Mice**

# TABLE OF CONTENTS

<i>ABBREVIATIONS</i> .....	IV
<i>1. INTRODUCTION</i> .....	1
1.1 Atherosclerosis .....	1
1.1.1 The healthy artery .....	1
1.1.2 Progress in the field of atherogenesis .....	3
1.1.3 Immunocytes in atherosclerotic plaques .....	3
1.1.4 Mouse models of atherosclerosis .....	5
1.1.5 Atherosclerosis in ApoE <sup>-/-</sup> mice .....	6
1.2 Complement system and activation .....	6
1.2.1 Complement cascade .....	6
1.2.2 Activation of the complement system .....	6
1.3 Complement cascade and atherosclerosis .....	9
1.4 Complement-based therapies .....	11
1.4.1 Complement-system-associated diseases .....	11
1.4.2 Complement therapeutics .....	12
1.4.3 Liver-specific C5 small interfering RNA (siRNA) from Alnylam Pharmaceuticals, Inc. ·	13
1.4.4 Complement component C5 and autoimmune diseases studies .....	13
1.5 Aims .....	16
<i>2. MATERIALS &amp; METHODS</i> .....	17
2.1 Materials .....	17
2.1.1 Equipment .....	17
2.1.2 Reagents and materials .....	18
2.1.3 Standard solutions and buffers .....	19
2.1.4 Antibodies for Immunofluorescence Microscopy .....	20
2.2 Mouse strains and husbandry .....	23
2.3 Mouse models .....	23
2.3.1 siRNA preparation and injection .....	23
2.3.2 Experimental protocol .....	23
2.4 Serum collection and body weighing .....	24
2.5 Blood and organ collection .....	24
2.6 Assessment of atherosclerosis in mice .....	25
2.6.1 <i>en-face</i> preparation and Sudan IV staining .....	25
2.6.2 Tissue sectioning .....	26
2.6.3 Oil-Red-O Hematoxylin (ORO/HE) staining and atherosclerotic lesion quantification ·	27
2.6.4 Immunofluorescence staining .....	27
2.6.5 Quantification of CD68 <sup>+</sup> macrophage and CD3e <sup>+</sup> T cell infiltration in the plaque areas ·	28
2.7 ELISA for C5 protein in the circulation .....	29
2.8 Human carotid artery tissues and atherosclerotic lesion analyses .....	30
2.9 Statistical analysis .....	31
<i>3. RESULTS</i> .....	32

3.1 mRNA Microarrays of Wt and ApoE <sup>-/-</sup> aortas of various ages reveal the presence of transcripts of complement cascade constituents in atherosclerotic plaques.....	32
3.2 Liver-specific C5 siRNA reduces atherosclerosis burden in young ApoE <sup>-/-</sup> mice maintained on normal mouse chow .....	37
3.2.1 Liver-specific C5 siRNA reduces serum C5 protein level in 32 weeks old ApoE <sup>-/-</sup> mice on a normal diet .....	38
3.2.2 Liver-specific C5 siRNA does not change blood lipid levels, body weight, blood cell numbers, and leukocyte percentages in 32 weeks old ApoE <sup>-/-</sup> mice on a normal mouse chow .....	39
3.2.3 Liver-specific C5 inhibition does not change blood leukocyte subsets in young ApoE <sup>-/-</sup> mice on normal mouse chow .....	44
3.2.4 Liver-specific C5 siRNA reduces atherosclerotic plaque burden in young ApoE <sup>-/-</sup> mice on a normal mouse chow .....	44
3.2.5 Liver-specific C5 siRNA inhibits macrophage/dendritic and T cell infiltration in atherosclerosis in young ApoE <sup>-/-</sup> mice on a normal chow .....	46
3.2.6 Effect of C5 siRNA on complement protein activation and deposition in normal chow-fed 32 weeks old ApoE <sup>-/-</sup> mice .....	48
3.3 The role of liver-specific complement C5 in atherosclerosis in aged ApoE <sup>-/-</sup> mice maintained on a normal mouse chow.....	49
3.3.1 Liver-specific C5 siRNA reduced serum C5 protein level in aged ApoE <sup>-/-</sup> mice on a normal chow .....	50
3.3.2 Liver-specific C5 siRNA does not change body weight and blood lipid level in aged ApoE <sup>-/-</sup> mice.....	51
3.3.3 C5 inhibition does not change blood leukocytes subsets in aged ApoE <sup>-/-</sup> mice on normal chow.....	53
3.3.4 Liver-specific C5 siRNA did not affect atherosclerosis plaque burden in aged ApoE <sup>-/-</sup> mice on a normal chow .....	56
3.3.5 Liver-specific C5 siRNA did not affect CD68 <sup>+</sup> macrophage/DC infiltration in atherosclerosis in aged ApoE <sup>-/-</sup> mice on a normal chow .....	57
3.3.6 Effect of C5 siRNA on complement protein deposition in normal chow-fed 76 weeks old ApoE <sup>-/-</sup> mice .....	59
3.4 The role of liver-specific complement C5 in atherosclerosis in ApoE <sup>-/-</sup> mice with a high-fat diet.....	61
3.4.1 Liver-specific C5 siRNA reduces serum C5 protein levels in 32 weeks old ApoE <sup>-/-</sup> mice on a high-fat diet .....	62
3.4.2 Liver-specific C5 siRNA does not change blood lipid levels, body weight, blood cell numbers, and leukocyte percentages in 32 weeks old ApoE <sup>-/-</sup> mice on a high-fat diet .....	62
3.4.3 Liver-specific C5 inhibition does not change the blood leukocytes subsets in young ApoE <sup>-/-</sup> mice on a high-fat diet.....	67
3.4.4 C5 siRNA did not affect atherosclerosis plaque burden in young ApoE <sup>-/-</sup> mice on a high-fat diet .....	68
3.4.5 C5 siRNA does not influence macrophage/DC and T cell infiltration in atherosclerosis in young ApoE <sup>-/-</sup> mice on a high-fat diet .....	69
3.4.6 Effect of C5 siRNA on complement protein activation and deposition in high-fat diet fed 32 weeks old ApoE <sup>-/-</sup> mice .....	70

3.4.7 C5 siRNA does not affect atherosclerotic plaque burden in young ApoE <sup>-/-</sup> mice on a short-term high-fat diet.....	72
3.5. Classical complement cascade activation in human atherosclerosis .....	73
4. <i>DISCUSSION</i> .....	75
4.1 Discovery of an ApoE-complement C5 axis which controls atherosclerosis in mice .....	75
4.2 C5-targeted therapy aims to reduce atherosclerosis .....	77
4.3 Possible effect of high-fat diet on C5-dependent atherosclerosis.....	79
4.4 Is the C5-dependent effect on atherosclerosis only the tip of an iceberg of a broader and possibly ubiquitous role of C5 and ApoE in unresolvable inflammation? .....	80
4.5 Liver-derived complement component C5 vs. local produced C5 in atherosclerosis.....	81
4.6 Complement studies in other atherosclerotic mouse models.....	82
4.6.1 Complement component C5 in atherosclerosis .....	82
4.6.2 Complement activation studies on atherosclerosis in ApoE <sup>-/-</sup> mice .....	83
4.6.3 Complement activation on atherosclerosis in LDLr <sup>-/-</sup> mice .....	83
4.7 Can C5-dependent atherogenesis in mice be translated to human atherosclerosis? .....	85
4.8 Young and aged ApoE <sup>-/-</sup> mice are suitable murine models to study of the roles of complement cascades in atherosclerosis .....	86
5. <i>SUMMARY</i> .....	88
6. <i>ZUSAMMENFASSUNG</i> .....	89
7. <i>REFERENCES</i> .....	90
8. <i>ACKNOWLEDGEMENTS</i> .....	103
9. <i>SUPPLEMENT</i> .....	104



## ABBREVIATIONS

ACK lysis buffer	Ammonium-Chloride-Potassium lysis buffer
AMD	Age-related macular degeneration
ANOVA	Analysis of variance
ASGPR	Asialoglycoprotein receptor
ApoE	Apolipoprotein E
aHUS	Atypical hemolytic uremic syndrome
BSA	Bovine serum albumin
CCC	Classical complement cascade
Chol	Cholesterol
CR	Complement receptors
CR1	C3b receptor
CR3	iC3b receptor
DAB	3,3'-Diaminobenzidine
DAPI	4',6-diamidino-2-phenylindole
DBA/2	C5 <sup>-/-</sup> mouse
EAE	Experimental autoimmune encephalomyelitis

EC	Endothelial cell
EDTA	Ethylenediamine tetra-acetic acid
ELISA	Enzyme-linked immunosorbent assay
ET-1	Endothelin
EvG	Elastic van Gieson
FACS	Fluorescence-activated cell sorting
fB	Factor B
fD	Factor D
FFPE	Formalin-fixed paraffin-embedded
FSC	Fetal calf serum
Foxp3	Forkhead box P3
Gal-Nac	N-acetylgalactosamine
GO	Gene ontology
GRA	Granulocyte
HCT	Hematocrit
HDL	High-density lipoprotein
HGB	Hemoglobin

Ig	Immunoglobulin
I/R	Ischemia/reperfusion
LCM	Laser capture microdissection
LDL	Low-density lipoprotein
LDLr	Low-density lipoprotein receptor
LLOD	Lower limit of quantification
LYM	Lymphocyte
MAC	Membrane attack complex
MBL	Mannan-binding lectin
MCH	Mean corpuscular hemoglobin
MCHC	Mean corpuscular hemoglobin concentration
MCV	Mean corpuscular volume
mDC	Monocyte-derived dendritic cells
MG	Myasthenia gravis
MO	Monocyte
MPV	Mean platelet volume
MS	Multiple sclerosis

NO	Nitric oxide
ORO	Oil red O staining
PBS	Phosphate buffered saline
PFA	Paraformaldehyde
PLT	Platelets, thrombocytes
PNH	Paroxysmal nocturnal hemoglobinuria
RA	Rheumatoid arthritis
RBC	Red blood cells, erythrocytes
RDW	Red blood cell distribution width
RISC	RNA-induced silencing complexes
RNA	Ribonucleic Acid
rpm	Revolutions per minute
s.c.	Subcutaneous
siRNA	Small interfering RNA
SLE	Systemic lupus erythematosus
SMCs	Smooth muscle cells
TC	Total cholesterol

TCC	Terminal complement complex
TCM	Central memory T cell
TCR	T cell receptor
TEM	Effector memory T cell
TG	Triglycerides
Th0	Naïve T cell
Treg cells	Regulatory T cells
VLDL	Very low-density lipoprotein
ZVH	Zentrale Versuchstierhaltung
v/v	Volume per volume
WBC	White blood cell, leukocyte
w/v	Weight per volume
-/-	Deficiency

# 1. INTRODUCTION

## 1.1 Atherosclerosis

Atherosclerosis is the leading cause of death worldwide<sup>1</sup>. The disease can be viewed as a chronic inflammatory condition of the arterial wall<sup>2</sup>. Atherosclerosis is mainly located in the intima of middle- and large-sized arteries. Atherosclerosis affects all three layers of the arterial wall, i.e., the intima, the media, and the adventitia. The adventitia constitutes the connective tissue coat that surrounds arteries<sup>3,4</sup>. Major features of the advanced atherosclerotic plaque are foamy macrophages, smooth muscle cells (SMCs), T cells, extracellular lipid, and necrotic cores<sup>5</sup>. Atherosclerosis leads to plaque formation and - if the disease becomes clinically significant - subsequent fissure, erosion or rupture of the plaque. In its late stages, atherosclerosis is associated with intraluminal thrombosis, resulting in oxygen depletion in the downstream territory leading to tissue infarcts<sup>2,6</sup>. Smoking, obesity, hypertension, stationary way of life, diabetes mellitus, and hyperlipidemia are well-recognized risk factors of atherosclerosis<sup>1</sup>.

### 1.1.1 The healthy artery

A normal large- or medium-sized artery consists of three layers, i.e., the intima, the media, and the adventitia. The innermost layer is known as the intima, which is composed of a single layer of endothelial cells and a sheet of elastic fibers named the internal elastic lamina. The media, i.e., the middle layer, is made up of SMCs and elastic fibers<sup>7</sup>. The outermost layer is the adventitia consisting of connective tissue harboring blood vessels, lymph vessels, tissue macrophages, mast cells, T cells, conventional or classical dendritic cells, and myofibroblasts<sup>8</sup>. The inner elastic lamina separates the intima from the media, while the outer external lamina isolates the media from the adventitia (Fig. 1.1).

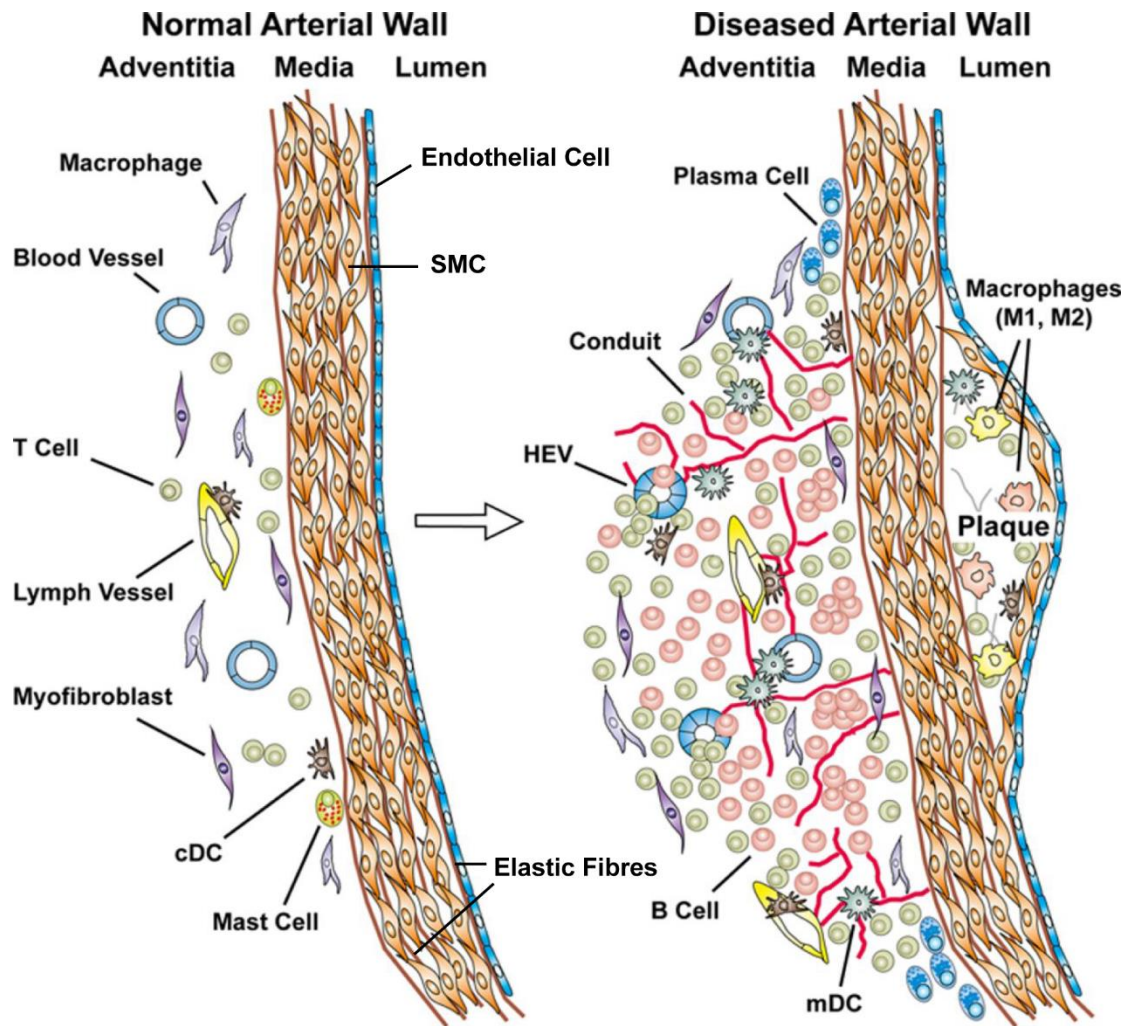


**Figure 1.1 Schematic graph of a normal and diseased artery<sup>8</sup>.** Reproduced from Mohanta, S.K., et al. 2014, Circulation Research. Normal and diseased arteries contain three layers: the intima, the media, and the adventitia. The normal intima contains a monolayer of endothelial cells. The normal media consists of several layers of smooth muscle cells (SMCs). Underneath the endothelial cell monolayer, few T cells together with conventional dendritic cells can be observed, while the adventitia harbors mast cells, macrophages, T cells, and myofibroblasts. During atherosclerosis progression, macrophages take up lipid to form foam cells, and SMCs migrate into the intima and proliferate. Thus, the atherosclerotic plaque consists of several inflammatory leukocytes, proliferating SMCs, and activated endothelial cells. Moreover, the adventitia adjacent to atherosclerosis contains a large number of T- and B-cells, other immunocytes, and newly formed high endothelial venules (HEVs) and conduits as well as aberrant lymphatic vessels. mDC designates monocyte-derived DC.

### **1.1.2 Progress in the field of atherogenesis**

Atherosclerosis is initiated by an accumulation of cholesterol in the arterial wall. Oxidized lipids and low-density lipoprotein (LDL) cause endothelial cells to express adhesion factors and chemokines. Subsequently, blood leukocytes adhere to the activated endothelium, then migrate into the intima<sup>9</sup>. Many macrophages in atherosclerotic plaques originate in blood-born monocytes, take up lipid to become lipid-laden foam cells<sup>10</sup>. The development of atherosclerotic plaque includes the migration of SMCs from the media to the intima, proliferation of SMCs, and an increase of extracellular matrix components such as collagen, elastin, and proteoglycans<sup>11</sup>. The macrophages and SMCs sustain apoptosis in advanced plaques. Extracellular lipid released by dead cells locates in the center of a plaque. Advanced plaques contain cholesterol crystals and microvessels as well. The last and clinically phases of atherosclerosis are associated with rupture of the plaque and intraluminal thrombus formation, which ultimately clog the artery leading to tissue infarcts, including myocardial infarcts and stroke<sup>12</sup>.

### **1.1.3 Immunocytes in atherosclerotic plaques**

Atherosclerotic plaques consist of various immunocytes, characteristically macrophages, and T cells<sup>13-14</sup>. However, the roles for each cell type and the sequence of events leading to advanced atherosclerosis are not entirely clear.

Foamy macrophages accumulate in the plaque and are pathological hallmarks of atherosclerosis. In 1979, Goldstein's group first found that macrophages express scavenger receptors for acetylated LDL uptake and degradation<sup>15</sup>. This discovery revealed that scavenger receptor-expressing macrophages promote foam cell formation and atherogenesis.

Ralph M. Steinman, in 1973, discovered dendritic cells (DCs) and characterized some general features of T cell responses that are initiated by DCs<sup>16</sup>. DCs were described in atherosclerosis for the first time in 1995 by Bobryshev<sup>13</sup>. DCs are found in the normal healthy artery wall and in all stages of atherosclerosis, indicating that DCs play



important roles in atherosclerosis. Subramanian et al. reported that Myd88-deficient CD11c<sup>+</sup> DCs reduced regulatory T cells (T<sub>reg</sub> cells) in atherosclerotic arterial walls and thereby promoted atherosclerotic lesion formation in aortic roots<sup>17</sup>. DCs can also influence atherosclerosis by secreting inflammatory cytokines, i.e., interleukin-6, tumor necrosis factor, interleukin-2, interleukin-23, granulocyte-macrophage-colony-stimulating factor with potent effects on T cells and other immune cells<sup>18</sup>.

T cells, one of the two major lymphocyte subtypes, play a significant role in the immune response. The T cell repertoire is formed in the thymus, and subsequently, T cells become activated and proliferate in secondary lymphoid tissues, including lymph nodes and spleen. T cells are heterogeneous. There are different stages and functional activation stages of T cells. These can be identified on the basis of surface activation markers. CD44 and Selectin-L (also known as CD62L) are well-recognized lymphocyte homing receptors, which mediate the interaction of lymphocytes with endothelial cells of high endothelium venules in secondary lymphoid tissues mediating recirculation events. Conventional murine T cells can be divided into three major populations, CD62L<sup>hi</sup>CD44<sup>lo</sup> naïve T cells (Th0), CD62L<sup>hi</sup>CD44<sup>hi</sup> central memory T cells (TCM), and CD62L<sup>lo</sup>CD44<sup>hi</sup> effector memory T cells (TEM). Naïve T cells refer to T cells that leave the thymus but are not yet activated by antigens in secondary lymphoid organs. These T cells perform immune surveillance by recirculating between the blood and secondary lymphoid organs. In contrast, memory T cells have encountered a specific antigen and have been activated, resulting in proliferation.

In 1986, Jonasson et al. discovered that T cells were present in atherosclerotic fibrous caps<sup>14</sup>. Since then, adaptive immune responses became a focus of atherosclerosis research. Wick et al. also observed that lymphoid cells were critical cellular constituents of atherosclerotic plaques<sup>19</sup>. Moreover, van der Wal et al. showed that CD4<sup>+</sup> T cells were more abundant than CD8<sup>+</sup> T cells in the early lesions and that the CD8<sup>+</sup>/CD4<sup>+</sup> ratio increased in both early and late human plaques<sup>20</sup>. In the lesion, 95% of the T cells express TCR  $\alpha$  and  $\beta$  subunits, and approximately 5% of T cells carry the TCR  $\gamma\delta$  in fatty streaks, and 4.3% in plaque<sup>21</sup> (only 1-2% T cells carry the TCR  $\gamma\delta$  in peripheral

blood)<sup>22</sup>. These data indicated that T cells might contribute to atherogenesis.

#### **1.1.4 Mouse models of atherosclerosis**

Atherosclerosis is a complex, chronic, and multi-factorial disease. Because of the generation and use of genetically modified mice and their use for atherosclerosis research, the current understanding of the mechanisms of the disease has grown rapidly<sup>23-26</sup>.

Genetically modified mice such as Apolipoprotein E-deficient mice, when maintained on a normal chow diet develop atherosclerosis because these mice are constitutively hyperlipidemic<sup>27,28</sup>. When maintained on a high-fat diet, some strains of mice, such as the C57BL/6 strain, develop atherosclerosis even more rapidly over time<sup>29,30</sup>.

In 1992, the Apolipoprotein E-deficient (ApoE<sup>-/-</sup>) mouse was generated by two independent research groups<sup>27,28</sup>. As mentioned above, ApoE<sup>-/-</sup> mice are constitutively hyperlipidemic when maintained under normal mouse chow<sup>29,30</sup>. The other most utilized model of atherosclerosis is the low-density lipoprotein receptor-deficient (LDLr<sup>-/-</sup>) mouse. This mouse was established in 1993 by Ishibashi et al<sup>31</sup>. In contrast to ApoE<sup>-/-</sup> mice, LDLr<sup>-/-</sup> mice require a high-fat diet such as a Western-type diet to become severely hyperlipidemic and to develop atherosclerosis. Both ApoE<sup>-/-</sup> and LDLr<sup>-/-</sup> mice generate atherosclerotic plaques, which are similar to their human counterparts, but the mice have different plasma lipid profiles<sup>30</sup>. In LDLr<sup>-/-</sup> mice, triglyceride and cholesterol levels are increasing because of the Western chow, while in ApoE<sup>-/-</sup> mice triglyceride levels do not significantly change<sup>32</sup>. ApoE<sup>-/-</sup> mice develop advanced lesions with an acellular necrotic core<sup>33</sup>, and in addition, atherosclerotic plaque ruptures rarely occur in the brachiocephalic artery of the long-term high-fat diet fed ApoE<sup>-/-</sup> mice<sup>34</sup>. However, plaques instability in the normal diet fed ApoE<sup>-/-</sup> mice does not regularly form occlusive thrombi revealing differences between humans and mice<sup>35</sup>. However, ApoE<sup>-/-</sup> mice are of great interest in performing longitudinal studies of plaque development, vascular fibrosis, and calcification, but not plaque rupture.

### **1.1.5 Atherosclerosis in ApoE<sup>-/-</sup> mice**

Compared to wild type C57BL/6 mice, which have mean total cholesterol (TC) of 2.1 mg/dl, ApoE<sup>-/-</sup> mice show substantial elevations, with mean TC at 19 mg/dl<sup>36</sup>. And this TC level will further increase 3-4 times on a high-fat diet (15% fat, 1.0% cholesterol, and 0.5% cholate)<sup>36</sup>.

In a normal diet fed ApoE<sup>-/-</sup> mice, early atherosclerotic lesions, fatty streaks are regularly observed at 3 months<sup>27,37</sup>. More complex lesions will be formed after 20-30 weeks, with many characteristics similar to human lesions, such as macrophages and SMC infiltration, fibrous plaque formation, and wall thinning<sup>37</sup>. By 10 months, calcification may be seen<sup>37</sup>. The progression will speed up with a high-fat diet<sup>37</sup>.

## **1.2 Complement system and activation**

### **1.2.1 Complement cascade**

Hans Ernst August Buchner found a "factor" or "principle which is capable of eliminating microbes in the blood. Later, in 1896, Jules Bordet found that blood contained two distinct molecules: a heat-stable and a heat-labile constituent. The heat-labile component was observed to be responsible for the general antimicrobial action of normal serum, and this is now termed the so-called "complement"<sup>38,39</sup>.

The complement system constitutes a group of components in human and animal body fluids or on cell surfaces<sup>40-42</sup>. Complement is a significant part of the innate immune system, which is the first line of defense/protection against pathogen-triggered diseases. Recent studies further showed that complement connects the innate and adaptive immune response, and removes antibody-antigen complexes (immune complexes)<sup>41-43</sup>. The system contains more than 30 components<sup>41-43</sup>, which are largely produced and maintained by hepatocytes<sup>43</sup>. Additionally, immune cells and endothelial cells synthesize several complement components locally<sup>44</sup>.

### **1.2.2 Activation of the complement system**

The complement system senses foreign pathogens and injured host cells by activating

the classical complement pathway (which is also termed the classical complement cascade, i.e., the CCC), the alternative complement pathway, and the mannan-binding lectin (MBL) complement pathway<sup>38</sup>.

The CCC can be activated by binding of antibody-antigen complexes to C1q during innate immune responses, and therefore the CCC bridges the innate and adaptive immune systems. Binding of the MBL to mannose-containing carbohydrates on bacteria or viruses initiates the MBL pathway. The alternative pathway is initiated by the spontaneous hydrolysis of C3 into C3a and C3b. Because of the inhibitors and regulators represented on the surface, i.e., factor H, factor I, CD59, C3b deposits on all normal cells does not lead to cell damage. The pathway is only triggered by the direct binding of the C3b protein to a microbe, foreign materials, and damaged cells.

Both the classical and MBL pathways require the C2 and C4 complement proteins for the formation of C3 convertase, which is formed from C4b-C2b complexes. In the alternative pathway, factor B can bind to C3b, which is produced by the CCC. D factor cleaves the C3bB complex into C3bBb and Ba. C3bBb, as a C3 convertase, includes the Bb component which can cleave C3 into C3a and C3b. C3bBb can be stabilized with binding to properdin (P factor), or it will hydrolyze rapidly (see Fig. 1.3).

Complement pathway activation leads to the generation of a protease called a C3 convertase that cleaves C3 to C3a and C3b. The C3b molecule contributes to generating a C5 convertase that produces the small key peptide mediators of inflammation, the products of C5, i.e., C5a and C5b. Following C6 binding site exposure by C5b, the C5bC6 binds to the target surfaces and initiates the formation of C5b-9 (MAC or TCC)<sup>45</sup>, which forms a pore in the cell membranes of pathogens or other target cells and induces the cells' lysis. Whether cell death is apoptotic or necrotic seems to be a function of C5b-9 quantity<sup>45</sup>.

Complement cascade activation results in lysis of the pathogen, opsonization, and pro-inflammatory activity by producing a large number of biologically active components.

C3b plays an important role in opsonization. It deposits on the surface of a target to

mark the target such a microorganism and then promotes the recognition and uptake by phagocytes<sup>46</sup>.

C3a and C5a can also recruit and activate inflammatory cells by potent chemotactic activity towards several innate and adaptive immune cells. C5a receptor (C5aR) is involved in chemotaxis, oxidative burst, and other inflammatory mechanisms. Moreover, it is highly expressed in myeloid cells, granulocytes, monocytes/macrophages, mast cells, DCs, T and B cells<sup>47, 48</sup>. C5aR was also found to be expressed in most organs and many different cell types like endothelial cells, neurons, astrocytes, microglia, and other tissue cells, including those of the kidney, lung, liver, spleen, intestine, and heart<sup>46,47</sup>. Using C5aR<sup>-/-</sup> mice or C5a/C5aR-inhibition in animal models, it has been shown that C5a plays an important role in various diseases, i.e., Alzheimer's disease, sepsis, Arthus reaction, asthma, in several models of ischemia-reperfusion injury<sup>47</sup>, and in atherosclerosis<sup>48</sup>.

C5a regulates neutrophil and monocyte activity and enhances cell adhesion, resulting in granulocyte degranulation and release of intracellular enzymes, generate toxic oxygen metabolites and initiating other cellular metabolites.

The complement component also has a variety of other immune functions via complement receptors (CR) expressed by immune cells. C3b/C4b receptor, CR1, known as CD35, promotes antigen presentation on B cells<sup>49</sup>, and transfers and eliminate immune complexes on red blood cells<sup>50</sup>. CR2 (CD21) regulates B cell activation by binding to CD19<sup>51</sup> and serves as a receptor for Epstein Barr virus, which is an important facilitator of T cell lymphomas and autoimmune diseases<sup>52</sup>. CR3 (CD11b/CD18) regulate T cell proliferation and IL-2 production<sup>53</sup>. CR3 and CR4 (CD11c / CD18) contribute to phagocytosis<sup>54</sup>. Activation of complement cascades generates C3a, C4a, and C5a, which in return lead to mast cell degranulation, vascular leakage, and smooth muscle contraction.

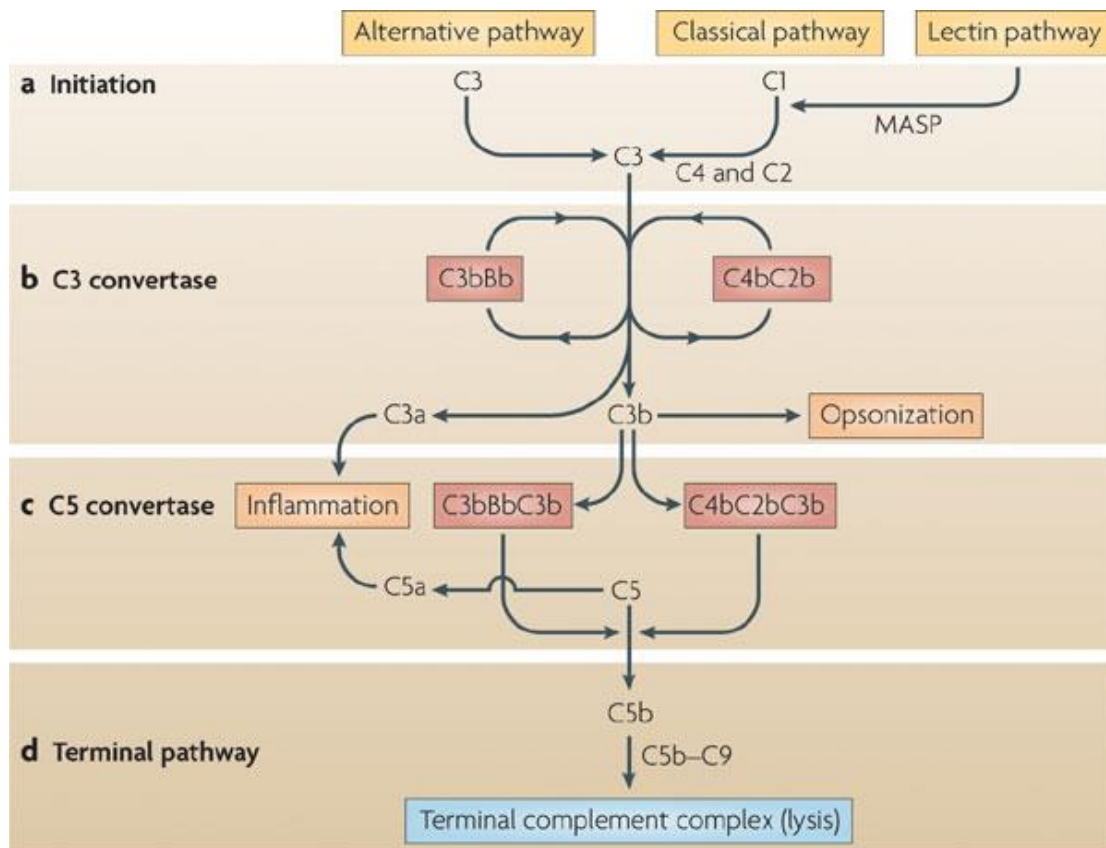


**Figure 1.2 Complement activation cascades<sup>46</sup>.** This schematic representation was taken from reference (Zipfel, P.F et al., 2009, Nat Rev Immunol). The complement pathways contain alternative, classical, and lectin pathways. The alternative pathway is activated by C3 hydrolysis spontaneously, which is modified by factor B and factor D. The CCC is activated by C1q binding to immune complexes, and the lectin pathway is initiated by MBL. Activation of C3 leads to the C5 activation and TCC formation, which is formed with C5a, C6, C7, C8, and multiple C9 molecules. C3b can serve as an opsonin when bound to an antigen's surface. C3a and C5a cause inflammation by activating and recruiting inflammatory cells. Mannan-binding lectin serine protease (MASP) indicates MBL-associated serine protease.

### 1.3 Complement cascade and atherosclerosis

While initial events in the pathogenesis of atherosclerosis remain to be fully understood, it is well accepted that lipid accumulation beneath endothelial cells is associated with major inflammatory tissue reactions, which in turn trigger additional inflammatory cascades to form an advanced plaque. However, how lipid triggers vascular inflammation is still unclear.

Complement might influence the progression of atherogenesis, as shown in human studies. Vlaicu's group showed that C5b-9 is present in the normal intima and the media but is induced significantly in the thickening intima, media, and the fibrous plaque<sup>55</sup>. Moreover, Cristea and Vlaicu's group reported that C5b-9 deposition was frequently associated with other complement components such as C1q, C3c, and C4 and immunoglobulins such as IgM, IgG, IgA<sup>56</sup>. In 1990, Rus and Vlaicu's group showed that decay-accelerating factor deposition in human thickened intima and fibrous plaques were significantly higher than those in fatty streaks or healthy blood vessel areas. Decay-accelerating factor and C5b-9 proteins were co-localized on nucleated cells and cell debris<sup>57</sup>. In 1989, factor H, factor B, and C3 were found at the same location as C5b-9 by Hansson's group, but not in normal arteries. The same investigators observed complement C3b receptor (CR1) and the iC3b receptor (CR3) to be expressed by approximately 20% of the total cells in complex human carotid lesions<sup>58</sup>. The mRNA levels for complement components were also increased in fibrous plaques when compared with normal arteries indicating local production of complement components. Yasojima observed that mRNAs for C1r, C1s, C4, C7, C8, and CD59 were increased in human aortic atherosclerotic plaques compared with normal artery<sup>59</sup>.

Previous functional studies in mice have, however, shown that the role of complement activation in atherosclerosis remains controversial. C6<sup>-/-</sup>ApoE<sup>-/-</sup> mice on a high-fat diet develop fewer plaques in the innominate artery compared to control ApoE<sup>-/-</sup> mice<sup>60</sup>. Inhibition of the C5a receptor in ApoE<sup>-/-</sup> mice on a normal diet decreased innominate artery plaque size<sup>48</sup>. These data indicated that complement system activation promotes atherosclerosis. However, C1q<sup>-/-</sup>LDLr<sup>-/-</sup> mice on normal diet developed more aortic root plaque<sup>61</sup>, and C3<sup>-/-</sup>ApoE<sup>-/-</sup>LDLr<sup>-/-</sup> mice have more plaques in total aorta when stained with *en-face* staining<sup>62</sup>, indicating that complement cascade activation protects the arterial wall from atherosclerosis. Finally, knockout of C5 does not appear to affect atherosclerosis in ApoE<sup>-/-</sup> mice on high fat diet<sup>63</sup>. Therefore, studies on the role of the complement cascades in atherosclerosis using animal models have so far produced

conflicting results, and thus the role of complement activation in atherosclerosis remains unclear.

## **1.4 Complement-based therapies**

### **1.4.1 Complement-system-associated diseases**

The immune system employs inflammation to protect the host from microbial damage, repair damaged tissue, and to remove dead cells and immune complexes. However, when inflammation becomes chronic, inflammation can cause disease. Complement system activation seems to drive a significant number of chronic inflammatory, autoimmune<sup>64</sup>, neurodegenerative<sup>65</sup>, and ischemia/reperfusion (I/R) injury-related diseases<sup>66</sup>. It is well established that complement constituents are increased in inflamed tissues and complement is involved in various autoimmune diseases, e.g., systemic lupus erythematosus (SLE)<sup>67</sup>, Alzheimer's disease plaques<sup>68</sup>, age-related macular degeneration (AMD)<sup>69</sup>, atypical hemolytic uremic syndrome (aHUS)<sup>70</sup>, paroxysmal nocturnal hemoglobinuria (PNH)<sup>71</sup>, rheumatoid arthritis (RA)<sup>72</sup>, myasthenia gravis (MG)<sup>73</sup> and others.

PNH is a rare and acquired fatal blood disease. Patients with PNH present somatic mutations in the PIG-A gene on the X chromosome in hematopoietic bone marrow stem cells, and deficiency of CD55 and CD59, which are surface proteins and inhibit the formation and function of the TCC. Therefore, red bloods are susceptible to damage by the complement system, resulting in chronic hemolytic anemia<sup>74</sup>.

aHUS is a disease characterized by microvascular hemolytic anemia, thrombocytopenia, and acute renal failure. The main pathogenesis of aHUS is the excessive activation of the alternative pathway, which forms MAC on the membrane of the host cells, resulting in cell lysis<sup>75</sup>.

AMD is an age-related disease, characterized by ocular nerve degeneration, and associated with several complement gene variations, including C2, C3, FB, Factor H, and Factor I<sup>69</sup>. Nozaki et al<sup>76</sup> found deposition of C3a and C5a in the drusen (the earliest



clinic pathologic feature of AMD, extracellular deposits under the retinal pigmented epithelium) of AMD patients and in a mouse model. And in the C3a and C5a knockout AMD mouse model, the expression of vascular endothelial growth factor decreased implicating complement in the pathogenesis of AMD.

SLE and SLE like disease are chronic, complex autoimmune diseases. In SLE patients, many organs, including the joints, skin, and kidneys<sup>77</sup>, are affected by complement activation. The deficiencies of C1q, C1r, C1s, C2, and C4<sup>78</sup> can increase the risk of these diseases in the patients. Only a small number of these patients exist with C3<sup>79</sup> and C5b-9<sup>75</sup> deficiency. Clinical data show that atherosclerosis is more prevalent in patients with SLE<sup>80</sup>. The complement protein deposition is easily observed in the inflamed tissues of the patients, such as C3, C4<sup>81</sup> and C5b-9<sup>82</sup>, supporting the complement system activation in SLE pathology.

#### **1.4.2 Complement therapeutics**

The purpose of clarifying the association between complement activation and the pathogenesis of many diseases is not only to assist in clinical diagnosis but also to develop novel treatments. In recent years, targeted therapeutics related to complement components or their receptors have also made considerable progress.

The first approved adjuvant therapy for clinical use is Eculizumab (Alexion), i.e., a humanized recombinant anti-C5 monoclonal antibody that specifically binds to complement C5 blocking the release of C5a and the C5b-9 complex. In PNH patients, anti-C5 treatment improves the quality of life but does not appear to affect mortality<sup>71,83</sup>. The anti-C5 antibody has also been successfully used to treat aHUS patients who developed C3 glomerulopathy<sup>84</sup>.

Pexelizumab (Alexion) is a humanized, monoclonal, single-chain antibody fragment targeting C5. It shows promising therapeutic benefits by reducing inflammation and organ dysfunction both in acute myocardial infarction and in patients undergoing coronary artery bypass graft with cardiopulmonary bypass<sup>85</sup>.

### **1.4.3 Liver-specific C5 small interfering RNA (siRNA) from Alnylam Pharmaceuticals, Inc.**

Alnylam Pharmaceuticals, Inc. was founded in 2002 to develop next-generation drugs based on the RNA interference technology (Andrew Fire and Craig Mello received the Nobel prize for Physiology or Medicine for the discovery of the technology). Alnylam has developed an RNAi therapeutics to target the liver-specific C5, currently under phase 2 clinical study in the USA. It features an attachment resulting in N-acetylgalactosamine (GalNAc)-tagged siRNA to target the liver specifically. It was demonstrated that ALN-CC5 targets hepatocytes to block the synthesis of C5 mRNA levels and subsequent dramatic lowering of C5 protein in mice, rats, and non-human primates<sup>73</sup>. In vivo, the highest dose reduces the circulating C5 concentration by 99%, and as reported by Alnylam that C5 knockdown is associated with up to 96.8% inhibition of serum complement activity<sup>86</sup>. In Phase I clinical trial for healthy people, subcutaneous injection of the drug can reduce complement hemolysis by more than 90% and can last for more than 2 months<sup>87</sup>. Clearly, this is an advantage for the pharmacokinetics and pharmacodynamics of siRNA in patients who require long-term acceptance of complement inhibition therapy.

### **1.4.4 Complement component C5 and autoimmune diseases studies**

The role of complement component C5 in complement system activation in the context of autoimmune diseases, i.e. RA<sup>88</sup>, AMD, SLE<sup>89</sup>, MS<sup>90</sup>, MG<sup>73</sup>, was studied in C5<sup>-/-</sup> (DBA/2) hybrid mice<sup>90</sup> or the use of anti-C5 specific antibody<sup>89</sup> and C5 siRNA<sup>73,88</sup> treatment. The anti-C5aR (anti-CD88)<sup>91</sup> antibody was also used for studying the effect of the C5a receptor in autoimmune disease.

In 1996, Yi Wang studied the role of C5 in SLE with the New Zealand black crossed New Zealand white F1 mice, which develop a notable syndrome similar to human SLE spontaneously. In the mice, chronic treatment with C5 antibody for 6 months significantly reduced the development of glomerulonephritis and increased survival, supporting the role of complement activation in the SLE mouse model<sup>89</sup>.

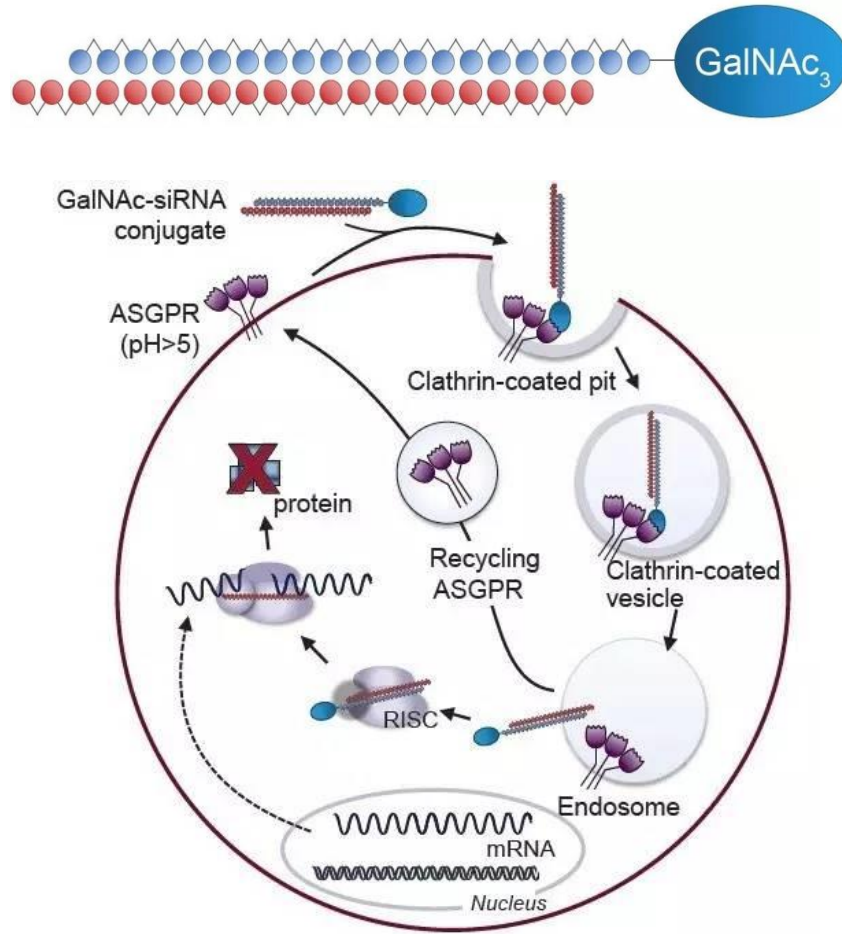


**Figure 1.3 GalNAc-siRNA C5 conjugate is an RNAi therapeutics targeting C5<sup>86</sup>.** This schematic representation was taken from Borodovsky. et al. (2014)<sup>86</sup>. Asialoglycoprotein receptor (ASGPR) is highly and specifically expressed in hepatocytes. siRNA conjugated to N-acetylgalactosamine (GalNAc) ligand, which binds to the ASGPR specifically, was efficiently delivered to hepatocytes by clathrin-coated pit-mediated uptake. siRNA binds to a helicase, ATP, and multiple proteins to form RNA-induced silencing complexes (RISCs). After specific binding to the C5 messenger RNA (mRNA), RISC cleaves the mRNA, eventually leading to C5 protein silencing. ASGPR is released from the endosome and recycled to the cell membrane.

Experimental autoimmune encephalomyelitis (EAE) is a mouse model for studying multiple sclerosis (MS). C5 deficiency in the EAE mouse model reduced the lesion areas and immune cell infiltration<sup>90</sup>, indicating that complement activation plays a role in the development of the course of the disease in the EAE model.

The C5 siRNA treatment significantly reduced the serum C5 level and the disease

symptoms in the two MG rat model<sup>73</sup>, demonstrating the liver-specific C5 plays a part in the development of MG.

## 1.5 Aims

Atherosclerosis is a prototypic chronic inflammatory disease of major clinical importance. Complement cascades play multiple roles in several inflammatory diseases, such as PNH and the aHUS. Complement proteins (i.e., C1q, C3, C5, C5b-9) were discovered in both the human and the mouse atherosclerotic plaque. However, the roles of complement cascades in atherosclerosis remain controversial. To understand the roles of complement cascades on atherosclerosis better, I chose N-acetylgalactosamine-conjugated C5 siRNA to examine liver-derived C5 on atherosclerosis in different dietary conditions as well as at various disease stages. In my Ph.D. thesis, the following questions will be addressed:

- 1) Are transcripts coding for complement cascades altered during atherosclerosis development?
- 2) Does liver-specific C5 control atherosclerosis in young ApoE<sup>-/-</sup> mice maintained under a normal chow diet?
- 3) Does liver-derived C5 affect atherosclerosis in young ApoE<sup>-/-</sup> mice maintained under a high-fat diet?
- 4) Does liver-derived C5 affect atherosclerosis development in aged ApoE<sup>-/-</sup> maintained under a normal mouse chow?
- 5) Are complement proteins expressed in human plaques?

## 2. MATERIALS & METHODS

The general reagents were purchased from Fluka (Buchs, Switzerland), Sigma (Deisenhofen, Germany), and Carl Roth (Karlsruhe, Germany) in analytical grade quality unless stated otherwise. All solutions were prepared with Millipore H<sub>2</sub>O (Milli-Q Plus ultrapure purification, Millipore, MA).

### 2.1 Materials

#### 2.1.1 Equipment

**Table 2.1 List of equipment**

Equipment	Type	Manufacturer
Balance	Analytical Plus	Ohaus
Black dissection wax	C3541	CR Scientific
Centrifuge	Centrifuge5415 R	Eppendorf
	Heraeus®Multifuge®3S-R	Thermo Scientific
Complete blood cell counter	scil Vet abc	scil animal care company GmbH
Confocal laser scanning microscopy	True Confocal Scanner-SP8	Leica
Cryostat microtome	Leica RM2235	Leica Biosystems
Digital camera	DSLR-a580	Sony
	Leica DFC365 FX	Leica Microsystems
Dissection Stereo microscope	Stemi 2000	Leica
Flow cytometers	Canto-II	BD
Flourescence microscope	DM 6000 B	Leica

Hematology analyzer	ScilVet ABC	Scil Animal Care
Light microscope	DM LB	Leica
Minutien Pin	26002-15	Fine Scientific Tools
pH-meter	InoLab level 1	WTW
Microplate reader	SpectraFluor Plus	Tecan
Ultrapure purification	Milli-Q Plus ultrapure purification	Millipore
Veroklav Laboratory Autoclave	Ype:500	Thermo Scientific
-80 °C freezer	C7736CD	Miele

### 2.1.2 Reagents and materials

**Table 2.2 List of reagents and materials**

<b>General Reagents and materials</b>	<b>Catalog number</b>	<b>Manufacturer</b>	<b>Storage or Specification</b>
10% bovine serum albumin (BSA)	70411/1	Aurion	4 °C
10% fetal calf serum (FCS)	DE14-801F	Lonza	-20 °C
4',6-diamidino-2'-phenylindole (DAPI)	H-1500	Vector Labs	-20 °C
96 Well Polystyrene Plate	Costar 9018	Corning	Room temperature
Acetone	K40718714	Merck	Room temperature under the hood
Ethylendiaminetetraacetic acid (EDTA)-coated tubes	41.1504.005	Sarstedt	Room temperature
Fluorescence mounting medium	S3023	DAKO	4 °C

Faramount mounting medium, Aqueous	S3025	DAKO	4 °C
Isopropanol	K40615718	Merck	Room temperature under hood
O.C.T. Compound	0827400006	Tissue-Tek	125mL
O.C.T. Cryomold	25608-922/924/916	Tissue-Tek	10x10x5/15x15x5/25x20x5mm
Oil red O (ORO)	S378	Romeis	Room temperature
Paraformaldehyde (PFA)	P-6148	Sigma-Aldrich	Room temperature
Sarstedt Microtube 1.1ml Z-Gel	50-809-211	Sarstedt	Room temperature
Triton X-100	9002-93-1	Sigma-Aldrich	Room temperature
Tween® 20	P1379	Sigma-Aldrich	Room temperature
Western Type Diet (High-fat diet)	EF TD88137 mod	ssniff-Spezialdiaeten GmbH	21.1% crude fat, and 17.3% crude protein

### 2.1.3 Standard solutions and buffers

**Table 2.3 List of standard solutions and buffers**

<b>Solution</b>	<b>Composition</b>	<b>Storage</b>
Ammonium-Chloride-Potassium (ACK) lysis buffer	0.15 mM NH <sub>4</sub> Cl, 1 mM KHCO <sub>3</sub> , 0.1 mM Na <sub>2</sub> EDTA, adjust to pH 7.3	Room temperature
Phosphate buffered saline (PBS) (10x)	80 g NaCl, 2 g KCl, 27 g Na <sub>2</sub> HPO <sub>4</sub> ·7H <sub>2</sub> O, 2.4 g KH <sub>2</sub> PO <sub>4</sub> into 800 mL ddH <sub>2</sub> O, then, adjust the pH to 7.4, add ddH <sub>2</sub> O to 1000 mL	Room temperature
PBS (1x)	Dilute PBS (10x) in 10 times with ddH <sub>2</sub> O	Room temperature



Fluorescence-activated cell sorting (FACS) buffer	PBS with 2% fetal calf serum (FCS)	Fresh prepared
0.05 M sodium Bicarbonate buffer	0.015 M Na <sub>2</sub> CO <sub>3</sub> , 0.035 M NaHCO <sub>3</sub> , adjust to pH 9.6	Room temperature
4% PFA	Dissolve 40 g paraformaldehyde in PBS (1000 ml final), pH 7.2-7.4	4 °C
PFA-sucrose solution	Dissolve 50 g sucrose into 1000mL 4% PFA	Room temperature
Sudan IV-staining solution	Dissolve 500 mg Sudan IV in a mixture of 35 mL ethanol, 50 mL acetone, and 20 mL ddH <sub>2</sub> O	Room temperature
Oil red O stock solution	Dissolve 1 g Oil red O powder in 200 mL 99% isopropanol	Room temperature
Oil red O working solution	Dilute 400 mL Oil red O stock solution with 300 mL of ddH <sub>2</sub> O. Stored at room temperature overnight, filtered before use.	Room temperature

### 2.1.4 Antibodies for Immunofluorescence Microscopy

**Table 2.4 List of antibodies for immunofluorescence staining**

Primary Antibodies					
Antibody	Target	Clone	Host	Reactivity	Manufacture
Anti-C1q	Complement protein C1q	9A7	Human	Mouse	abcam
Anti-C3	Complement protein C3	Polyclonal	Goat	Human	Complement Technologies
Anti-C4	Complement protein C4	16D2	Rar	Mouse	Hycult
Anti-C5	Complement protein	Polyclonal	Rabbit	Human	Complement

	C5				Technologies
Anti-C5	Complement protein C5	Polyclonal	Rabbit	Mouse	abcam
Rabbit IgG	Isotype control	Polyclonal	Rabbit	Mouse	abcam
Anti-CD68	Macrophages, microglia cells, some DCs	FA-11	Rat	Mouse	Serotec
Anti-CD3e	Naïve or primed T cells	145-2C11	A. Hamster	Mouse	BD PharMingen
Anti-CD31	Endothelial cells, some peripheral leukocytes, platelet, bone marrow-derived hematopoietic stem cells and embryonic stem cells	MEC13.3	Rat	Mouse	BD PharMingen
SMA-Cy3	Smooth Muscle cells	1A4	Mouse	Mouse	Sigma
<b>Secondary Antibodies</b>					
<b>Antibody</b>	<b>Host</b>	<b>Format</b>	<b>Manufacture</b>		
Anti-rat IgG	Donkey	Alexa 488	Dianova		
		Cy3			
		Cy5			
	Goat	Cy3			
Anti-rabbit IgG	Donkey	Cy3	Dianova		
		Cy5			
	Goat	Alexa 488	Invitrogen		

		Cy3	Dianova
		Cy5	
Anti-mouse IgG	Goat	Cy3	
		Cy5	
	Donkey	Cy3	
		Cy5	
Anti-goat IgG	Donkey	FITC	
		Cy3	
		Cy5	
Anti-A. Hamster IgG	Donkey	Cy3	
		Cy5	

Table 2.5 List of antibodies for Enzyme-linked immunosorbent assay (ELISA)

Primary Antibodies						
Antibody	Target		Clone	Host	Reactivity	Manufacture
Anti-C5	Complement protein C5		Polyclonal	Goat	Human	Complement Technologies
Secondary Antibody						
Antibody	Clone	Conjugate	Format	Host	Reactivity	Manufacture
Bovine Anti-Goat IgG-HRP (H+L)	Polyclonal	Horseradish Peroxidase	IgG (H+L)	Bovine	Goat	Jackson ImmunoResearch

## 2.2 Mouse strains and husbandry

Male ApoE<sup>-/-</sup> mice (on C57BL/6J background) were housed in the animal laboratory facility of the Ludwig-Maximilians-University München (LMU), the Zentrale Versuchstierhaltung (ZVH), Klinikum Universität München (KUM). Mice were kept on a 12-hour light-dark cycle. Mice had free access to water and mouse chow. Depending on experiment objectives, mice were fed a normal diet (ssniff Spezialdiäten GmbH) or the high-fat diet (21.1% crude fat, 17.3% crude protein, 5% crude fiber with 4.3% crude ash; E15721-347, EF TD88137 mod, ssniff Spezialdiäten GmbH, Germany). According to the German animal protection law, animal experiments were reviewed and approved by the government of Upper Bavaria (Regierung von Oberbayern).

## 2.3 Mouse models

### 2.3.1 siRNA preparation and injection

In order to block the complement pathways, GalNAc conjugated siRNA targeting C5 (C5 siRNA; AD-61679.7, 20 mg/mL in DPBS) and GalNAc conjugated siRNA targeting luciferase (control siRNA; AD-48349.3, 20 mg/mL in DPBS) as control (received from Alnylam Pharmaceuticals) were used for C5 protein knockdown in the circulation. The control siRNA, luciferase siRNA, was chosen as a control because it targets the luciferase protein, which does not exist in the vertebrate transcriptome. The dose of siRNA for injection was 0.15 mg/g body weight. These siRNAs were applied immediately after 20 times dilution with PBS. Mice were injected with subcutaneous injection (s.c.). The site for injection was s.c. in the neck area.

### 2.3.2 Experimental protocol

1. 23 ApoE<sup>-/-</sup> mice (12-13 weeks old) were randomized for treatment with C5 siRNA or control siRNA every two weeks for 20 weeks. There were 12 mice in the C5 siRNA group, and others in control.
2. 18 ApoE<sup>-/-</sup> mice (58-59 weeks old) were randomized for treatment with C5 siRNA or

control siRNA every two weeks for 18 weeks. There were 9 mice in each group.

3. 21 ApoE<sup>-/-</sup> mice (12-13 weeks old) were randomized for treatment with C5 siRNA or control siRNA every two weeks for 20 weeks. They were fed a high-fat diet for 16 weeks, starting at 14-15 weeks old. There were 10 mice in the C5 siRNA group, and others in control.

4. Six ApoE<sup>-/-</sup> mice (8-9 weeks old) were randomized for treatment with C5 siRNA or control siRNA every two weeks for four weeks. They were fed a high-fat diet for 3.5 weeks. There were three mice in each group.

## **2.4 Serum collection and body weighing**

Serum was collected every two weeks before and after siRNA treatment at different time intervals, for the C5 concentration in circulation detecting. After fixing the mouse in a fixture, approximately 20-30 µl of blood from the tail vein was collected in serum-separating tubes. After the centrifugation, serum in the supernatant was transferred into new tubes and stored at -80 °C. Mice were weighed every two weeks before and after siRNA treatment regularly.

## **2.5 Blood and organ collection**

Mice were anesthetized by i.p. injection of Ketamine Hydrochloride (80 mg/kg) and Xylazine (5 mg/kg), and 700-1000 µl of blood were drawn by cardiac puncture. 20-30 µl of blood was kept in serum-separating tubes, and serum was prepared for determining the C5 concentration in circulation using ELISA. About 100-200 µl of blood was collected in EDTA tubes, and plasma was prepared from different blood cells counting with animal blood counter and for determination of concentrations of total cholesterol, Cholesterol (Chol) and triglyceride (TG) (in collaboration with Institute of Laboratory Medicine, Clinical Chemistry and Molecular Diagnostics, Universitäts Klinikum München). 400-500 µl of blood was collected in 10mL tubes with 5 ml 5 mM EDTA, and single blood cells were prepared for FACS.

Subsequently, mice were perfused with 5 ml 5 mM EDTA and followed by 10 ml PBS

to ensure the removal of blood from the aorta and other organs. The aortic roots were then collected and immersed in Tissue-Tek® O.C.T. compound and frozen in N-pentane to prepare fresh-frozen tissue blocks. These blocks were stored at -80 °C. The total aortas were collected for *en-face* Sudan IV staining.

## **2.6 Assessment of atherosclerosis in mice**

In order to assess atherosclerosis progression, the area of plaques may be quantified throughout the arterial tree. Previous studies already identified areas of atherosclerosis, which developed faster than others, such as the aortic valve leaflet and the root of the aortic arch<sup>92</sup> implicating that the location for assessing atherosclerosis within the aorta determines the outcome of the analyses.

Cross-section and *en-face* staining techniques are applied to determine the degree of atherosclerosis. Cross-sections can be used for histological staining or immunohistochemistry of different markers, which could be quantified for specific purposes of the atherosclerosis study. The *en-face* assay requires to open the aorta, then, fixing it onto a flat black wax dish, followed with Sudan IV staining. Imaging software, such as ImageJ, is used for plaque development quantification and plaque structure evaluation.

### **2.6.1 *en-face* preparation and Sudan IV staining**

The total plaque load in the thoracic and abdominal aorta were analyzed using the Sudan IV staining of *en-face* prepared tissues. The adventitia was carefully removed, and the entire aorta was dissected under a dissection microscope. The outer curvature of the aortic arch and the inner curvature of the entire aorta was cut open along longitudinally to expose the intimal surface. The aortas were pinned down with the luminal surface upside with needles onto a black wax plate for fixation in PFA-sucrose solution overnight at 4 °C. The consistency in the pinning of the aorta was ensured. Then, pinned aortas were rinsed three times with PBS for 10 min, followed by

incubation in Sudan IV solution for 10 min. The aortas were then rinsed two times with 70% ethanol, and covered with PBS.

In order to quantify the percentages of lipid deposition in the thoracic, abdominal, and entire aorta, images were taken using a digital camera (Sony, DSLR-a580) with a standard bar.

The Sudan IV positive area in the aorta was quantified using Java-based image processing software ImageJ. The percentage area of the lesion was calculated using the Sudan IV positive area and area of the thoracic, abdominal and total aorta. The images to be measured were opened with the software ImageJ. Then, the image scale was set with the standard bar on the images. After the calibration for the image, on the measurement toolbar 'polygon selections' icon was used to outline and measure the area of the thoracic aorta and abdominal aorta. The aorta was separated into the thoracic and abdominal aorta at the level of the diaphragm<sup>93</sup>. The Sudan IV positive lesion areas on each part were outlined and traced with 'polygon selections'. Then the selected lesions were checked through the microscope. The selections were saved to the 'ROI Manager'. The data were exported using the 'measure' in the ROI Manager.

The percentage of the area of the lesion in the aorta area was calculated respectively. The sum of the thoracic aorta area and abdominal aorta area together is total aorta area. And the percentage of lesions in the total aorta was calculated with the total lesion area and the total aorta area.

### **2.6.2 Tissue sectioning**

The tissue blocks were sectioned in a cryotome maintained at -20 °C. 10 µm thick aortic root serial sections were collected on glass slides. The slides were stored at -80 °C until further use.

### **2.6.3 Oil-Red-O Hematoxylin (ORO/HE) staining and atherosclerotic lesion quantification**

Frozen aortic root cryosections (10  $\mu$ m) were warmed on a hot plate maintained at 37 °C for one min immediately followed by air-dry for 30-60 min at room temperature. The sections are serial and in 100  $\mu$ m intervals, respectively, starting from the origin of the aortic roots. In total, 6-8 sections per mouse heart were stained in ORO working solution for 10 min, then immersed in 60% isopropanol and washed with tap water briefly. They were then stained with hematoxylin for 6 min, followed by washing in running water (pH>7) for 10 min. The cover slides were mounted on tissue sections with an aqueous Faramount Mounting Medium. Images were taken with a microscope (Leica DM6000B, Leica Microsystems) connected to a camera (Leica DFC295, Leica Microsystems). All pictures of sections were taken with a 10x objective and 10x ocular lens.

Atherosclerotic plaque areas were quantified with the ORO pictures using ImageJ software. The ORO images were opened with the software ImageJ. The image scale was set with the standard bar on the images. After the calibration for the image, the measurement toolbar 'polygon selections' icon was selected to encircle the intimal layer area of the aortic root by repetitive clicks. The intimal layer was defined by the internal elastic lamina and the lumen. The intima area was saved to the 'ROI Manager.' The data were exported using the 'measure' in the ROI Manager.

### **2.6.4 Immunofluorescence staining**

Immunofluorescence staining was performed for CD68<sup>+</sup> macrophage/DC, CD3e<sup>+</sup> T cells, SMA<sup>+</sup> SMC, CD31<sup>+</sup> EC, and complement components C3, C4, and C5. 10  $\mu$ m fresh frozen tissue sections were prepared by microtome and stored at -80 °C. In total, 6-8 sections per mouse heart were thawed on a 37 °C hot plate for 30 seconds, followed by 30-60 min air-dry at room temperature. For fixation, sections were incubated with a pre-cooled 4% PFA solution for 5 minutes at 4 °C, then rinsing with PBS. Before and



after the fixation in 100% acetone for 2 min, sections were submerged in 50% acetone and then rehydrated in PBS for 10 min.

After fixation, sections were incubated overnight with primary antibodies diluted at the appropriate dilution in PBS with 0.25% BSA at room temperature. Sections were washed three times with PBS for 5 min, followed by incubation with the fluorescent-labeled secondary antibodies diluted in PBS with 0.25% BSA and 0.2% DAPI nuclear stain for one hour in the dark. After three times washes, slides were mounted with Fluoromount-G mounting media. For negative controls, primary antibodies were omitted, whereas the rest of the procedure was done as described. No specific immunostaining was observed in the control sections.

#### **2.6.5 Quantification of CD68<sup>+</sup> macrophage and CD3e<sup>+</sup> T cell infiltration in the plaque areas**

The serial aortic root cryosections (10  $\mu$ m), which are in 100  $\mu$ m intervals respectively, were stained with CD68 and CD3e antisera with the immunofluorescence staining method above. A total of 6-8 sections per mouse heart was used for analysis. Stained sections were examined using a confocal laser scanning microscope TCS SP8 (Leica, Germany) with appropriate excitation and emission filters. All pictures of sections were taken with a 20x objective and a 10x ocular lens.

The CD68<sup>+</sup> macrophage and CD3e<sup>+</sup> T cell infiltration in the plaque areas were quantified with CD68 and CD3e antibody stained pictures using the software ImageJ. The images were opened with the software ImageJ. The image scale was set with the standard bar on the images. After the calibration for the image, the intimal layer was encircled using the 'polygon selections' tool. The intimal layer was defined by the internal elastic lamina and the lumen. The intima area was saved to the 'ROI Manager.' Then the immunofluorescence pictures of CD68 were segmented by thresholding to create binary images<sup>94</sup>. The 'area fraction' of CD68<sup>+</sup> macrophage in plaque area and the plaque area can be exported with the 'measure' tool in the 'ROI Manager.'

In order to count the CD3e<sup>+</sup> T cell numbers in the plaque area, the CD3e antibody and DAPI stained pictures were merged into one picture. The CD3e and DAPI double-positive cells were counted as the CD3e<sup>+</sup> T cells.

## **2.7 ELISA for C5 protein in the circulation**

In order to obtain an estimate of C5 levels in circulation, approximately 20-30 µl of mouse blood, which was collected in 2.4 and 2.5, was centrifuged at 10,000 rpm for 15 min. The serum was then collected, and the C5 level was measured by ELISA, described below.

10 serum samples from 8 weeks old ApoE<sup>-/-</sup> mice without siRNA treatment were pooled as a positive control and standard curve sample. Pooled serum was frozen in 10 µl aliquots. A new aliquot was thaw for every assay.

96 wells flat plates were first coated with 100 µl diluted samples at the dilution of 1:5000 in dilution buffer. Pooled serum was used as a positive control and no serum as a negative control. As a non-specific background C5 negative control, serum from C5<sup>-/-</sup> mouse (DBA/2) to show the specificity of the assay. They were diluted at the same dilution as samples. For the standard curve, pooled serum was initially diluted at a dilution of 1:1000 and then eight serial 2x dilutions in sample dilution buffer.

ELISA plates were first coated with mouse serum (including all samples, controls, and standards curve dilutions) overnight at 4 °C, then blocked with 350 µl per well of blocking buffer (2% (w/v) BSA in PBS, filter through a 0.2 µm filter prior to use), incubated at room temperature for 2 hours. Subsequently, 100 µl per well of primary antibody (Gout anti-human C5 Antibody), diluted in antibody buffer at a dilution of 1:1000 and incubated at room temperature for 60 min, was used to detect bound C5 protein.

Following this step, 100 µl per well of secondary antibody (Bovine anti-goat IgG-HRP) diluted into an Antibody Buffer at a dilution of 1:500 and incubated for 1 hour at room temperature in the dark. Last, 100 µl per well of TMB mixed equal parts substrate A

and B before use and incubated for 3-5 min at room temperature in the dark. The ELISA reaction was stopped with 100 µl per well of 2 N sulfuric acid. The reaction was stopped at an OD value between 0.7 and 0.9 for the highest signal wells. Absorbance was read at 450 nm using a plate reader. Between incubations, plates were washed five times with 300 µl per well of wash buffer (0.05% (v/v) Tween 20 in DPBS).

OD values were first subtracted from background value (no serum background), and these values were then transferred in GraphPad Prism 8, and a standard curve was plotted with known C5 values (dilution fold) on the x-axis against absorbance values on the y-axis. Fit standard curve in GraphPad Prism 8 using a Sigmoidal 4-parameter fit. Input background-subtracted OD values for samples and controls into Prism and interpolated arbitrary values for C5 protein concentration. The data were normalized to the pre-dose values.

## **2.8 Human carotid artery tissues and atherosclerotic lesion analyses**

Human carotid atherosclerotic plaques were analyzed and quantified<sup>95</sup>. Briefly, atherosclerotic plaques were obtained from patients with high-grade carotid artery stenosis (>70%) after carotid endarterectomy. Healthy control carotid arteries were obtained from the Forensic Medicine Institute (type 0–I). The study was performed according to the Guidelines of the World Medical Association Declaration of Helsinki. The ethics committee of the Faculty of Medicine, Technical University of Munich (TUM) approved the study.

Human carotid plaques were segmented in blocks of 3 to 4 mm, fixed in formalin overnight, decalcified in 0.5 M EDTA (pH 7.2), and formalin-fixed paraffin-embedded (FFPE), or fresh frozen in Tissue-Tec (Sakura Finetek) for immunofluorescent staining of lipid. Hematoxylin-eosin and Elastic van Gieson (EvG) staining were performed to assess atherosclerosis. Specimens were divided into early (II–III) and advanced stages of atherosclerosis (V–VII) according. After staining, the stained slides were scanned by a ScanScope microscope (Leica) to obtain digital histological images of the whole

aorta sections. By ScanScope, each aorta section was translated into a TIF file. The TIF images were opened with the software ImageJ. The image scale was set with the standard bar on the images. After the calibration for the image, atherosclerotic plaques and media layers were encircled using the 'polygon selections' tool. The intimal layer was defined by the internal elastic lamina and lumen. The intima area and media were saved to the 'ROI Manager.' Immunohistochemical pictures of CD68 or C1q or ApoE or C5 were segmented by thresholding to create binary images<sup>94</sup>. Then the 'area fraction' of CD68<sup>+</sup> macrophage or C1q<sup>+</sup> area or ApoE<sup>+</sup> area or C5<sup>+</sup> area within intima or media layers was quantified by click "measure" tool in the 'ROI Manager.'

## **2.9 Statistical analysis**

Measurements are expressed as means of n samples  $\pm$  SEM. All calculations were carried out using Microsoft Excel and/or GraphPad Prism 8 software. Significance was analyzed using two-tailed unpaired Student's *t*-test, one-way analysis of variance (ANOVA), and two-way ANOVA, with statistical significance, assumed at  $p$  value $<0.05$ , and statistically highly significant assumed at  $p$  value $<0.001$ .

### 3. RESULTS

#### **3.1 mRNA Microarrays of Wt and ApoE<sup>-/-</sup> aortas of various ages reveal the presence of transcripts of complement cascade constituents in atherosclerotic plaques**

Multicellular organisms develop into different tissues, each with various functions due to specific gene expression profiles at different times and territories. If a certain gene is abnormally expressed, it may affect the body's normal physiological activity or even lead to disease. Similarly, if the body encounters certain injuries, it will usually respond with distinct gene expression patterns. Whole transcriptome mRNA expression arrays were examined by microarray, which is based on a Gene chip to study gene expression changes, and such tissues can then be compared and analyzed for differences in gene expression between physiological and pathological conditions.

Recently, Skerka and Zipfel observed through in vitro studies that ApoE is a CCC inhibitor by binding to activated C1q<sup>95</sup>. We found that C1q-ApoE complexes emerge in choroid plexus inflammation in Alzheimer's disease and in atherosclerosis, and that pharmacological targeting the complement component C5 alleviates choroid plexus inflammation, atherosclerosis and intermediate-sized Alzheimer plaque loads as well as Alzheimer plaque-associated inflammation in several mouse models<sup>95</sup>. Here, I examined the functional impacts of C1q-ApoE complexes in atherosclerosis.

ApoE-deficient mice on normal mouse chow develop atherosclerosis during aging. We hypothesized that complement cascades might be induced in atherosclerotic plaques of ApoE<sup>-/-</sup> mice due to the lack of its endogenous complement inhibitor (ApoE). We examined whether complement activation controls atherosclerosis development in this mouse model during aging.

In order to validate this hypothesis, members of our group had earlier harvested the whole aorta from Wt and ApoE<sup>-/-</sup> mice of various ages. These plaques were prepared

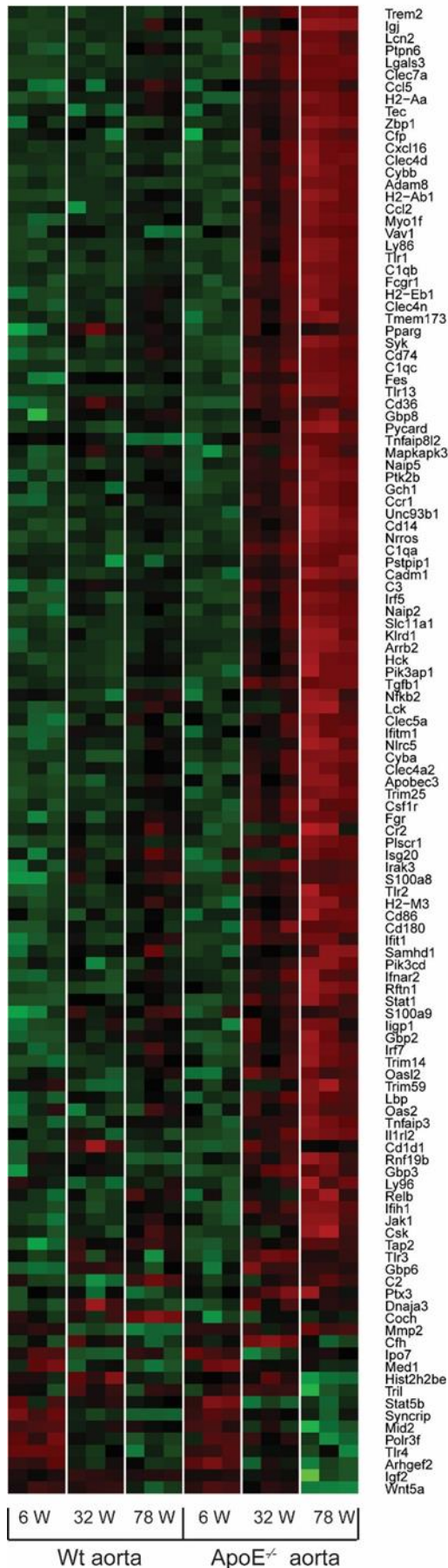
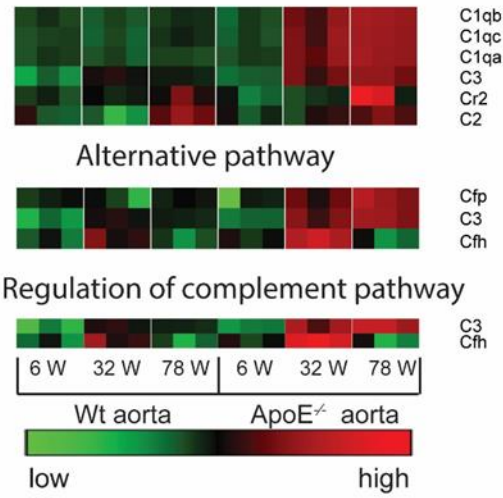
for microarray analyses in the previous studies<sup>95-97</sup>. Total aortas were from 6w, 32w, and 78w old Wt and ApoE<sup>-/-</sup> mice. Microarray analyses were performed by Michael Beer and Markus Hildner at the Friedrich-Schiller University of Jena Medical School.

This approach allowed me to mine the transcriptomes for the complement pathway-associated molecules. We examined differentially expressed genes of interest by using several gene ontology (GO) terms involved in complement cascades, that is an innate immune response (GO: 0045087), classical complement pathway (GO: 0006958), alternative complement pathway (GO: 0006957), regulation of complement activation (GO: 0030449).

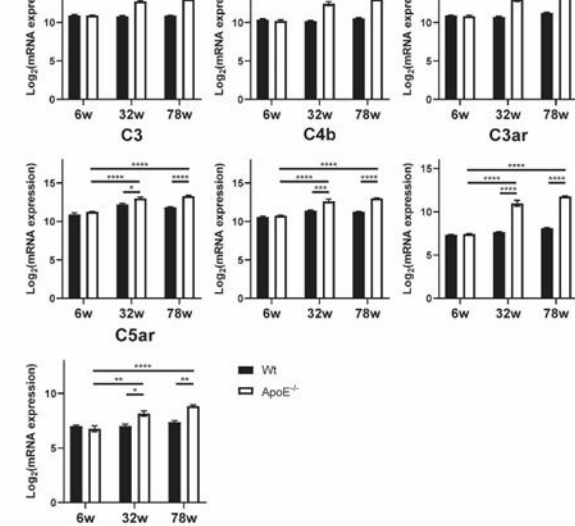
There are few immune response-related genes that are up- and down-regulated in the Wt aorta during aging (Fig. 3.1 A: innate immune response GO term). However, immune response-related genes were dramatically upregulated in the aortas of adult and aged ApoE<sup>-/-</sup> mice. There are no significant differences observed between Wt and ApoE<sup>-/-</sup> aortas at 6 weeks of age, but large differences were noted in ApoE<sup>-/-</sup> aortas at 32 weeks and 78 weeks of age when compared with age-matched Wt aortas (Fig. 3.1 A).

We specifically focused on the GO term of the CCC, the alternative complement pathway, and the regulation of complement activation (Fig. 3.1 B).

Atherosclerosis plaques begin to form in the aorta during the time window of 8-12 weeks when maintained on a normal chow diet though 6-weeks old ApoE<sup>-/-</sup> mice do not develop atherosclerosis plaques in the aorta. The CCC-related genes, i.e., C1qa, C1qb, C1qc, C4b, were strongly upregulated in the diseased aorta, but not in 6-week old ApoE<sup>-/-</sup> mice (Fig. 3.1 C). Complement C3 and complement receptors expressed by leukocytes (C3ar1, C5ar1) were also strongly induced during atherosclerosis (Fig. 3.1 C). Following CCC activation, C3b will initiate a constitutive amplification loop of the alternative complement cascade, also referred to as C3-triggered amplification loop. In addition, Factor H mRNA was detectable without differences between groups. Some of these data were represented in my previous publication<sup>95</sup>.

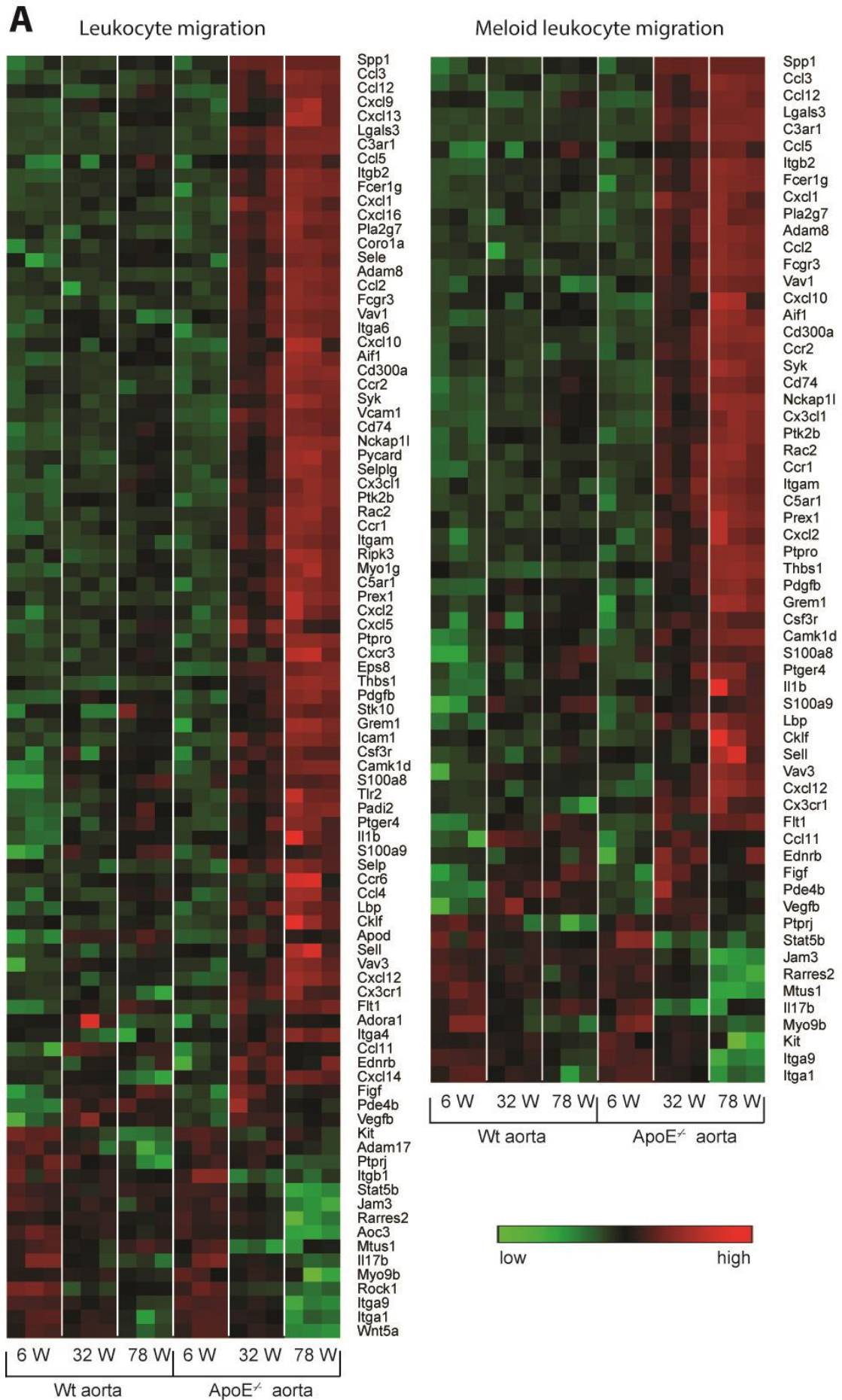
**A** Innate immune response**B** Classical pathway

## Regulation of complement pathway



**Figure 3.1 Transcriptomes of Wt and ApoE<sup>-/-</sup> aorta during aging** Microarray heatmaps of the whole aorta from different age groups of Wt and ApoE<sup>-/-</sup> mice. **A-B.** Heatmaps of differentially regulated genes in total aorta RNA extracts. Gene expression in aortas was displayed separately from 6, 32, and 78 weeks old Wt and ApoE<sup>-/-</sup> mice. The following GO terms were analyzed from total genes: innate immune response (GO: 0045087), classical pathway (GO: 0006958), alternative pathway (GO: 0006957), regulation of complement activation (GO: 0030449). **C.** Aorta complement gene mRNA expression (log<sub>2</sub> value). Means ± SEM. One-way ANOVA with Bonferroni's post-hoc test; \* P<0.05, \*\* P<0.01, \*\*\* P<0.005, \*\*\*\* P<0.001. 6 weeks Wt (n=3); 32 weeks Wt (n=3); 78 weeks Wt (n=3); 6 weeks ApoE<sup>-/-</sup> (n=3); 32 weeks ApoE<sup>-/-</sup> (n=3); 78 weeks ApoE<sup>-/-</sup> (n=3).







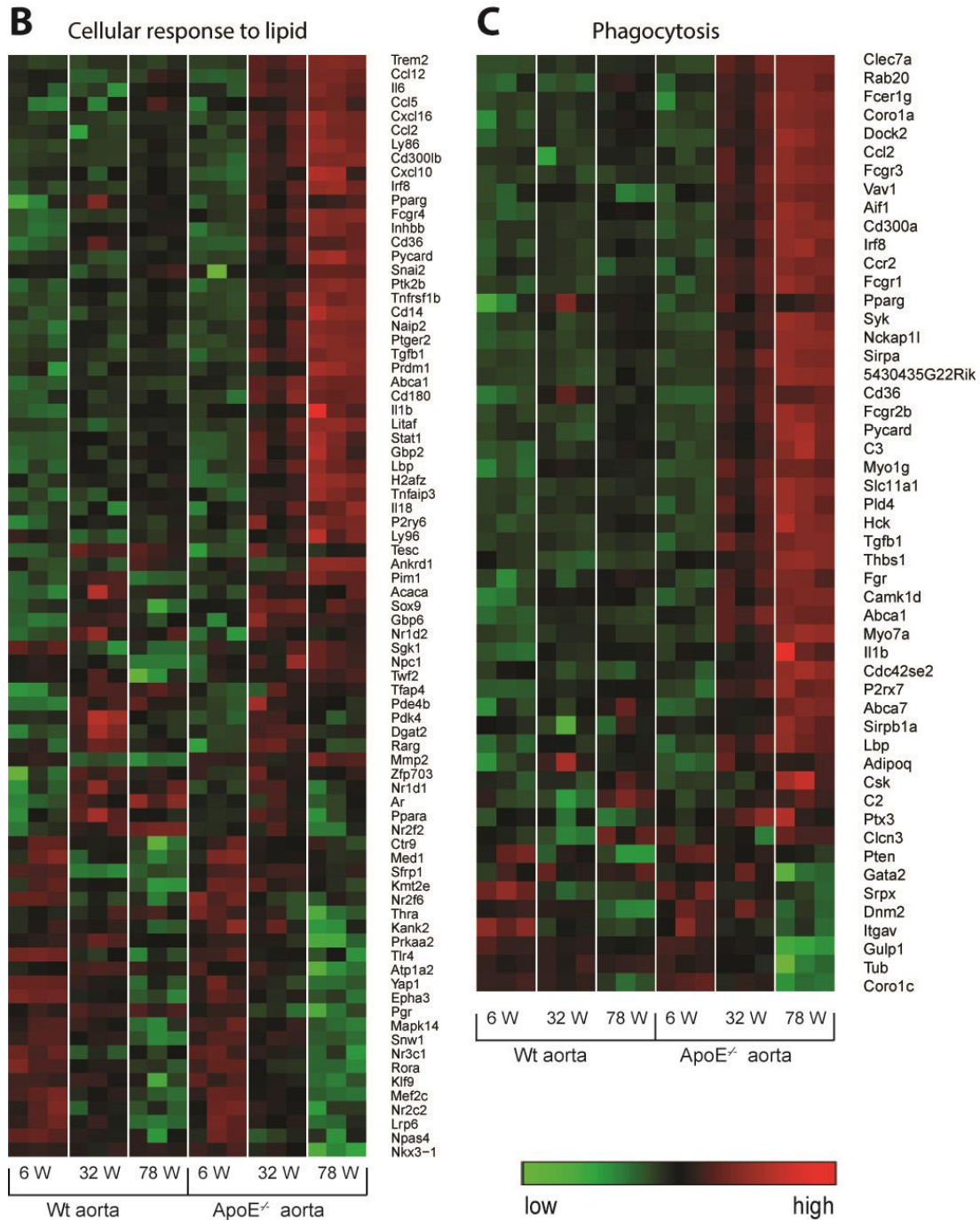


**Figure 3.2 Other transcriptomes of Wt and ApoE<sup>-/-</sup> aorta during aging** Microarray heatmaps of the whole aorta from different age groups of Wt and ApoE<sup>-/-</sup> mice. Heatmaps of differentially regulated genes in total aorta RNA extracts. Gene expression in aortas was displayed separately from 6, 32, and 78 weeks old Wt and ApoE<sup>-/-</sup> mice. The following GO terms were analyzed from total genes: **A.** Leukocyte migration (GO: 0050900), meloid leukocyte migration (GO: 0097529), **B.** Phagocytosis (GO: 0006909), **C.** Cellular response to lipid (GO: 0071396). One-way ANOVA. 6 weeks Wt (n=3); 32 weeks Wt (n=3); 78 weeks Wt (n=3); 6 weeks ApoE<sup>-/-</sup> (n=3); 32 weeks ApoE<sup>-/-</sup> (n=3); 78 weeks ApoE<sup>-/-</sup> (n=3).

These data supported our hypothesis that the CCC was strongly induced during atherosclerosis in ApoE<sup>-/-</sup> mice.

Oxidized lipids can activate the CCC, which in turn will release anaphylatoxin C3a and C5a to recruit leukocytes to the injury sites. The deposition of C3b on the lipid surface will increase macrophage phagocytosis and cellular response to lipids<sup>98</sup>. We next examined the GO terms related to the functional impact of complement activation, i.e., leukocyte migration, myeloid cell migration, phagocytosis, and cellular response to lipid (Fig. 3.2). In conclusion, our data support the hypothesis that the CCC may be involved in atherosclerosis progression.

### **3.2 Liver-specific C5 siRNA reduces atherosclerosis burden in young ApoE<sup>-/-</sup> mice maintained on normal mouse chow**

In order to examine whether complement cascades control atherosclerosis development, we chose to specifically target complement C5, which is a biologically inactive proprotein resulting in the generation of the potent downstream inflammatory mediators of all three complement cascades, C5a and C5b. Complement C5 is expressed mainly by hepatocytes, but a small amount can also be produced by locally infiltrating leukocytes under distinct physiological and disease conditions<sup>99</sup>. However, we did not detect complement C5 mRNA expression in the aorta transcriptomes in our microarray data analyses (see above), indicating that locally expressed C5 was under the detection threshold of the microarray.

The deficiency of ApoE in mice leads to spontaneous hyperlipidemia. These mice develop visible atherosclerotic plaques in the aorta at the age of 8-12 weeks, and atherosclerotic plaque progression can be observed during aging<sup>30</sup>. Oxidation-specific epitopes in extracellular lipid activate complement cascades and result in surface opsonization by C3b, generation of locally acting anaphylatoxins C3a and C5a, which in turn recruit leukocytes and elicit tissue inflammation<sup>47,100</sup>. In order to test the possibility that lipid accumulated underneath the dysfunctional endothelial cells triggers complement activation and leads to leukocyte infiltration and inflammation

during atherosclerosis in ApoE<sup>-/-</sup> mice, we first treated 12 weeks old ApoE<sup>-/-</sup> mice with C5 siRNA for 20 weeks. Then, we harvested tissues at the age of 32 weeks (Fig. 3.3). 23 mice were randomly separated into two groups: 12 ApoE<sup>-/-</sup> mice were treated with C5 siRNA every two weeks for 20 weeks and 11 ApoE<sup>-/-</sup> mice, as a control group, were injected with siRNA targeting luciferase. In order to examine the effect of C5 siRNA on atherosclerosis, a series of measurements were performed: a) blood was taken throughout the whole injection period: before treatment, at 2 weeks, at 12 weeks, and at 20 weeks after treatment to determine the concentration of C5 in the circulation; b) body weight was measured every two weeks; c) blood parameters were measured with complete blood leukocyte counts after 20 weeks treatment; d) leukocytes percentages were examined by FACS after 20 weeks treatment; e) atherosclerotic plaque burden was determined by *en-face* staining, and aortic root plaque areas were determined with ORO/HE-stained sections; f) plaque complement proteins were examined by immunofluorescence staining (see below Fig. 3.4 - Fig.3.9). The work introduced in this section was published<sup>95</sup>.

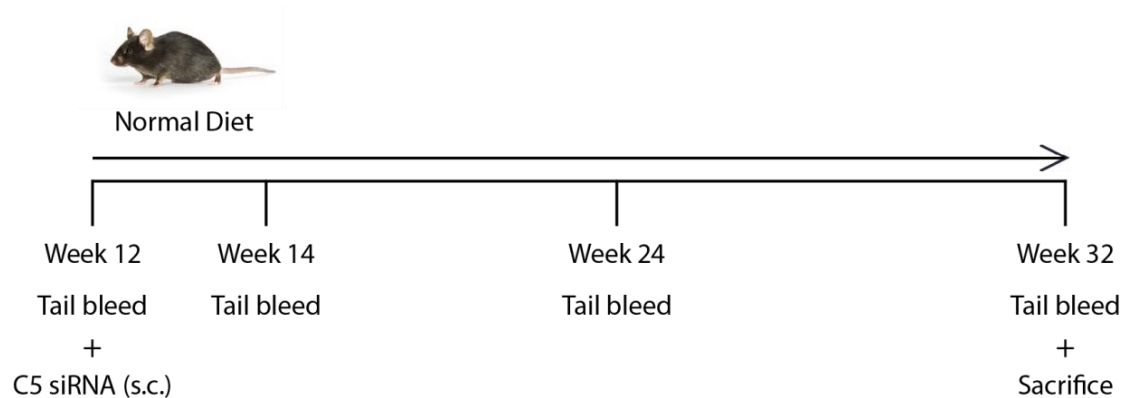


**Figure 3.3 Experimental design.** 12 weeks old male ApoE<sup>-/-</sup> mice (C5 siRNA treated mice: n=12; control siRNA treated mice: n=11), were treated with C5 or control siRNA every two weeks for 20 weeks and were given water and normal chow *ad libitum*. They were tail-bled at the age of 12 weeks, 14 weeks, 24 weeks, and 32 weeks.

### 3.2.1 Liver-specific C5 siRNA reduces serum C5 protein level in 32 weeks old ApoE<sup>-/-</sup> mice on a normal diet

Complement protein C5 concentration in serum was quantified by ELISA. Complement

protein C5 levels were determined before treatment and 2 weeks, 12 weeks, and 20 weeks after treatment. Serum C5 levels decreased dramatically up to 93% after 2 weeks of treatment, and the low levels were maintained throughout the treatment period (Fig. 3.4). By contrast, the levels of serum C5 in control siRNA-treated mice remained unaffected (Fig. 3.4). These data demonstrated that liver-specific C5 siRNA effectively silences serum C5 protein, and indicated that circulating C5 protein was mainly derived from the liver (Fig. 3.4).

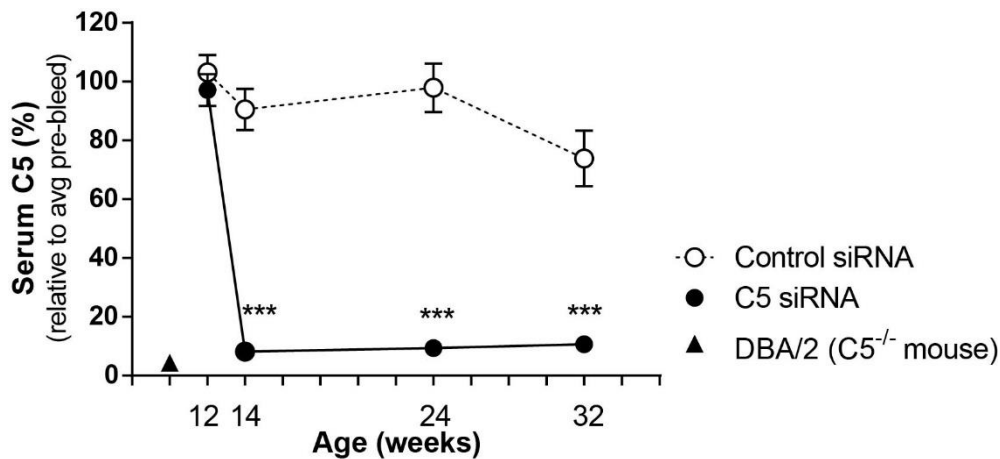


**Figure 3.4 Liver-specific C5 siRNA effectively silenced C5 in the circulation of young ApoE<sup>-/-</sup> mice on a normal mouse chow.** Blood was collected before injection, 2 weeks, 12 weeks, and 20 weeks after injection from the caudal vein. Complement C5 levels were measured by ELISA. Serum of C5-deficient mice (DBA/2) was used as a non-specific background negative control. The line graph shows group means  $\pm$  SEM; two-tailed Student's t-test; \*\*\*  $p < 0.005$  versus before injection; liver-specific C5 siRNA treated mice:  $n = 12$  mice; control siRNA treated mice:  $n = 11$  mice.

### 3.2.2 Liver-specific C5 siRNA does not change blood lipid levels, body weight, blood cell numbers, and leukocyte percentages in 32 weeks old ApoE<sup>-/-</sup> mice on a normal mouse chow

We next examined whether C5 siRNA impacts body weight, blood lipid levels, and blood cells.

#### 3.2.2.1 Lipid metabolism

Atherosclerosis is thought to involve passive lipid, specifically LDL, deposition in the

vessel wall. In order to study whether the C5 siRNA injection influences the blood lipid levels, plasma lipid levels were determined in the plasma of 32 weeks old ApoE<sup>-/-</sup> mice after 20 weeks C5 or control siRNA treatments. LDL, HDL, and total cholesterol levels and LDL, HDL, and total triglyceride levels between C5 siRNA-treated mice and control mice were not different (Fig. 3.5 A, B).

### **3.2.2.2 Body weight**

Mice were weighed before treatment and every 2 weeks after injection. Body weight of mice in both of the groups increased over time, but there was no statistically discernable alteration between the two different groups ( $p=0.6175$ ) (Fig. 3.5 C). This data indicated that C5 inhibition did not affect the body weight in young ApoE<sup>-/-</sup> mice.

### **3.2.2.3 Blood cell counts**

In order to study whether C5 siRNA affects other blood parameters, the blood of 32 weeks old ApoE<sup>-/-</sup> mice treated with siRNA for 20 weeks was analyzed with a complete blood cell counter. There are no differences in white blood cells (WBCs), red blood cells (RBC), platelets (PLT), lymphocytes (LYM), monocytes (MO), and granulocytes (GRA) between C5 siRNA and control groups (Fig. 3.5 D). Hence, C5 protein knock-down in the circulation did not alter the number of white blood cells. Other red blood cell parameters including total RBC, hemoglobin (HGB), hematocrit (HCT), mean corpuscular volume (MCV), mean corpuscular hemoglobin (MCH), mean corpuscular hemoglobin concentration (MCHC), and red blood cell distribution width (RDW), were not statistically significantly different between the C5 siRNA group and control siRNA group (Fig. 3.5 E).

Platelet parameters, including total platelet number (PLT) and mean platelet volume (MPV), were also not statistically different between C5 siRNA-treated and the control siRNA-treated groups (Fig. 3.5 E).

Liver-specific C5 inhibition did not affect the percentages of LYM, MO, and GRA within total white blood cells (Fig. 3.5 F).

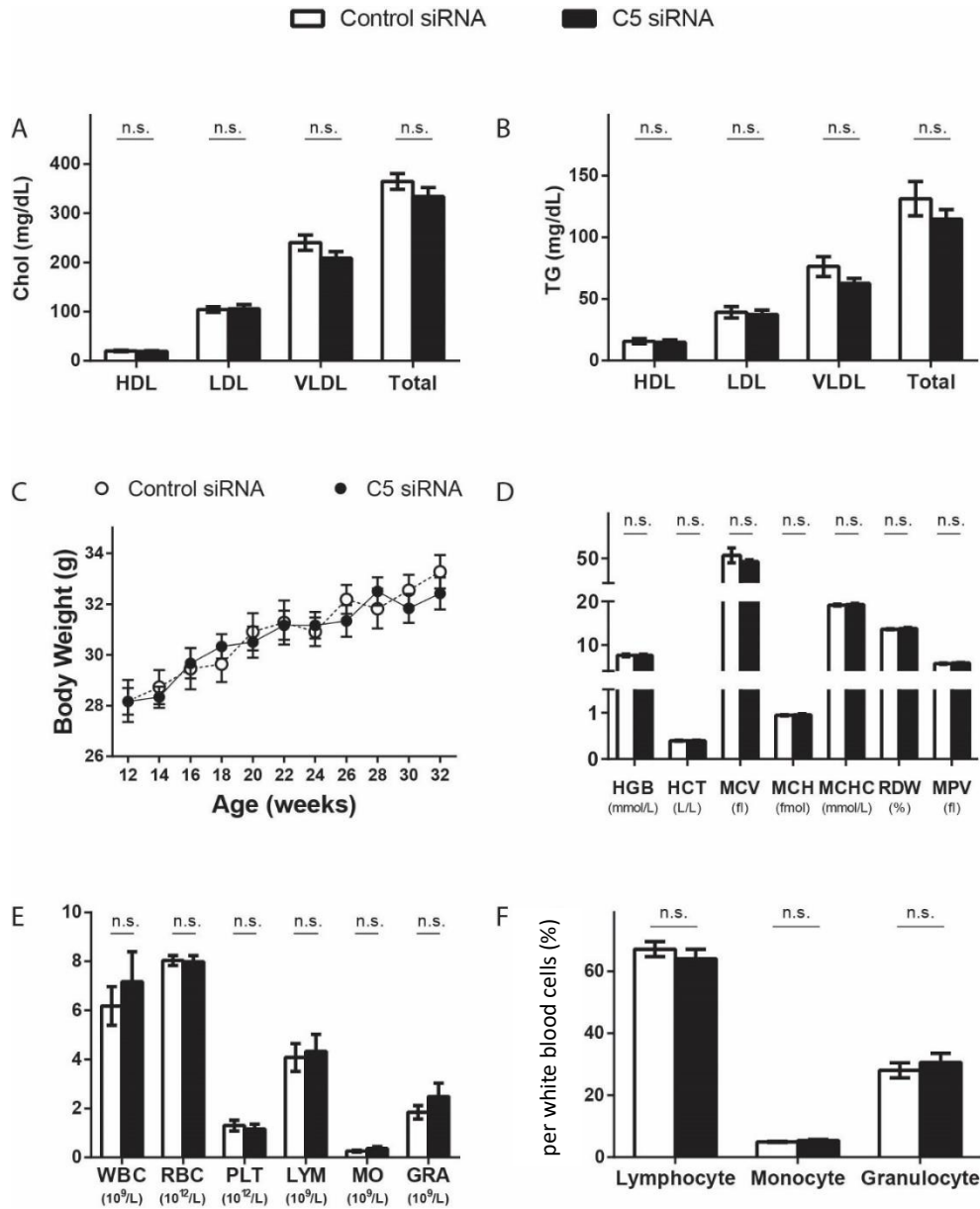


**Figure 3.5 Liver-specific C5 siRNA does not impact blood lipid, body weight, blood cell concentration and leukocyte percentages of 32 weeks old ApoE<sup>-/-</sup> mice. (A-B) Blood lipid.** Plasma was collected after 20 weeks of siRNA treatment. Chol and triglyceride TG levels were measured. I greatly acknowledge the help of Prof. Daniel Teupser and Dr. Wolfgang Wilfert (Institute of Laboratory Medicine, Clinical Chemistry and Molecular Diagnostics, Universitätsklinikum München). Chol: cholesterol; TG: triglyceride. HDL: high-density lipoprotein; LDL: low-density lipoprotein; VLDL: very low-density lipoprotein. **C. Body weight.** Body weight was determined before treatment and every 2 weeks thereafter. **(D-F) Blood cell concentration and leukocyte percentage.** Data represent means  $\pm$  SEM; two-tailed Student's t-test, n.s.: no significant difference; liver-specific C5 siRNA-treated mice:

n=12 mice; control siRNA-treated mice: n=11 mice. HGB: hemoglobin; HCT: hematocrit; MCV: mean corpuscular volume; MCH: mean corpuscular hemoglobin; MCHC: mean corpuscular hemoglobin concentration; RDW: red blood cell distribution width; MPV: mean platelet volume. WBCs: white blood cells; RBC: red blood cells; PLT: platelets; LYM: lymphocytes; MO: monocytes; and GRA: granulocytes.

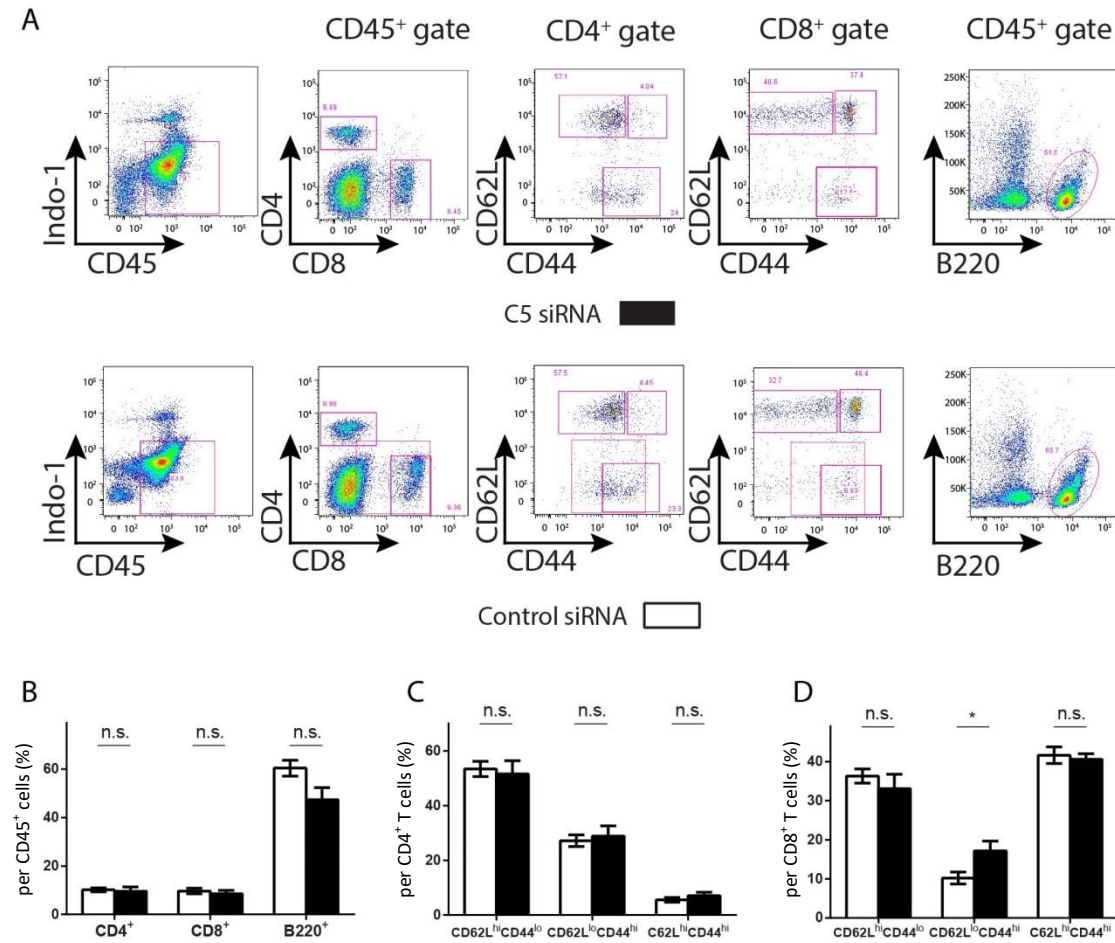


**Figure 3.6 Effects of liver-specific C5 siRNA on leukocyte subsets in the circulation of 32 weeks old ApoE<sup>-/-</sup> mice on normal mouse chow, part A. Flow cytometric analysis of leukocytes from 32 weeks old C5 siRNA and control siRNA treated ApoE<sup>-/-</sup> mice. A. Gating strategies: CD4<sup>+</sup> T cells (CD45<sup>+</sup>CD4<sup>+</sup> gate), CD8<sup>+</sup> T cells (CD45<sup>+</sup>CD8<sup>+</sup> gate), CD4<sup>+</sup> Th0 (CD45<sup>+</sup>CD4<sup>+</sup>CD62L<sup>hi</sup>CD44<sup>lo</sup> gate), CD4<sup>+</sup> TCM (CD45<sup>+</sup>CD4<sup>+</sup>CD62L<sup>hi</sup>CD44<sup>hi</sup> gate), CD4<sup>+</sup> TEM (CD45<sup>+</sup>CD4<sup>+</sup>CD62L<sup>lo</sup>CD44<sup>hi</sup> gate), CD8<sup>+</sup> Th0 (CD45<sup>+</sup>CD8<sup>+</sup>CD62L<sup>hi</sup>CD44<sup>lo</sup> gate), CD8<sup>+</sup> TCM (CD45<sup>+</sup>CD8<sup>+</sup>CD62L<sup>hi</sup>CD44<sup>hi</sup> gate), CD8<sup>+</sup> TEM (CD45<sup>+</sup>CD8<sup>+</sup>CD62L<sup>lo</sup>CD44<sup>hi</sup> gate), B cells (CD45<sup>+</sup>B220<sup>+</sup> gate). B. The frequencies of CD4<sup>+</sup> T cells, CD8<sup>+</sup> T cells, and B cells were compared in circulation in the normal diet fed 32 weeks old ApoE<sup>-/-</sup> mice treated with C5 siRNA and control siRNA. C. The frequencies of CD4<sup>+</sup> Th0, TEM and TCM were compared in circulation in the normal diet fed 32 weeks old ApoE<sup>-/-</sup> mice treated with C5 siRNA or**



control siRNA. **D.** The frequencies of CD8<sup>+</sup> Th0, TEM and TCM were compared in circulation in normal chow-fed 32 weeks old ApoE<sup>-/-</sup> mice treated with C5 siRNA or control siRNA. Data represent means  $\pm$  SEM; Student's-t test, n.s.: no significant difference, \* p<0.05; C5 treated mice: n=6 mice; control siRNA treated mice: n=6 mice.

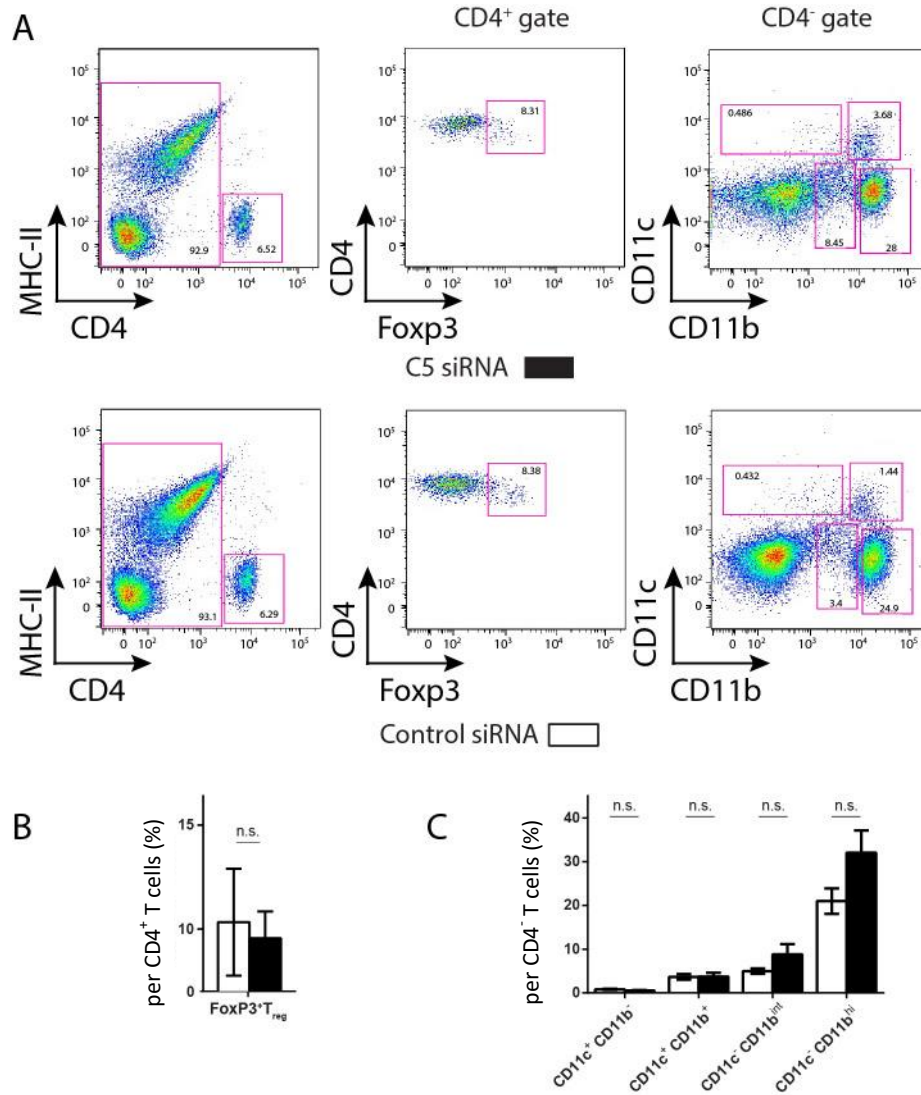


**Figure 3.7 Effects of liver-specific C5 siRNA on leukocyte subsets in the circulation of 32 weeks old ApoE<sup>-/-</sup> mice, part B. Flow cytometric analyses of leukocytes from 32 weeks old ApoE<sup>-/-</sup> mice treated with C5 siRNA or control siRNA. **A.** Gating strategies: T<sub>reg</sub> cells (CD45<sup>+</sup>CD4<sup>+</sup>Foxp3<sup>+</sup> gate), CD11c<sup>+</sup>CD11b<sup>-</sup> cells (CD45<sup>+</sup>CD4<sup>+</sup>CD11c<sup>+</sup>CD11b<sup>-</sup> gate), CD11c<sup>+</sup>CD11b<sup>+</sup> cells (CD45<sup>+</sup>CD4<sup>+</sup>CD11c<sup>+</sup>CD11b<sup>+</sup> gate), CD11c<sup>+</sup>CD11b<sup>int</sup> cells (CD45<sup>+</sup>CD4<sup>+</sup>CD11c<sup>+</sup>CD11b<sup>int</sup> gate), CD11c<sup>+</sup>CD11b<sup>hi</sup> (CD45<sup>+</sup>CD4<sup>+</sup>CD11c<sup>+</sup>CD11b<sup>hi</sup> gate). **B.** The frequencies of T<sub>reg</sub> cells were compared in the circulation of 32 weeks old ApoE<sup>-/-</sup> mice treated with C5 siRNA or control siRNA. **C.** The frequencies of**



CD11c<sup>+</sup>CD11b<sup>-</sup> cells, CD11c<sup>+</sup>CD11b<sup>+</sup> cells, CD11c<sup>-</sup>CD11b<sup>int</sup> cells, and CD11c<sup>-</sup>CD11b<sup>hi</sup> cells were compared within circulation in 32 weeks old ApoE<sup>-/-</sup> mice treated with liver-specific C5 siRNA or control siRNA. Data represent means  $\pm$  SEM; Student's t-test, n.s.: no significant difference; Liver-specific C5 siRNA treated mice: n=6 mice; control siRNA treated mice: n=6 mice.

### **3.2.3 Liver-specific C5 inhibition does not change blood leukocyte subsets in young ApoE<sup>-/-</sup> mice on normal mouse chow**

In order to examine whether liver-specific C5 siRNA influences circulating leukocyte subsets, blood leukocytes were examined using quantitative FACS analyses.

20 weeks of liver-specific C5 siRNA treatment does not change the percentage of CD4<sup>+</sup> T cell and CD8<sup>+</sup> T cell subpopulations (Fig. 3.6 B), and B220<sup>+</sup> B cells (Fig. 3.6 B).

We next examined T cell activation and differentiation markers. Conventional murine T cells can be divided into three major populations, CD62L<sup>+</sup>CD44<sup>-</sup> Th0, CD62L<sup>+</sup>CD44<sup>+</sup> TCM, and CD62L<sup>-</sup>CD44<sup>+</sup> TEM. In CD4<sup>+</sup> T cells, Th0 cells comprised the majority, whereas TEM cells were minor populations. C5 siRNA treatment does not change the percentages of either subset (Fig. 3.6 C). In CD8<sup>+</sup> T cells, Th0 cells were the major subset. Otherwise, the ratio of TCM cells was low. The proportion of TEM cells in CD8<sup>+</sup> T cells was slightly higher in the C5 inhibition group compared to the control group (Fig. 3.6 D). Forkhead box P3<sup>+</sup> (Foxp3<sup>+</sup>) T<sub>reg</sub> cells ratio among CD4<sup>+</sup> T cells did not differ between C5 siRNA-treated mice and control mice (Fig. 3.7 B). The frequencies of CD11c<sup>+</sup>CD11b<sup>-</sup> cells, CD11c<sup>+</sup>CD11b<sup>+</sup> cells, CD11c<sup>-</sup>CD11b<sup>int</sup> cells, and CD11c<sup>-</sup>CD11b<sup>hi</sup> cells were compared within the circulation in 32 weeks old ApoE<sup>-/-</sup> mice treated with C5 siRNA and control siRNA, and there was no significant difference between these two groups (Fig. 3.7 C).

### **3.2.4 Liver-specific C5 siRNA reduces atherosclerotic plaque burden in young ApoE<sup>-/-</sup> mice on a normal mouse chow**

In order to evaluate the effect of liver-specific C5-mediated complement cascade activation in plaque burden, *en-face* analysis of the whole aorta was examined<sup>101</sup>. Sudan IV was used to label lipids in red, and the main arterial trunk was stained (Fig. 3.8 A).

Liver-specific C5 siRNA-treated mice revealed markedly reduced atherosclerosis plaque burden as evidenced by decreased *en-face* staining. The 32 weeks old control siRNA mice developed  $2.876 \pm 0.735\%$  Sudan IV-positive plaque in the total aortas,  $4.184 \pm 1.148\%$  in the thoracic aortas and  $0.688 \pm 0.120\%$  in the abdominal aortas. The age-matched C5 siRNA treated ApoE<sup>-/-</sup> mice developed  $0.9997 \pm 0.164\%$  plaque in the total aortas,  $1.367 \pm 0.246\%$  in the thoracic aortas, and  $0.3571 \pm 0.097\%$  in the abdominal aortas. C5 siRNA-treated mice showed significantly reduced total lesion sizes of the whole aortas (65.24% reduction;  $P=0.030$ ). The mean lipid-positive area in the thoracic aorta was also significantly less (69.21% reduction,  $P=0.035$ ) in C5 siRNA-treated mice compared with controls, and 48.10% reduction in abdominal aorta lesion sizes in C5 siRNA-treated mice vs. control siRNA-treated mice ( $P=0.045$ ).

Hence, by 32-weeks of age, the administration of C5 siRNA resulted in a dramatic decrease in plaque formation in ApoE<sup>-/-</sup> mice.

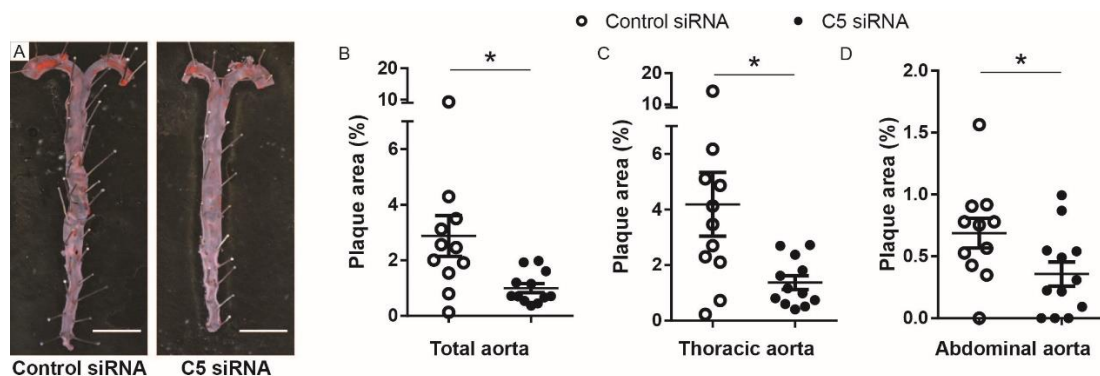


**Figure 3.8 Liver-specific C5 mediate reduced atherosclerotic lesions in the aortas of 32 weeks old normal diet fed ApoE<sup>-/-</sup> mice.** **A. *en-face* Sudan IV staining.** The total aortas were pinned and stained with Sudan IV. Representative aorta from mice treated with control siRNA or liver-specific C5 siRNA. Scale bar: 500 μm. **B.** The percent Sudan IV staining of the total aortic surface. **C.** The percent Sudan IV staining of the thoracic aorta. **D.** The percent Sudan IV staining of the abdominal aorta. Data represent means ± SEM; Student's t-test, n.s.: no significant difference, \*  $p<0.05$ ; liver-specific C5 siRNA-treated mice:  $n=12$ ; control siRNA-treated mice:  $n=11$ .

In order to analyze whether C5 siRNA impact on plaque composition, fresh frozen aortic root sections were prepared for further studies. Lipid content in the plaques was

determined by ORO/HE staining of the fresh-frozen cross-sections. Lesions at the aortic root were quantified at 6-8 sections, which were located 300, 400, 500, 600, and 700  $\mu\text{m}$  proximal from its bottom side. As shown in Fig. 3.9 A, the lesion area was dramatically reduced ( $p$  value=0.0092) in C5 siRNA treated ApoE<sup>-/-</sup> mice when compared to the controls (Fig. 3.9 B).

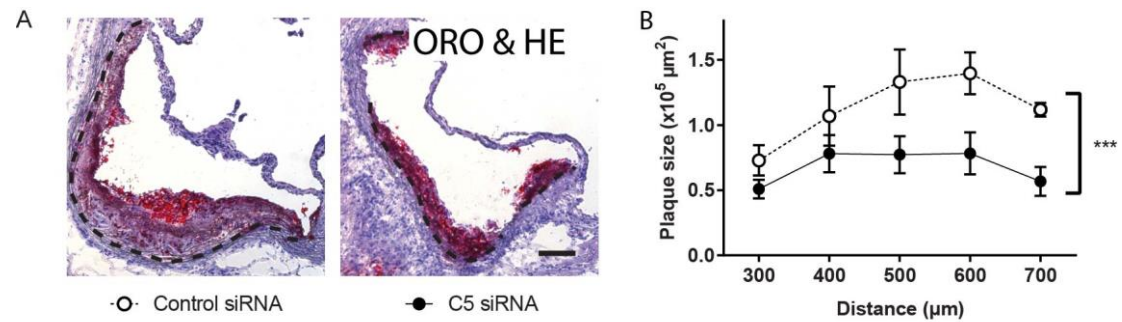


**Figure 3.9 Liver-specific C5 treatment led to a marked reduction of atherosclerotic lesions in aortic roots of 32 weeks old normal diet fed ApoE<sup>-/-</sup> mice.** *A.* Aortic root plaques from normal chow-fed 32 weeks old C5 siRNA and control siRNA-treated ApoE<sup>-/-</sup> mice. 10  $\mu\text{m}$  fresh frozen sections of the aortic root were stained with ORO/HE staining. Scale bar: 100  $\mu\text{m}$ . *B.* Mean plaque sizes of the individual cross-sections of the aortic root. Data are represented as the mean  $\pm$  SEM, two-way ANOVA, \* \* \*  $p < 0.005$ ; liver-specific C5 siRNA-treated mice:  $n=4$ ; control siRNA-treated mice:  $n=4$ .

### 3.2.5 Liver-specific C5 siRNA inhibits macrophage/dendritic and T cell infiltration in atherosclerosis in young ApoE<sup>-/-</sup> mice on a normal chow

Foamy macrophages accumulate in the plaque and are the pathological hallmark of atherosclerosis<sup>15</sup>. CD68 is highly expressed on macrophages, as well as DCs in the plaque. Aortic root sections were stained for CD68 antibody using immunofluorescence staining (Fig. 3.10 A).

The CD68<sup>+</sup> area in atherosclerotic plaques was higher in control siRNA-treated mice compared to C5 siRNA-treated mice (Fig. 3.10 B). Our data indicated that liver-specific C5 inhibition inhibits CD68<sup>+</sup> macrophage/DC infiltration in atherosclerotic plaque of 32 weeks ApoE<sup>-/-</sup> mice fed with a normal diet.

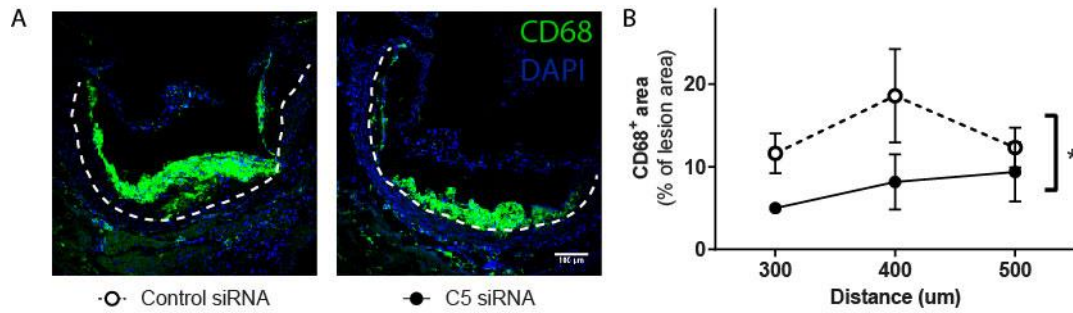


**Figure 3.10 Liver-specific C5 reduced CD68<sup>+</sup> macrophage/DC infiltration in atherosclerotic plaques of 32 weeks old ApoE<sup>-/-</sup> mice on a normal diet.** **A.** Aortic root plaques from 32 weeks old liver-specific C5 siRNA or control siRNA treated ApoE<sup>-/-</sup> mice. 10 μm fresh-frozen sections of the aortic root were stained for CD68<sup>+</sup> macrophages/DCs. Scale bars: 100 μm. **B.** Quantification of CD68<sup>+</sup> area in aortic root plaque. Data are representative for the means ± SEM, Two-way ANOVA, \*: p < 0.05; Liver-specific C5 siRNA-treated mice: n=4; control siRNA-treated mice: n=4.

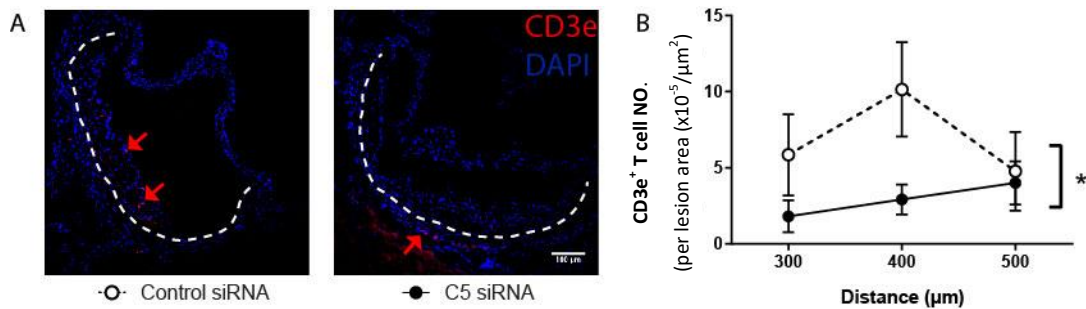


**Figure 3.11 Liver-specific C5 reduced CD3e<sup>+</sup> T cell numbers in atherosclerotic plaques of normal mouse chow-fed 32 weeks old ApoE<sup>-/-</sup> mice.** **A.** Aortic root plaques from normal chow-fed 32 weeks old liver-specific C5 siRNA- and control siRNA-treated ApoE<sup>-/-</sup> mice. 10 μm fresh-frozen sections of the aortic root were examined by CD3e<sup>+</sup> T cell immunofluorescence staining. The red arrows in the images show the CD3e<sup>+</sup> T cells. Scale bars: 100 μm. **B.** Quantification of CD3e<sup>+</sup> numbers in aortic root plaque. Data are representative for the means ± SEM, Two-way ANOVA, \*: p < 0.05; Liver-specific C5 siRNA-treated mice: n=4; control siRNA-treated mice: n=4.

The role of T cells in the development and progression of atherosclerosis has been intensively studied for many years. We next examined whether liver-specific C5 siRNA impact T cell infiltration in atherosclerosis. The accumulation of T cells in aortic root lesions was counted by combined CD3e immunostaining (Fig. 3.11 A). The lesional CD3e<sup>+</sup> T cells content in liver-specific C5 siRNA-treated mice was less than the control

group (Fig. 3.11 B), indicating that liver-specific C5 siRNA reduced CD3e<sup>+</sup> T cell infiltration in 32 weeks old ApoE<sup>-/-</sup> mice on a normal diet.

### 3.2.6 Effect of C5 siRNA on complement protein activation and deposition in normal chow-fed 32 weeks old ApoE<sup>-/-</sup> mice

We hypothesized that attenuation of plaque progression observed in liver-specific C5 treated ApoE<sup>-/-</sup> mice was due to the absence of complement proteins, including C3, C4, and C5 activation within the plaque. To test this hypothesis, we next stained complement proteins in atherosclerotic plaques. 10 µm fresh-frozen sections of the aortic roots from the liver-specific C5 siRNA and control groups were stained with immunofluorescence. Complement was assessed by staining for C3, C4 (Fig. 3.13), and C5 (Fig. 3.12) deposition.

C3 and C4 deposition were detected strongly in plaques from both mice groups (Fig. 3.13). C5 deposition was detected weakly in the aortic root plaques of C5-treated mice, though strongly in plaques from the control mice (Fig. 3.12). These results indicated that complement cascades are activated during the initiation of atherosclerosis; C5 inhibition did not affect the C3, C4 deposition; however, C5 inhibition influenced the C5 deposition in the plaque in the initiation period of atherosclerosis.

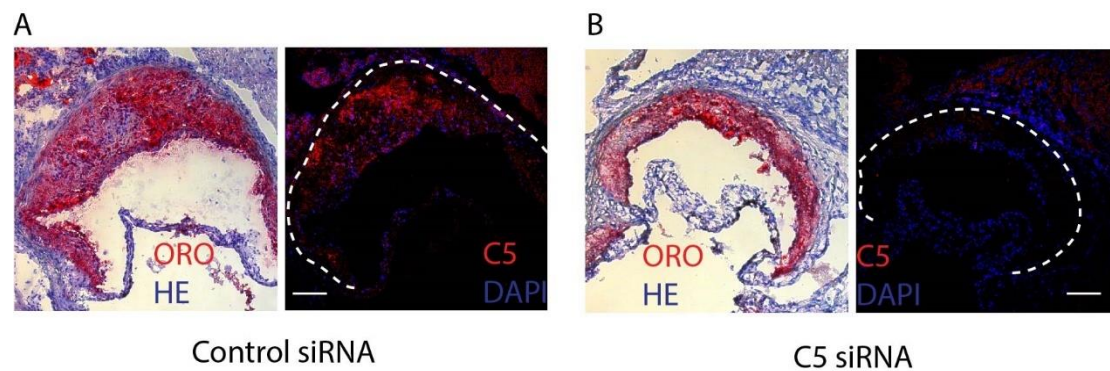


**Figure 3.12 Liver-specific C5 reduced C5 deposition in atherosclerotic plaque of normal diet fed 32 weeks old ApoE<sup>-/-</sup> mice. (A-B)** Aortic root plaque from normal chow-fed 32 weeks old C5 siRNA- or control siRNA-treated ApoE<sup>-/-</sup> mice. 10 µm fresh frozen sections of aortic roots were examined by C5 antibody immunofluorescence staining (right). Left pictures show the ORO/HE-stained sections next to the sections stained with C5-antibody. Scale bars: 100 µm.



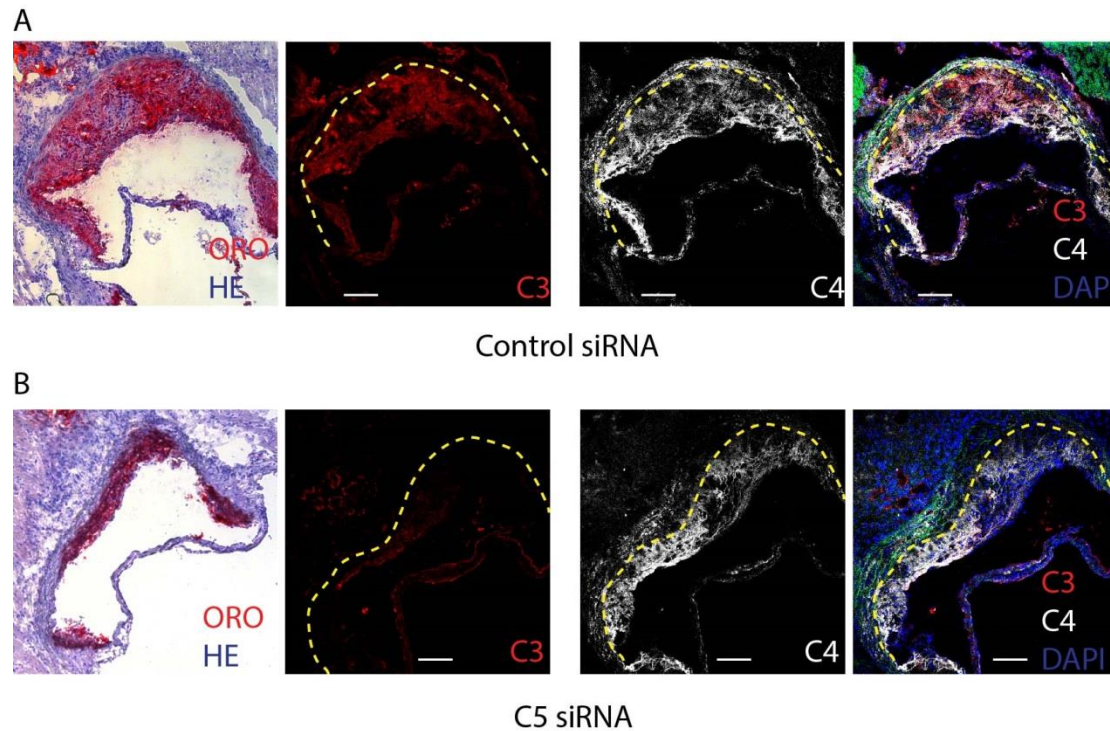


**Figure 3.13 C3 and C4 deposition in atherosclerotic plaques of normal chow-fed 32 weeks old *ApoE*<sup>-/-</sup> mice. (A-B)** Aortic root plaque from normal chow-fed 32 weeks old C5 siRNA- and control siRNA-treated *ApoE*<sup>-/-</sup> mice. 10  $\mu$ m fresh-frozen sections of the aortic root were examined by C3 and C4 antibody immunofluorescence staining. Left pictures show the ORO/HE-stained sections next to the sections stained with C3 and C4 antibody. Scale bars: 100  $\mu$ m. The green area in the pictures shows the autofluorescence.

### 3.3 The role of liver-specific complement C5 in atherosclerosis in aged *ApoE*<sup>-/-</sup> mice maintained on a normal mouse chow

Our data indicated that complement activation plays an important role in the formation of atherosclerotic plaques because, in the absence of complement C5 mice, the rate of progression of atherosclerosis was greatly decreased in young *ApoE*<sup>-/-</sup> mice. To further explore whether complement activation plays a role in atherosclerotic plaque development, complement activation inhibition was studied in aged *ApoE*<sup>-/-</sup> mice, which harbor advanced atherosclerotic plaques after maintaining them on a normal mouse chow. 58 weeks old *ApoE*<sup>-/-</sup> mice were treated with C5 siRNA every two weeks for 18 weeks. They were fed with a normal mouse chow throughout their lives (Fig.

3.14).

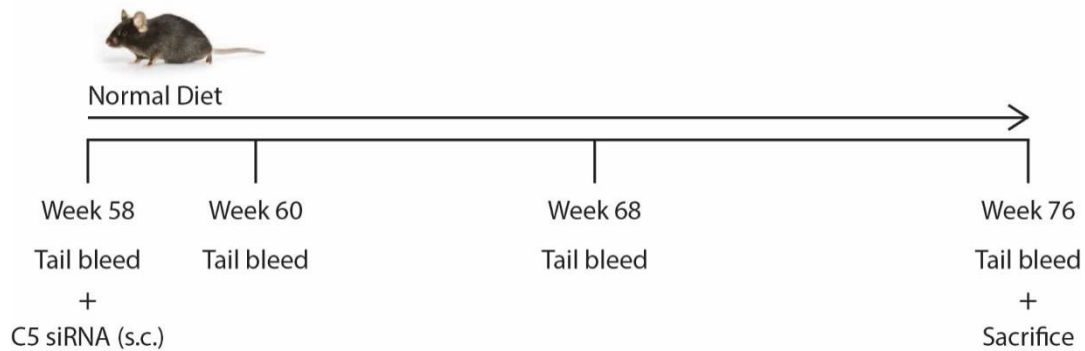


**Figure 3.14 Experimental design.** 58 weeks old male ApoE<sup>-/-</sup> mice (C5 siRNA treated mice: n=9; control siRNA-treated mice: n=9), were treated with C5 or control siRNA every two weeks for 18 weeks and were given water and normal chow *ad libitum*. They were tail-bled at the age of 58 weeks, 60 weeks, 70 weeks, and 76 weeks.

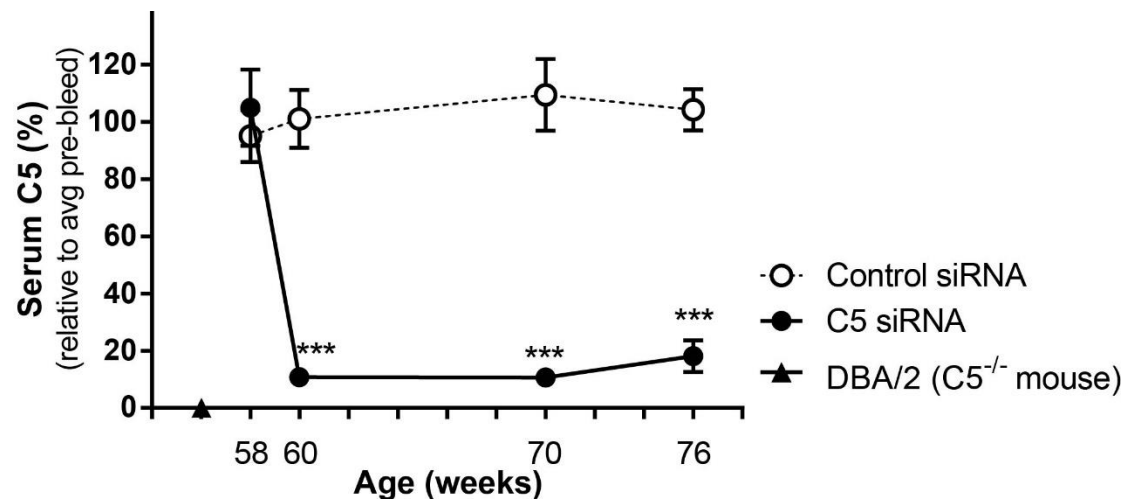


**Figure 3.15 C5 siRNA effectively silenced C5 in the circulation of aged ApoE<sup>-/-</sup> mice on a normal chow for 4 months.** Blood was collected before injection and 2, 12 and 18 weeks thereafter. Complement C5 levels were measured by ELISA. Serum of C5-deficient mice (DBA/2) was used as a negative background control. The line graph shows group means  $\pm$  SEM, two-tailed Student's t-test, \*\*\* P<0.005 versus before injection; liver-specific C5 siRNA-treated mice: n=9; control siRNA-treated mice: n=9.

### 3.3.1 Liver-specific C5 siRNA reduced serum C5 protein level in aged ApoE<sup>-/-</sup> mice on a normal chow

The serum of C5 siRNA and control groups were collected before siRNA application

and 2, 10, and 18 weeks thereafter. In order to determine the effect of C5 siRNA knockdown on aged ApoE<sup>-/-</sup> mice, C5 levels in serum were quantified by ELISA. 2 weeks after siRNA application, serum C5 levels decreased more than 99% in the C5 siRNA group, but no change was observed in the control group (Fig. 3.15). C5 levels in serum were maintained steadily throughout the experiment indicating that C5 siRNA silenced C5 level effectively in the circulation of aged ApoE<sup>-/-</sup> mice for extended periods of time.

### **3.3.2 Liver-specific C5 siRNA does not change body weight and blood lipid level in aged ApoE<sup>-/-</sup> mice**

#### **3.3.2.1 Lipid metabolism**

In order to study whether the C5 inhibition affects blood cholesterol and triglyceride levels, plasma lipid levels were studied in 76 weeks old C5 siRNA mice and control mice after 18 weeks of siRNA application. The cholesterol plasma levels, including HDL, LDL, and VLDL, and the total cholesterol levels were similar in these two groups. Further, plasma levels of triglycerides were unchanged by siRNA C5 treatment (Fig. 3.16 A, B) indicating that C5 knockdown did not influence plasma cholesterol and triglyceride levels in aged ApoE<sup>-/-</sup> mice on normal chow.

#### **3.3.2.2 Body weight**

Body weights of mice were measured before and every 2 weeks after treatment. Compared to the body weight before injection, the body weight of both siRNA C5 and control mice was unchanged (Fig. 3.16 C). This data indicated that C5 inhibition did not affect the body weight in aged ApoE<sup>-/-</sup> mice.

#### **3.3.2.3 Blood cell counts**

In order to evaluate the overall health and a wide range of disorders following liver-



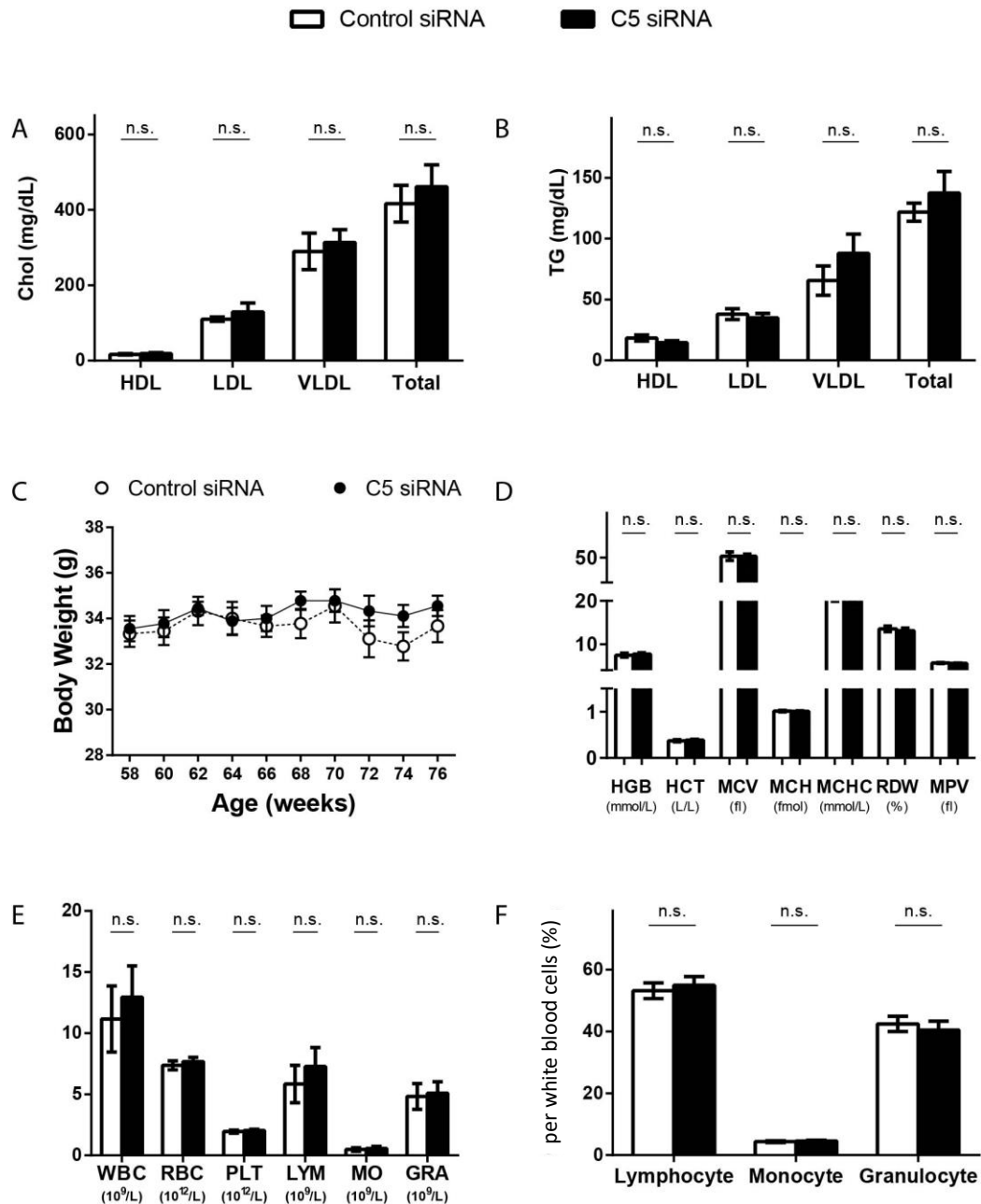


**Figure 3.16 C5 siRNA does not impact blood lipid level, body weight, blood cell count, and leukocyte percentages of 76 weeks old ApoE<sup>-/-</sup> mice on normal chow. (A-B) Blood lipid level.** Plasma was collected after 18 weeks of siRNA treatment. Chol and TG levels were determined by Prof. Daniel Teupser and Dr. Wolfgang Wilfert. Chol: cholesterol; TG: triglyceride. HDL: high-density lipoprotein; LDL: low-density lipoprotein; VLDL: very low-density lipoprotein. **C. Body weight.** Body weight was determined before treatment and every 2 weeks after treatment. **(D-F) Blood cell concentration and leukocyte percentages.** Data represent means  $\pm$  SEM; Two-tailed Student's t-test, n.s.: no significant difference; liver-specific C5 siRNA treated mice: n=9; control siRNA treated mice: n=9. HGB: hemoglobin; HCT: hematocrit; MCV: mean corpuscular volume; MCH: mean corpuscular hemoglobin;

MCHC: mean corpuscular hemoglobin concentration; RDW: red blood cell distribution width; MPV: mean platelet volume. WBCs: white blood cells; RBC: red blood cells; PLT: platelets; LYM: lymphocytes; MO: monocytes; and GRA: granulocytes.

specific C5 siRNA treatment in aged ApoE<sup>-/-</sup> mice, the blood of 76 weeks old ApoE<sup>-/-</sup> mice treated with siRNA for 18 weeks was analyzed with a complete blood cell counter. WBC count, including LYM, MO, and the GRA were not affected by C5 inhibition (Fig. 3.16 E, F). Red blood cell count and other parameters, including HGB, HCT, MCV, MCH, MCHC, and RDW, were not significantly different between the two mouse groups (Fig. 3.16 D). PLA counts and means of MPV were also not changed (Fig. 3.16 D).

Hence, liver-specific C5 inhibition did not alter major blood parameters of the aged ApoE<sup>-/-</sup> mice on a chow diet.

### **3.3.3 C5 inhibition does not change blood leukocytes subsets in aged ApoE<sup>-/-</sup> mice on normal chow**

To study the impacts of C5 siRNA treatment on leukocyte subsets in independent assays, isolated blood cells from aged ApoE<sup>-/-</sup> mice fed with normal chow diet, which were treated with C5 siRNA or control siRNA for 18 weeks, were analyzed by flow cytometry.

A considerable percentage of blood CD45<sup>+</sup> leukocytes were B220<sup>+</sup> B cells (Fig. 3.17 B). Percentages of B220<sup>+</sup> B cells and T cell receptor  $\beta$  (TCRb<sup>+</sup>) T cells in blood CD45<sup>+</sup> leukocytes were not different between C5 siRNA-treated and control groups (Fig. 3.17 B). Subtypes of CD4<sup>+</sup> T cells and CD8<sup>+</sup> T cells in total TCRb<sup>+</sup> T cells were also similar in the two groups (Fig. 3.17 C). In CD4<sup>+</sup> T cells, CD62L<sup>lo</sup>CD44<sup>hi</sup> TEM T cells comprised the majority, whereas CD62L<sup>hi</sup>CD44<sup>hi</sup> TCM cells were a minor fraction.

However, Th0 cells in CD4<sup>+</sup> T cells were lower in the C5 inhibition group compared to the control group (Fig. 3.17 D). In CD8<sup>+</sup> T cells, the percentages of each subset were unchanged by C5 inhibition (Fig. 3.17 E). Also, Foxp3<sup>+</sup> T<sub>reg</sub> cells ratio per CD4<sup>+</sup> T cells did not differ between C5-treated and control mice (Fig. 3.18 B). Percentages of

CD11b<sup>+</sup>CD11c<sup>+</sup>, CD11b<sup>+</sup>CD11c<sup>-</sup>, CD11b<sup>-</sup>CD11c<sup>hi</sup>, CD11b<sup>-</sup>CD11c<sup>int</sup> cells in CD4<sup>-</sup> cells were not affected by C5 inhibition (Fig. 3.18 C). The Th0 T cell result requires confirmation and possibly further studies.

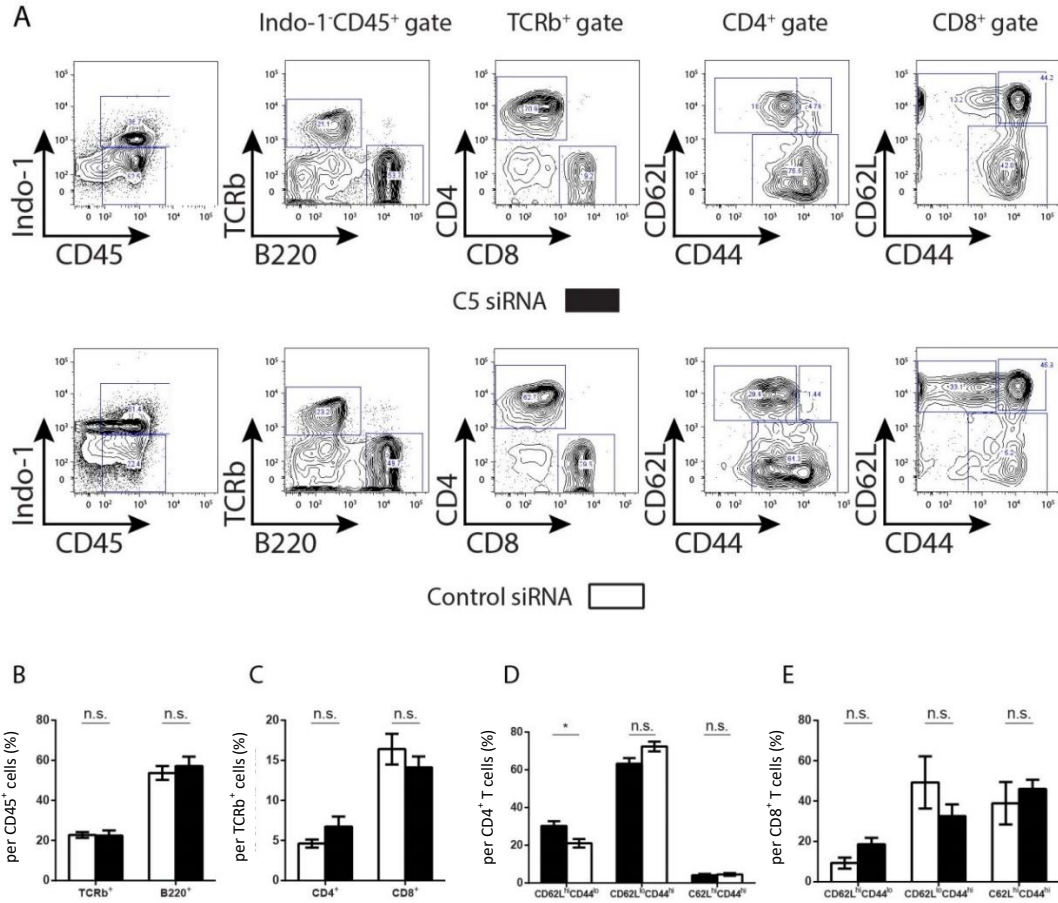


**Figure 3.17 Effects of C5 siRNA on leukocyte subsets in the circulation of 76 weeks old ApoE<sup>-/-</sup> mice on normal chow, part A. FACS analyses of leukocytes from 76 weeks old C5 siRNA- and control siRNA-treated ApoE<sup>-/-</sup> mice. A. Gating strategies: T cells (CD45<sup>+</sup>TCRb<sup>+</sup> gate), B cells (CD45<sup>+</sup>B220<sup>+</sup> gate), CD4<sup>+</sup> T cells (CD45<sup>+</sup>TCRb<sup>+</sup>CD4<sup>+</sup> gate), CD8<sup>+</sup> T cells (CD45<sup>+</sup>TCRb<sup>+</sup>CD8<sup>+</sup> gate), CD4<sup>+</sup> Th0 (CD45<sup>+</sup>CD4<sup>+</sup>CD62L<sup>hi</sup>CD44<sup>lo</sup> gate), CD4<sup>+</sup> TCM (CD45<sup>+</sup>CD4<sup>+</sup>CD62L<sup>hi</sup>CD44<sup>hi</sup> gate), CD4<sup>+</sup> TEM (CD45<sup>+</sup>CD4<sup>+</sup>CD62L<sup>lo</sup>CD44<sup>hi</sup> gate), CD8<sup>+</sup> Th0 (CD45<sup>+</sup>CD8<sup>+</sup>CD62L<sup>hi</sup>CD44<sup>lo</sup> gate), CD8<sup>+</sup> TCM (CD45<sup>+</sup>CD8<sup>+</sup>CD62L<sup>hi</sup>CD44<sup>hi</sup> gate), CD8<sup>+</sup> TEM (CD45<sup>+</sup>CD8<sup>+</sup>CD62L<sup>lo</sup>CD44<sup>hi</sup> gate). B. The frequencies of circulating T cells and B cells were compared in 76 weeks old ApoE<sup>-/-</sup> mice treated with C5 siRNA and control siRNA. C. The frequencies of circulating CD4<sup>+</sup> T cells and CD8<sup>+</sup> T cells were compared in 76 weeks old ApoE<sup>-/-</sup> mice treated with C5 siRNA or control siRNA. D. The frequencies of circulating CD4<sup>+</sup> Th0, TEM, and TCM were compared in 76 weeks old ApoE<sup>-/-</sup> mice treated with C5 siRNA or control**

siRNA. **E.** The frequencies of circulating CD8<sup>+</sup> Th0, TEM and TCM cells were compared in 76 weeks old ApoE<sup>-/-</sup> mice treated with C5 siRNA or control siRNA. Data represent means  $\pm$  SEM; Student's t-test, n.s.: no significant difference, \* p<0.05; C5 treated mice: n=6; control siRNA-treated mice: n=4.

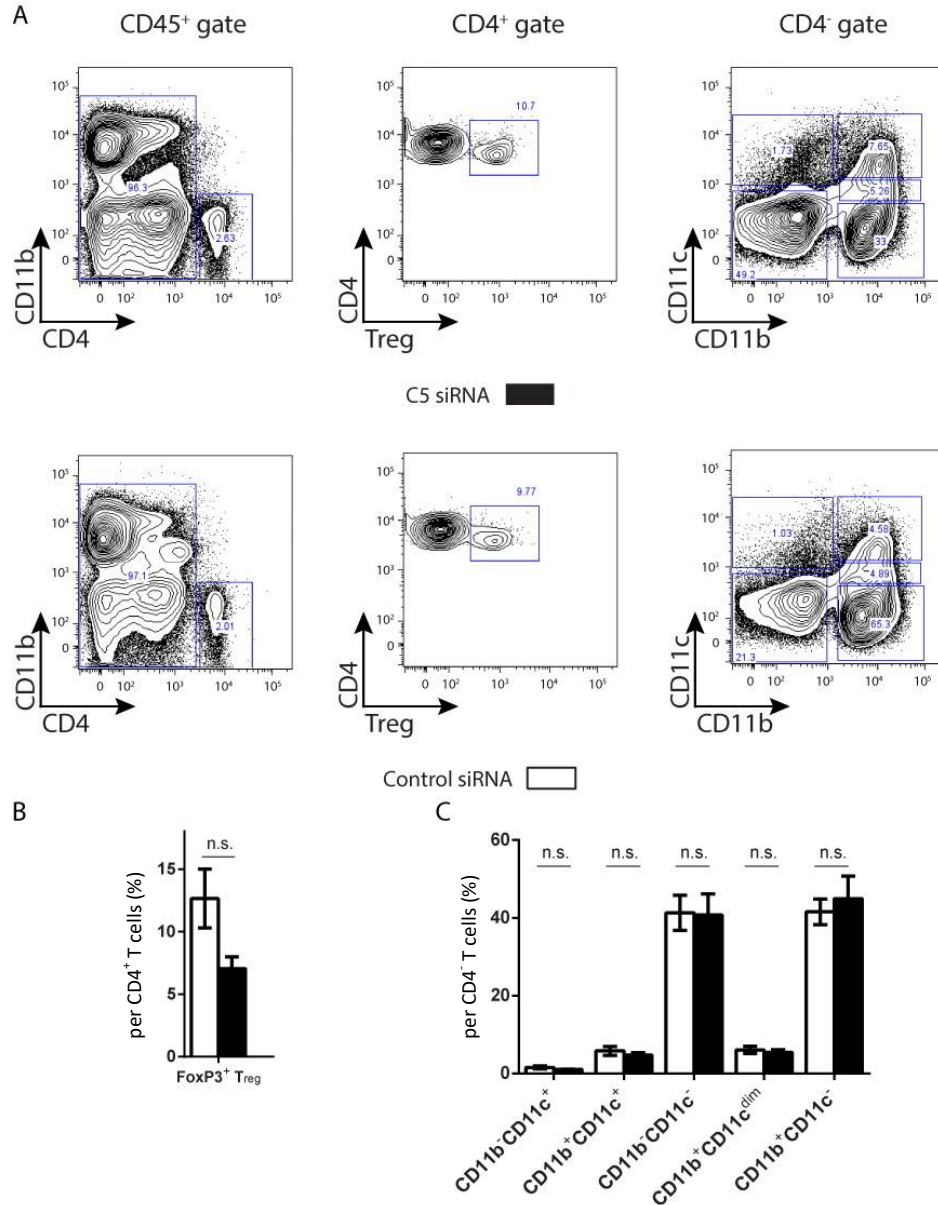


**Figure 3.18 Effects of C5 siRNA on leukocyte subsets in the circulation of 76 weeks old ApoE<sup>-/-</sup> mice, part B. FACS analyses of leukocytes from 76 weeks old ApoE<sup>-/-</sup> mice treated with C5 siRNA or control siRNA. A.** Gating strategies: T<sub>reg</sub> cells (CD45<sup>+</sup>CD4<sup>+</sup>Foxp3<sup>+</sup> gate), CD11b<sup>-</sup>CD11c<sup>+</sup> cells (CD45<sup>+</sup>CD4<sup>-</sup>CD11b<sup>-</sup>CD11c<sup>+</sup> gate), CD11b<sup>+</sup>CD11c<sup>+</sup> cells (CD45<sup>+</sup>CD4<sup>-</sup>CD11b<sup>+</sup>CD11c<sup>+</sup> gate), CD11b<sup>-</sup>CD11c<sup>-</sup> cells (CD45<sup>+</sup>CD4<sup>-</sup>CD11b<sup>-</sup>CD11c<sup>-</sup> gate), CD11b<sup>+</sup>CD11c<sup>dim</sup> cells (CD45<sup>+</sup>CD4<sup>-</sup>CD11b<sup>+</sup>CD11c<sup>dim</sup> gate), CD11b<sup>+</sup>CD11c<sup>-</sup> cells (CD45<sup>+</sup>CD4<sup>-</sup>CD11b<sup>+</sup>CD11c<sup>-</sup> gate). **B.** The frequencies of T<sub>reg</sub> cells were

compared within circulation in 76 weeks old ApoE<sup>-/-</sup> mice treated with the liver-specific C5 siRNA and control siRNA. **C.** The frequencies of CD11b<sup>-</sup>CD11c<sup>+</sup> cells, CD11b<sup>+</sup>CD11c<sup>+</sup> cells, CD11b<sup>-</sup>CD11c<sup>-</sup> cells, CD11b<sup>+</sup>CD11c<sup>dim</sup>, and CD11b<sup>+</sup>CD11c<sup>-</sup> cells were compared within circulation in 76 weeks old ApoE<sup>-/-</sup> mice treated with the liver-specific C5 siRNA and control siRNA. Data represent means  $\pm$  SEM; Student's-t test, n.s.: no significant difference; liver-specific C5 siRNA-treated mice: n=6; control siRNA-treated mice: n=4.

### 3.3.4 Liver-specific C5 siRNA did not affect atherosclerosis plaque burden in aged ApoE<sup>-/-</sup> mice on a normal chow

Aortas were harvested after 18 weeks of siRNA application, then examined after *en-face* staining and quantified (Fig. 3.19 A). Compared to the control group, 18 weeks C5 siRNA silencing did not affect plaque sizes in the total aortas or in each thoracic and abdominal segment separately (Fig. 3.19 B-D).

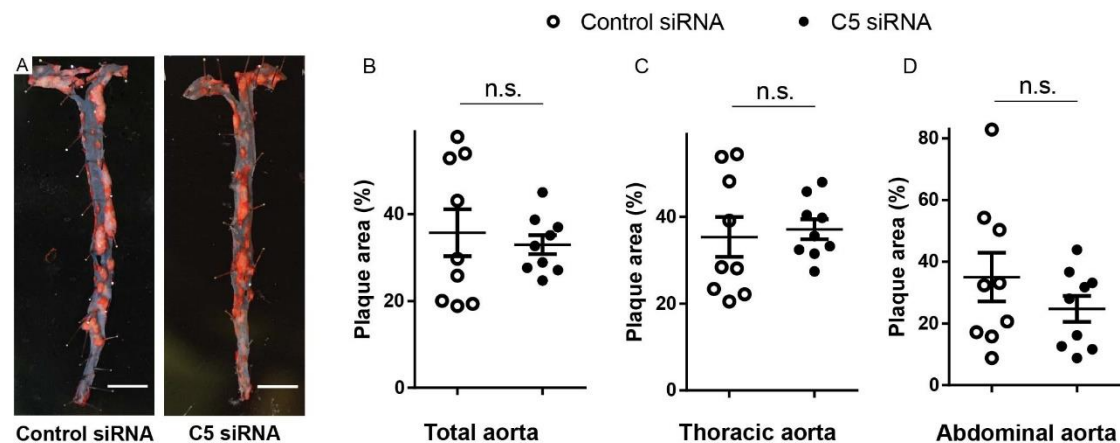


**Figure 3.19 C5 did not affect atherosclerotic lesion sizes in aortas of 76 weeks old normal chow-fed ApoE<sup>-/-</sup> mice.** **A.** *en-face* Sudan IV staining. Total aortas were pinned and stained with Sudan IV. Representative aortas from mice treated with control siRNA or C5 siRNA; Scale bar: 500  $\mu$ m. **B.** The percent Sudan IV staining of the total aortic surface. **C.** The percent Sudan IV staining of the thoracic aorta. **D.** The percent Sudan IV staining of the abdominal aorta. Data represent means  $\pm$  SEM; Student's t-test, n.s.: no significant difference; liver-specific C5 siRNA treated mice: n=9; control siRNA treated mice: n=9.

To examine whether C5 siRNA impacts plaque sizes, freshly prepared cross-sectional aortic root sections were stained with ORO/HE staining and quantified (Fig. 3.20 A).

There was no significant difference between the siRNA C5 group and the control group (Fig. 3.20 B) indicating that C5 inhibition did not influence atherosclerotic plaque sizes in aged ApoE<sup>-/-</sup> mice when compared to controls. In order to confirm these results in the small cohort of mice, future studies will have to analyze a higher number of mice. Moreover, the effects of the liver-specific C5 inhibition on stabilization of atherosclerotic plaque in normal chow-fed aged mice have not yet been examined. The major structural determinants of vulnerability, including the content of collagen, the size of the necrotic core, and the thickness of the fibrous cap, should be examined in the future.

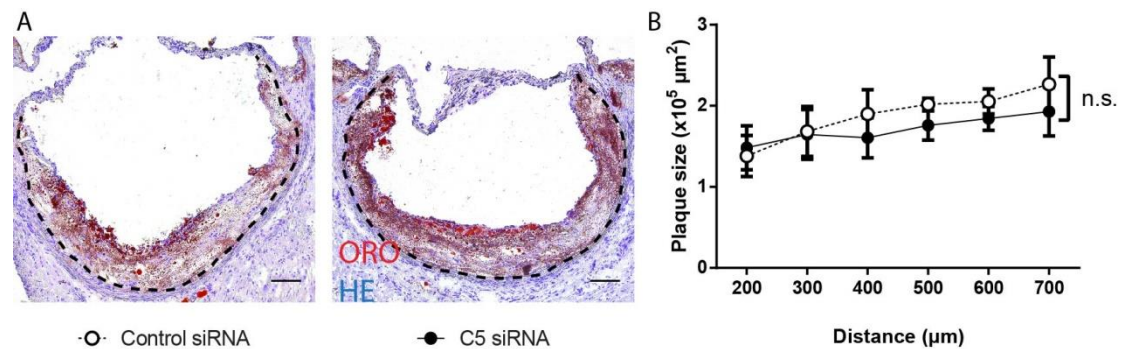


**Figure 3.20 C5 siRNA did not affect plaque sizes in aortic roots of 76 weeks old normal chow-fed ApoE<sup>-/-</sup> mice.** **A.** Aortic root plaques from 76 weeks old C5 siRNA-treated ApoE<sup>-/-</sup> mice or control siRNA-treated ApoE<sup>-/-</sup> mice. 10 μm fresh-frozen sections of the aortic root were stained with Oil-Red-O/HE. Scale bar: 100 μm. **B.** Mean plaque sizes of the individual cross-sections of the aortic roots of C5 siRNA-treated ApoE<sup>-/-</sup> mice or control siRNA-treated ApoE<sup>-/-</sup> mice. Data represent means ± SEM, two-way ANOVA, n.s.: no significant difference; C5 siRNA-treated mice: n=4; control siRNA-treated mice: n=4.

### 3.3.5 Liver-specific C5 siRNA did not affect CD68<sup>+</sup> macrophage/DC infiltration in atherosclerosis in aged ApoE<sup>-/-</sup> mice on a normal chow

Macrophages are pathological hallmarks of infiltrates in the advanced plaque of the aged ApoE<sup>-/-</sup> mice<sup>15</sup>. In order to examine whether the C5 inhibition influences the macrophage content in plaques of aged ApoE<sup>-/-</sup> mice, CD68<sup>+</sup> macrophages were stained on aortic root sections of 76 weeks old ApoE<sup>-/-</sup> mice treated with C5 siRNA for 18 weeks (Fig. 3.21 A). CD68<sup>+</sup> macrophage area/plaque areas were not affected by C5



inhibition (Fig. 3.21 B).

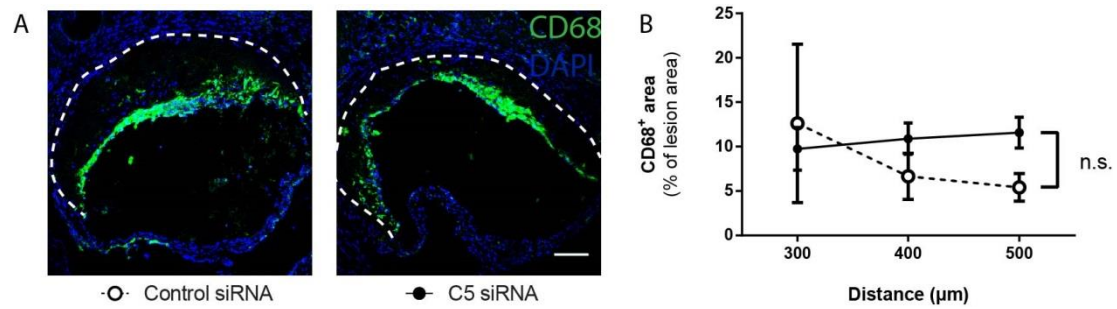


**Figure 3.21 C5 did not affect CD68<sup>+</sup> macrophage/DC infiltration in atherosclerotic plaque of 76 weeks old ApoE<sup>-/-</sup> mice on normal chow.** *A.* Aortic root plaques from 76 weeks old C5 siRNA- or control siRNA-treated ApoE<sup>-/-</sup> mice. 10 μm fresh-frozen sections of the aortic root were stained with CD68<sup>+</sup> macrophages/DCs. Scale bars: 100 μm. *B.* Quantification of CD68<sup>+</sup> area in aortic root plaque. Data represent means ± SEM, two-way ANOVA, n.s.: no significant difference; C5 siRNA treated mice: n=4; control siRNA treated mice: n=4.

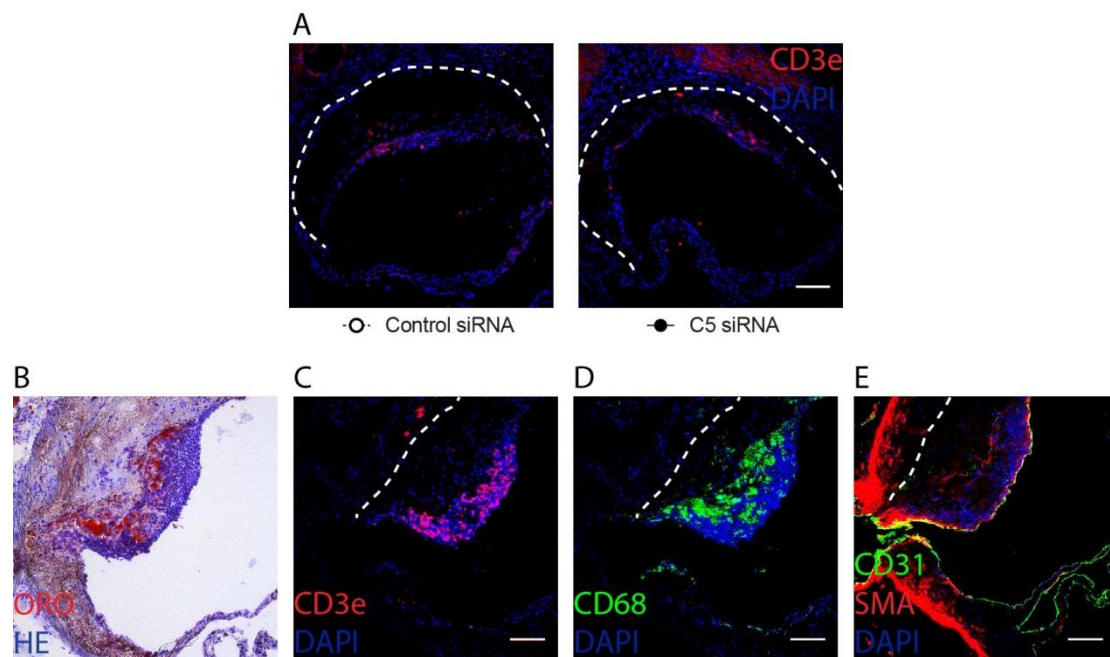


**Figure 3.22 CD3e<sup>+</sup> T cells in atherosclerotic plaques of 76 weeks old ApoE<sup>-/-</sup> mice on a normal diet.** *A.* Aortic root plaques from 76 weeks old C5 siRNA and control siRNA treated ApoE<sup>-/-</sup> mice. 10 μm fresh frozen sections of the aortic root were stained with CD3e<sup>+</sup> T cell immunofluorescence staining. Scale bars: 100 μm. *B-E.* Aggregates of CD3e<sup>+</sup> T cell in aortic root sections of control siRNA treated ApoE<sup>-/-</sup> mice. 10 μm fresh frozen sections of the aortic root in control mice were stained with ORO/HE,

CD3e<sup>+</sup> T cell, CD68<sup>+</sup> macrophage/DC, SMA<sup>+</sup> SMC, and CD31<sup>+</sup> EC immunofluorescence staining. Scale bars: 100  $\mu$ m.

There were 3 in 9 mice in the control siRNA group, which contained aggregates of nuclei in the aortic root sections stained with ORO/HE (Fig. 3.22 B), but no C5 siRNA treated mice showed a similar structure (n=9). CD3e<sup>+</sup> T cells were stained in aortic root sections (Fig. 3.22 A and C). CD3e<sup>+</sup> staining showed a large number of cells in the aggregates in the aortic root sections, which were identified as CD3e<sup>+</sup> T cells (Fig. 3.22 C). Except for these 3 mice, CD3e<sup>+</sup> T cell positive areas did not differ in C5 siRNA-treated mice versus the other 6 control mice, showing in Fig. 3.22 A. The CD68, SMA, and CD31 staining pictures show the cells in the aggregations of nuclei in the aortic root are not CD68<sup>+</sup> macrophage/DCs, SMCs and CD31<sup>+</sup> ECs (Fig. 3.22 D and E). The structure of T cells aggregates in the aged aortic root plaques in the control group and whether the C5 inhibition affects the T cells infiltration is still unclear.

### **3.3.6 Effect of C5 siRNA on complement protein deposition in normal chow-fed 76 weeks old ApoE<sup>-/-</sup> mice**

In order to study the role of C5 inhibition on complement protein deposition within the plaque, we performed immunofluorescence staining for C3, C4, and C5. C5 siRNA treatment did not alter C3 and C4 levels within atherosclerotic plaques of normal chow-fed 76 weeks old ApoE<sup>-/-</sup> mice when compared to their controls (Fig. 3.24). C5 deposition in the plaques from C5 siRNA-treated aged mice was reduced when compared to the controls, however (Fig. 3.23).

In conclusion, these data demonstrated that liver-derived complement C5 promotes atherosclerosis when ApoE<sup>-/-</sup> mice are fed with chow diet, and atherosclerosis plaque burden is reduced by C5 siRNA. Our data indicate new therapeutic treatment strategies for atherosclerosis. We next examined the roles of C5 on atherosclerosis when ApoE<sup>-/-</sup> mice were maintained on a high-fat diet.



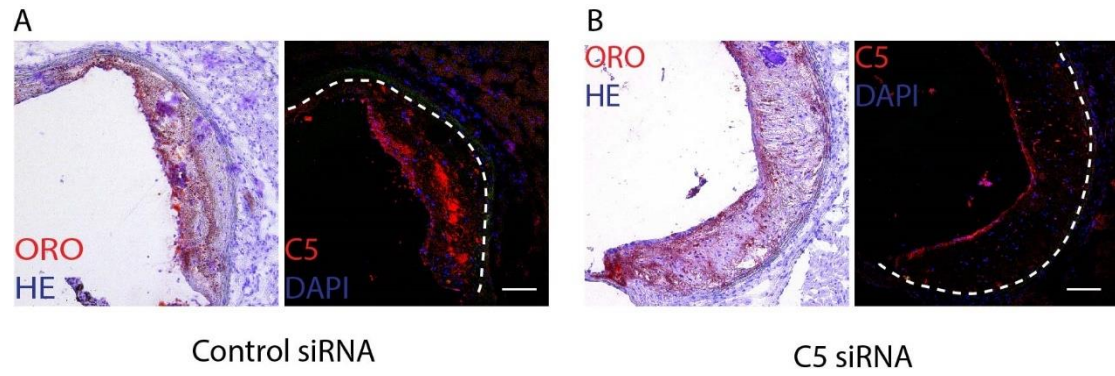


**Figure 3.23 C5 deposition in atherosclerotic plaque of normal chow-fed 76 weeks old  $ApoE^{-/-}$  mice.** (A-B) Aortic root plaques from 76 weeks old C5 siRNA- or control siRNA-treated  $ApoE^{-/-}$  mice. 10  $\mu m$  fresh-frozen sections of the aortic root were examined by C5 antibody immunofluorescence staining (right). Left pictures show the ORO/HE-stained sections next to the sections stained for C5. Scale bars: 100  $\mu m$ .

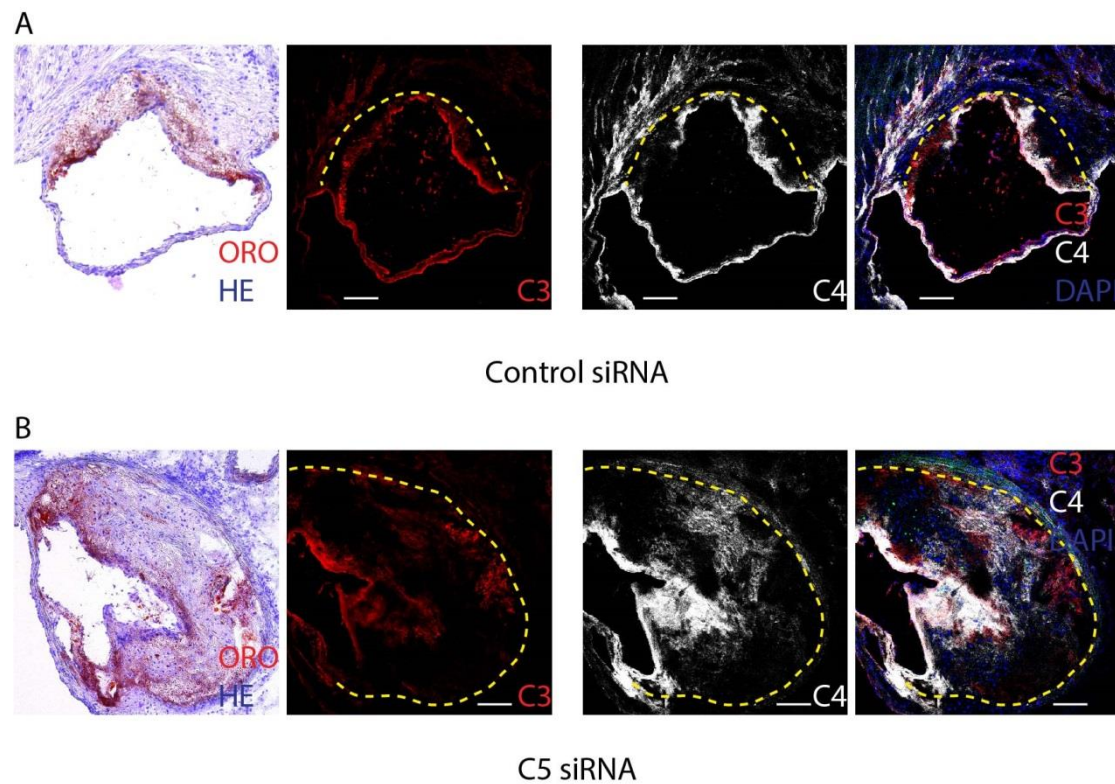


**Figure 3.24 C3 and C4 deposition in atherosclerotic plaques of normal chow-fed 76 weeks old  $ApoE^{-/-}$  mice.** (A-B) Aortic root plaques from normal chow-fed 76 weeks old C5 siRNA- or control siRNA-treated  $ApoE^{-/-}$  mice. 10  $\mu m$  fresh-frozen sections of the aortic root were examined by C3 and C4 antibodies immunofluorescence staining. Left pictures show the ORO/HE-stained sections next to the sections stained with C3 and C4 antibodies. Scale bars: 100  $\mu m$ . The green area in the pictures shows the

autofluorescence.

### 3.4 The role of liver-specific complement C5 in atherosclerosis in ApoE<sup>-/-</sup> mice with a high-fat diet

Our data reported above demonstrated that complement activation promotes atherosclerosis initiation rather than affects the late stages of the disease. In contrast, an article published in 2001 indicated that C5 deficiency did not change atherosclerosis plaque load in the aortic root of ApoE<sup>-/-</sup> mice after 18 weeks on the high-fat diet when compared to the control group<sup>63</sup>. Importantly, the mice were fed with a high-fat diet, whereas in the majority of our experiments, we used a normal mouse chow. ApoE<sup>-/-</sup> mice fed with a high-fat diet will develop atherosclerosis faster compared to normal chow. However, atherosclerotic plaque formation becomes less dependent on the immune system. These experiments are, therefore not strictly comparable. We hypothesized that atherosclerotic plaque sizes would differ depending on the diet as immune mechanisms of mice on a high-fat diet are compromised when compared to a normal diet. Therefore, we repeated our experiments under high-fat diet conditions in our experimental system.

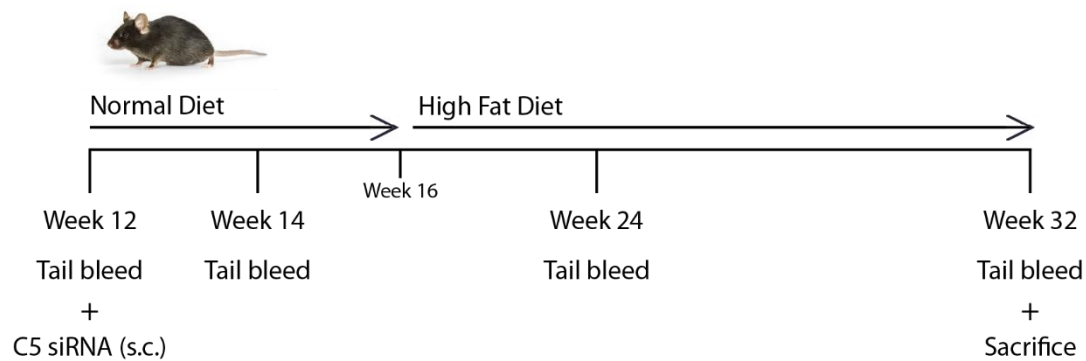


**Figure 3.25 Experimental design.** 12 weeks old male ApoE<sup>-/-</sup> mice (C5 siRNA-treated mice: n=10; control siRNA-treated mice: n=11), were treated with C5 or control siRNA every two weeks for 20 weeks and were given water and high-fat chow *ad libitum*. They were tail bled at the age of 12 weeks, 14 weeks, 24 weeks and 32 weeks.

To examine the role of complement activation during atherosclerosis, ApoE<sup>-/-</sup> mice were

treated with C5 siRNA and subjected them (together with their controls) to a high-fat diet. These 2 groups of mice (C5 siRNA-treated group or control siRNA-treated groups) were then characterized and compared (Fig. 3.25).

#### 3.4.1 Liver-specific C5 siRNA reduces serum C5 protein levels in 32 weeks old ApoE<sup>-/-</sup> mice on a high-fat diet

As the data mentioned above, C5 siRNA knocks down C5 levels (94%) in the serum of ApoE<sup>-/-</sup> mice on a high-fat diet and on normal chow (Fig. 3.26).

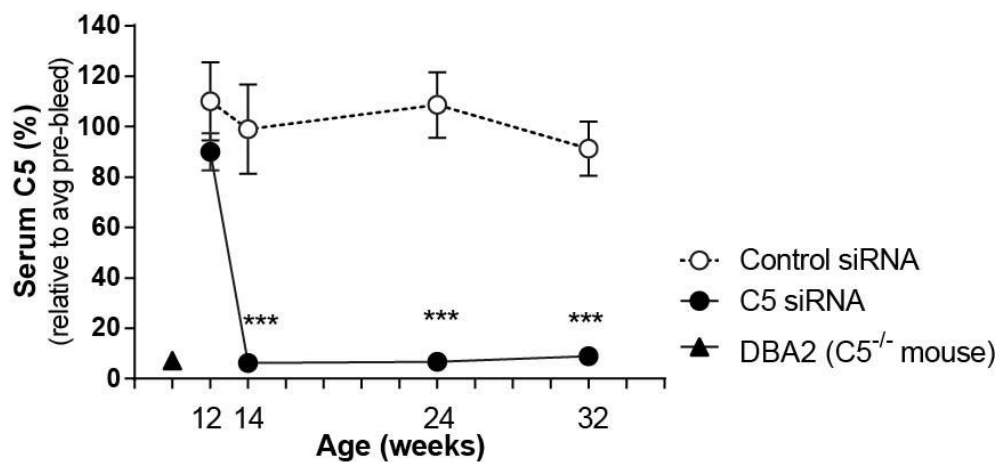


**Figure 3.26 Liver-specific C5 siRNA effectively silenced C5 in the circulation of young ApoE<sup>-/-</sup> mice on a high-fat diet.** Blood was collected before injection, 2 weeks, 12 weeks, and 20 weeks after injection from the caudal vein. Complement C5 levels were measured by ELISA. Serum of C5-deficient mice (DBA/2) was used as a non-specific background negative control. The line graph shows group means  $\pm$  SEM; two-tailed Student's t-test; \*\*\*  $p < 0.005$  versus before injection; liver-specific C5 siRNA treated mice:  $n = 10$ ; control siRNA treated mice:  $n = 11$ .

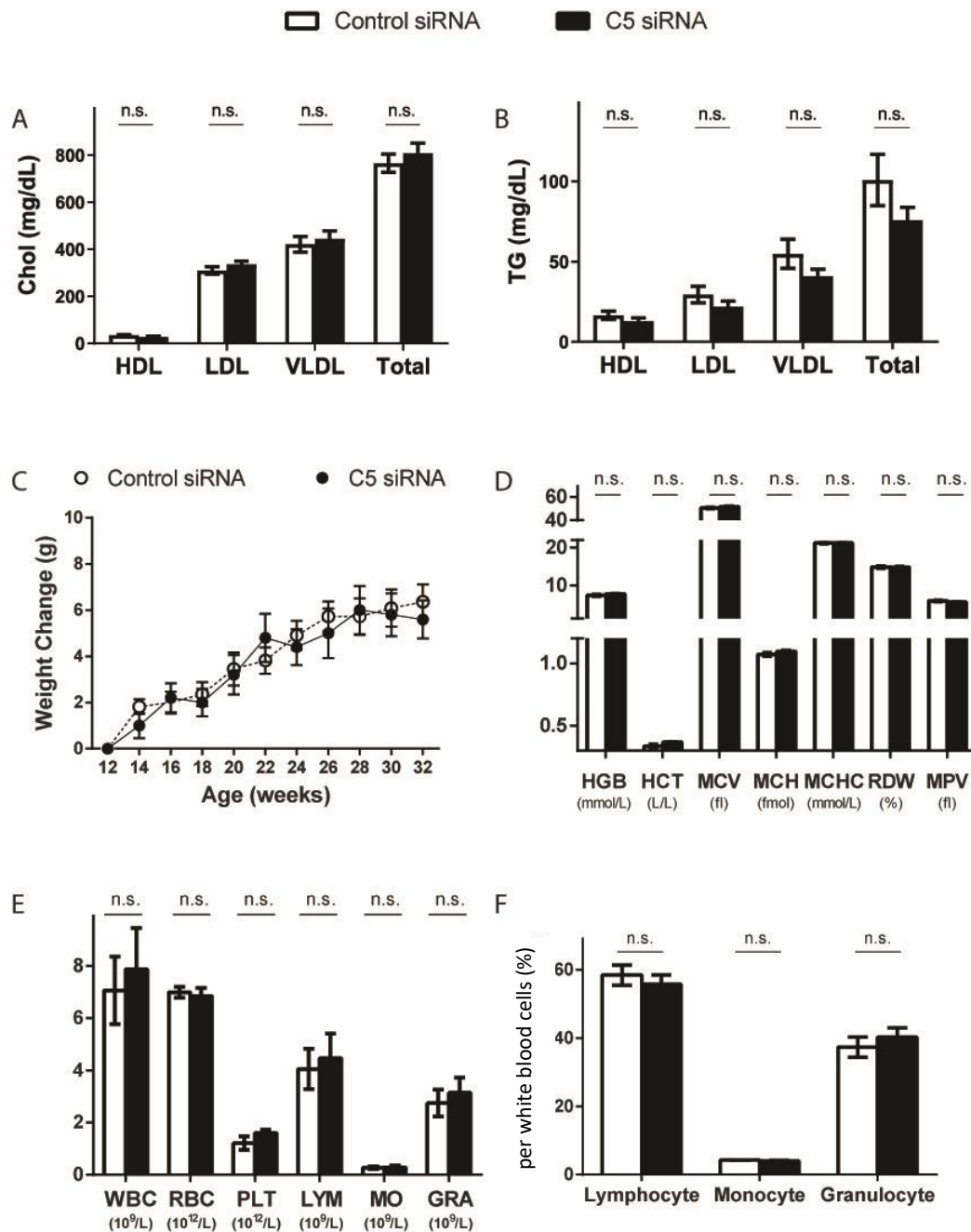
#### 3.4.2 Liver-specific C5 siRNA does not change blood lipid levels, body weight, blood cell numbers, and leukocyte percentages in 32 weeks old ApoE<sup>-/-</sup> mice on a high-fat diet

In order to determine whether C5 siRNA affected blood cell counts in high-fat diet fed ApoE<sup>-/-</sup> mice, plasma lipid levels were determined. C5 siRNA did not influence the cholesterol and triglyceride levels in high-fat diet fed ApoE<sup>-/-</sup> mice (Fig. 3.27 A-B). As expected, their plasma lipid levels were significantly higher than the plasma lipid levels

of mice on a normal diet (not shown).

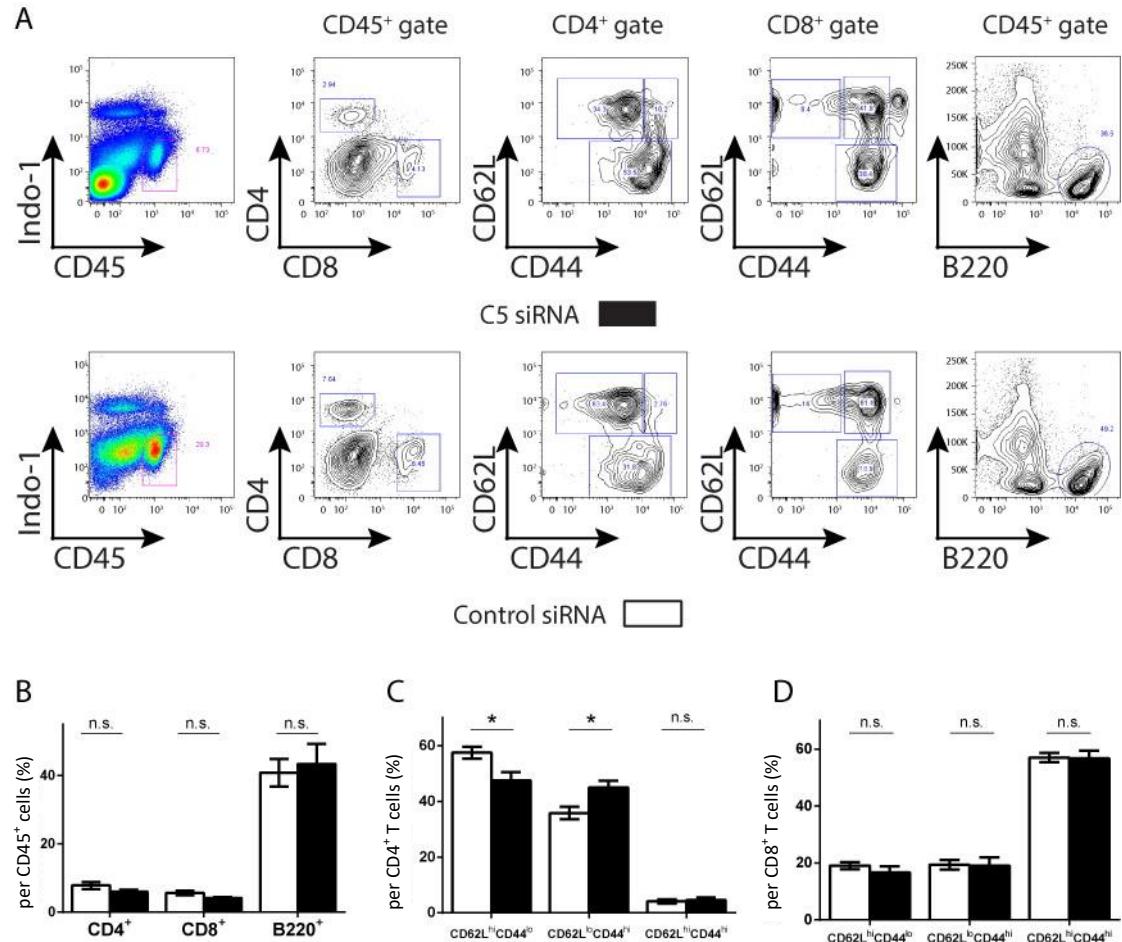
Two groups of mice were weighed every two weeks, and their body weight increased steadily during aging, reflecting the high calory intake. C5 siRNA did not affect the weight gain in the two groups (Fig. 3.27 C).

In order to determine whether C5 siRNA affected blood cell counts in ApoE<sup>-/-</sup> mice in a high-fat diet condition, complete blood was obtained after 20 weeks of C5 siRNA injections and analyzed with a complete blood cell counter. In both the liver-specific C5 siRNA and the control group mice, blood cells numbers, concentrations and other parameters were not changed after the high-fat diet period (Fig. 3.27 D-F).



**Figure 3.27 Liver-specific C5 siRNA does not impact blood lipid levels, body weight gain, blood cell concentration and leukocyte percentage of 32 weeks old ApoE<sup>-/-</sup> mice on a high-fat diet. (A-B) Blood lipid level.** Plasma was collected after 18 weeks of siRNA treatment. Chol and TG levels were measured by our collaborators, Prof. Daniel Teupser and Wolfgang Wilfert. Chol: cholesterol; TG: triglyceride. HDL: high-density lipoprotein; LDL: low-density lipoprotein; VLDL: very low-density lipoprotein. **C. Body weight gain.** Body weight was weighed before treatment and every 2 weeks after treatment. **(D-E) Blood cell concentration and leukocyte percentage.** Data represent means  $\pm$  SEM; two-tailed Student's t-test, n.s.: no significant difference; C5 siRNA-treated mice: n=10; control siRNA treated mice:




n=11. HGB: hemoglobin; HCT: hematocrit; MCV: mean corpuscular volume; MCH: mean corpuscular hemoglobin; MCHC: mean corpuscular hemoglobin concentration; RDW: red blood cell distribution width; MPV: mean platelet volume. WBCs: white blood cells; RBC: red blood cells; PLT: platelets; LYM: lymphocytes; MO: monocytes; and GRA: granulocytes.



**Figure 3.28 C5 siRNA did not affect leukocyte subsets in the circulation of 32 weeks old ApoE<sup>-/-</sup> mice on a high-fat diet, part A. Flow cytometric analysis of leukocytes from 32 weeks old C5 siRNA and control siRNA treated ApoE<sup>-/-</sup> mice. A. Gating strategies: CD4<sup>+</sup> T cells (CD45<sup>+</sup>CD4<sup>+</sup> gate), CD8<sup>+</sup> T cells (CD45<sup>+</sup>CD8<sup>+</sup> gate), CD4<sup>+</sup> Th0 (CD45<sup>+</sup>CD4<sup>+</sup>CD62L<sup>hi</sup>CD44<sup>lo</sup> gate), CD4<sup>+</sup> TEM (CD45<sup>+</sup>CD4<sup>+</sup>CD62L<sup>lo</sup>CD44<sup>hi</sup> gate), CD4<sup>+</sup> TCM (CD45<sup>+</sup>CD4<sup>+</sup>CD62<sup>hi</sup>CD44<sup>hi</sup> gate), CD8<sup>+</sup> Th0 (CD45<sup>+</sup>CD8<sup>+</sup>CD62L<sup>hi</sup>CD44<sup>lo</sup> gate), CD8<sup>+</sup> TEM (CD45<sup>+</sup>CD8<sup>+</sup>CD62L<sup>lo</sup>CD44<sup>hi</sup> gate), CD8<sup>+</sup> TCM (CD45<sup>+</sup>CD8<sup>+</sup>CD62<sup>hi</sup>CD44<sup>hi</sup> gate), B cells (CD45<sup>+</sup>B220<sup>+</sup> gate). B. The frequencies of CD4<sup>+</sup> T cells, CD8<sup>+</sup> T cells and B cells were compared in circulation in high-fat diet fed 32 weeks old ApoE<sup>-/-</sup> mice treated with C5 siRNA and control siRNA. The bar graph shows the percentages of CD4<sup>+</sup> T cells, CD8<sup>+</sup> T cells and B cells in CD45<sup>+</sup> leucocytes. C. The frequencies of CD4<sup>+</sup> Th0, TEM and TCM were compared in**



A

CD45 <sup>+</sup> gate	CD4 <sup>+</sup> gate	CD4 <sup>-</sup> gate
		

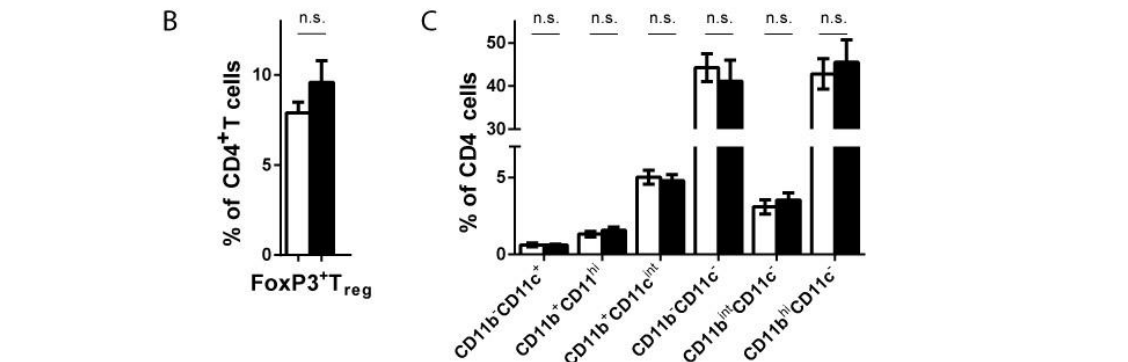


**Figure 3.29 C5 siRNA did not affect leukocyte subsets in the circulation of 32 weeks old ApoE<sup>-/-</sup> mice on a high-fat diet, part B. FACS analyses of leukocytes from high-fat diet fed 32 weeks old ApoE<sup>-/-</sup> mice treated with the C5 siRNA and control siRNA. A. Gating strategies: T<sub>reg</sub> cells**

(CD45<sup>+</sup>CD4<sup>+</sup>Foxp3<sup>+</sup> gate), CD11b<sup>-</sup>CD11c<sup>+</sup> cells (CD45<sup>+</sup>CD4<sup>-</sup>CD11b<sup>-</sup>CD11c<sup>+</sup> gate), CD11b<sup>+</sup>CD11c<sup>hi</sup> cells (CD45<sup>+</sup>CD4<sup>-</sup>CD11b<sup>+</sup>CD11c<sup>hi</sup> gate), CD11b<sup>+</sup>CD11c<sup>int</sup> cells (CD45<sup>+</sup>CD4<sup>-</sup>CD11b<sup>+</sup>CD11c<sup>int</sup> gate), CD11b<sup>-</sup>CD11c<sup>-</sup> cells (CD45<sup>+</sup>CD4<sup>-</sup>CD11b<sup>-</sup>CD11c<sup>-</sup> gate), CD11b<sup>int</sup>CD11c<sup>-</sup> cells (CD45<sup>+</sup>CD4<sup>-</sup>CD11b<sup>int</sup>CD11c<sup>-</sup> gate), CD11b<sup>hi</sup>CD11c<sup>-</sup> cells (CD45<sup>+</sup>CD4<sup>-</sup>CD11b<sup>hi</sup>CD11c<sup>-</sup> gate). **B.** The frequencies of T<sub>reg</sub> cells were compared within circulation in high-fat diet fed 32 weeks old ApoE<sup>-/-</sup> mice treated with the liver-specific C5 siRNA and control siRNA. **C.** The frequencies of CD11b<sup>-</sup>CD11c<sup>+</sup> cells, CD11b<sup>+</sup>CD11c<sup>+</sup> cells, CD11b<sup>-</sup>CD11c<sup>-</sup> cells, CD11b<sup>+</sup>CD11c<sup>dim</sup>, and CD11b<sup>+</sup>CD11c<sup>-</sup> cells were compared within circulation in high-fat diet fed 32 weeks old ApoE<sup>-/-</sup> mice treated with liver-specific C5 siRNA and control siRNA. Data represent means ± SEM; Student's-t test, n.s.: no significant difference; liver-specific C5 siRNA-treated mice: n=8 mice; control siRNA-treated mice: n=6 mice.

### 3.4.3 Liver-specific C5 inhibition does not change the blood leukocytes subsets in young ApoE<sup>-/-</sup> mice on a high-fat diet

The data above showed that the C5 siRNA did not affect circulating leukocytes subsets in young and aged ApoE<sup>-/-</sup> mice on a normal diet (Fig. 3.5, 3.6, 3.7, 3.16, 3.17, 3.18). In order to determine whether C5 siRNA influence the leukocyte subsets in the circulation in the ApoE<sup>-/-</sup> mice in the high-fat diet condition, the leukocyte concentrations in the blood were also analyzed with FACS (Fig. 3.28 A and Fig. 3.29 A).

C5 siRNA did not influence the concentration of CD45<sup>+</sup>CD4<sup>+</sup> T cells, CD45<sup>+</sup>CD8<sup>+</sup> T cells, CD45<sup>+</sup>B220<sup>+</sup> B cells (Fig. 3.28 B), CD45<sup>+</sup>CD4<sup>+</sup> Th0, CD45<sup>+</sup>CD4<sup>+</sup> TEM, CD45<sup>+</sup>CD4<sup>+</sup> TCM (Fig. 3.28 C), CD45<sup>+</sup>CD8<sup>+</sup> Th0, CD45<sup>+</sup>CD8<sup>+</sup>TEM, CD45<sup>+</sup>CD8<sup>+</sup> TCM (Fig. 3.28 D), CD45<sup>+</sup> T<sub>reg</sub> cells (Fig. 3.29 B), CD45<sup>+</sup>CD4<sup>-</sup>CD11b<sup>-</sup>CD11c<sup>+</sup> cells, CD45<sup>+</sup>CD4<sup>-</sup>CD11b<sup>+</sup>CD11c<sup>hi</sup> cells, CD45<sup>+</sup>CD4<sup>-</sup>CD11b<sup>+</sup>CD11c<sup>int</sup> cells, CD45<sup>+</sup>CD4<sup>-</sup>CD11b<sup>-</sup>CD11c<sup>-</sup> cells, CD45<sup>+</sup>CD4<sup>-</sup>CD11b<sup>int</sup>CD11c<sup>-</sup> cells, and CD45<sup>+</sup>CD4<sup>-</sup>CD11b<sup>hi</sup>CD11c<sup>-</sup> cells (Fig. 3.29 C). But in the CD4<sup>+</sup> T cells, the Th0 and TEM were changed. The concentration of CD4<sup>+</sup> Th0 was reduced, and CD4<sup>+</sup> TEM were increased in the C5 siRNA group compared to the control (Fig. 3.28 C).



### 3.4.4 C5 siRNA did not affect atherosclerosis plaque burden in young ApoE<sup>-/-</sup> mice on a high-fat diet

In order to explore whether the C5 siRNA affected atherosclerotic plaque development in the ApoE<sup>-/-</sup> mice under high-fat diet conditions after 20 weeks siRNA treatment, whole aortas were examined with the *en-face* analysis (Fig. 3.30 A). The Sudan IV positive plaque areas in the whole aortas (Fig. 3.30 B), thoracic aorta parts (Fig. 3.30 C) and abdominal aorta parts (Fig. 3.30 D) were similar in the siRNA group versus the control group.

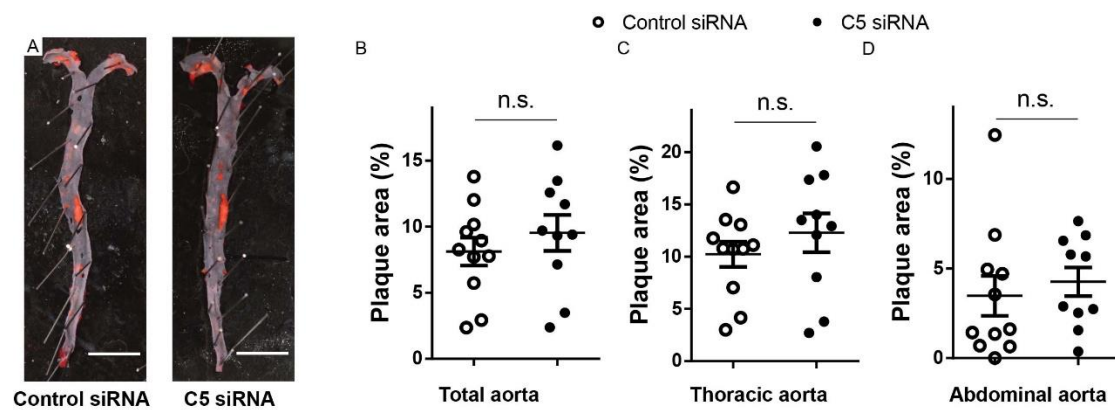


**Figure 3.30** C5 siRNA did not affect atherosclerotic lesion sizes in aortas of 32 weeks old high-fat diet fed ApoE<sup>-/-</sup> mice. **A.** *en-face* Sudan IV staining. Total aortas were pinned and stained with Sudan IV. Representative aortas from mice treated with control siRNA and liver-specific C5 siRNA; Scale bar: 500  $\mu$ m. **B.** The percent Sudan IV staining of the total aortic surface. **C.** The percent Sudan IV staining of the thoracic aorta. **D.** The percent Sudan IV staining of the abdominal aorta. Data represent means  $\pm$  SEM; Student's-t test, n.s.: no significant difference; liver-specific C5 siRNA treated mice: n=10; control siRNA treated mice: n=11.

To evaluate the effect of C5 siRNA in plaque composition, we stained 10 $\mu$ m fresh frozen aortic root sections with ORO/HE staining (Fig. 3.31 A) and quantified the plaque size. The plaque areas were not significantly different in the C5 siRNA and control groups (Fig. 3.31 B).

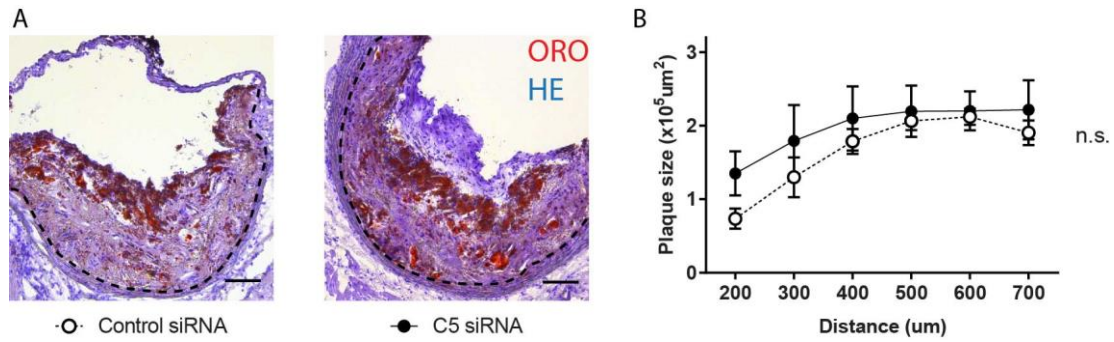


**Figure 3.31 Liver-specific C5 mediated regression of atherosclerotic lesions in aortic roots of 32 weeks old high-fat diet fed ApoE<sup>-/-</sup> mice.** *A.* Aortic root plaque from high-fat diet fed 32 weeks old C5 siRNA and control siRNA treated ApoE<sup>-/-</sup> mice. 10 µm fresh frozen sections of the aortic root were stained with ORO/HE staining. Scale bar: 100µm. *B.* Mean plaque sizes of the individual cross-sections of the aortic root. Data are represented as the mean ± SEM, Two-way ANOVA, n.s.: no significant difference; liver-specific C5 siRNA-treated mice: n=5; control siRNA-treated mice: n=5.

### 3.4.5 C5 siRNA does not influence macrophage/DC and T cell infiltration in atherosclerosis in young ApoE<sup>-/-</sup> mice on a high-fat diet

In order to determine the CD68<sup>+</sup> macrophage/DCs and CD3e<sup>+</sup> T cells infiltration, the aortic root sections were stained with immunofluorescence CD68 and CD3e antibodies staining (Fig. 3.32 A and Fig. 3.33 A).

The fraction of the CD68<sup>+</sup> macrophage/dendritic areas and CD3e<sup>+</sup> T cell numbers in the atherosclerotic plaques were not significantly different in the C5 siRNA and control siRNA groups (Fig. 3.32 B and Fig. 3.33 B).

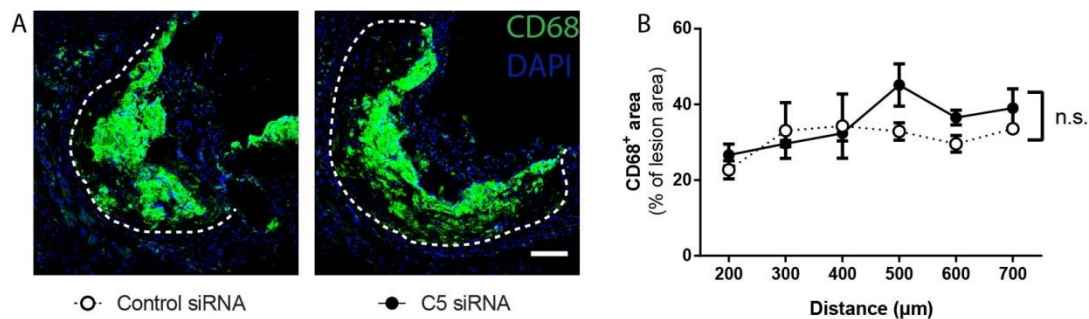


**Figure 3.32 C5 did not affect CD68<sup>+</sup> macrophage/DC infiltration in atherosclerotic plaque of 32 weeks old ApoE<sup>-/-</sup> mice on a high-fat diet.** *A.* Aortic root plaque from high-fat diet-fed 32 weeks old

C5 siRNA and control siRNA-treated ApoE<sup>-/-</sup> mice. 10  $\mu$ m fresh frozen sections of the aortic root were stained with CD68<sup>+</sup> macrophages/DCs immunofluorescence staining. Scale bars: 100  $\mu$ m. **B.** Quantification of CD68<sup>+</sup> area in aortic root plaque. Data represent the means  $\pm$  SEM, two-way ANOVA, n.s.: no significant difference; C5 siRNA-treated mice: n=4; control siRNA treated mice: n=4.

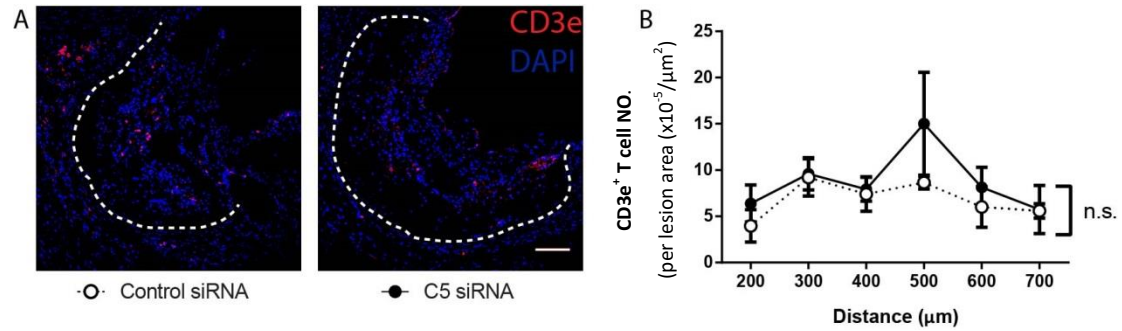


**Figure 3.33 C5 did not affect CD3e<sup>+</sup> T cells in atherosclerotic plaques of 32 weeks old ApoE<sup>-/-</sup> mice on a high-fat diet.** **A.** Aortic root plaques from high-fat diet fed 32 weeks old C5 siRNA and control siRNA treated ApoE<sup>-/-</sup> mice. 10  $\mu$ m fresh frozen sections of the aortic root were stained with CD3e<sup>+</sup> T cell immunofluorescence staining. Scale bars: 100  $\mu$ m. **B.** Quantification of CD3e<sup>+</sup> numbers in aortic root plaque. Data represent the means  $\pm$  SEM, two-way ANOVA, n.s.: no significant difference; liver-specific C5 siRNA-treated mice: n=4; control siRNA-treated mice: n=4.

### 3.4.6 Effect of C5 siRNA on complement protein activation and deposition in high-fat diet fed 32 weeks old ApoE<sup>-/-</sup> mice

In both the normal diet fed young and aged ApoE<sup>-/-</sup> mice, C5 siRNA reduced the C5 deposition in the plaques from them (Fig. 3.12 and Fig. 3.23), but did not affect the C3 or C4 deposition. Next, I examined complement protein deposition in the aortic root plaques from the high-fat diet fed 32 weeks ApoE<sup>-/-</sup> mice with immunofluorescence staining. There was no apparent difference of C3, C4 (Fig. 3.35), and C5 (Fig. 3.34) deposition in the aortic root plaques between the C5 siRNA and control siRNA group.

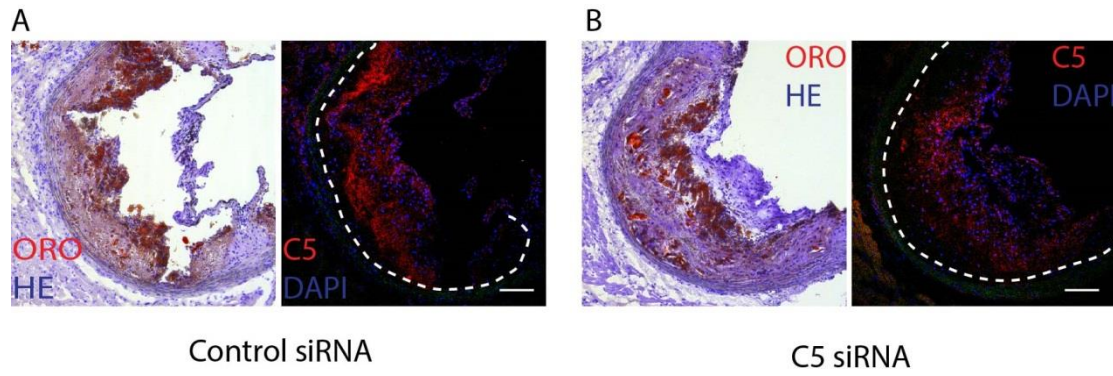


**Figure 3.34 C5 siRNA reduced C5 deposition in atherosclerotic plaque of the high-fat diet fed 32 weeks old ApoE<sup>-/-</sup> mice.** (A-B) Aortic root plaque from the high-fat diet fed 32 weeks old C5 siRNA- and control siRNA-treated ApoE<sup>-/-</sup> mice. 10 μm fresh frozen sections of the aortic root were examined by C5 antibody immunofluorescence staining (right). Left pictures show the ORO/HE-stained sections next to the sections stained with C5-antibody. Scale bars: 100 μm.

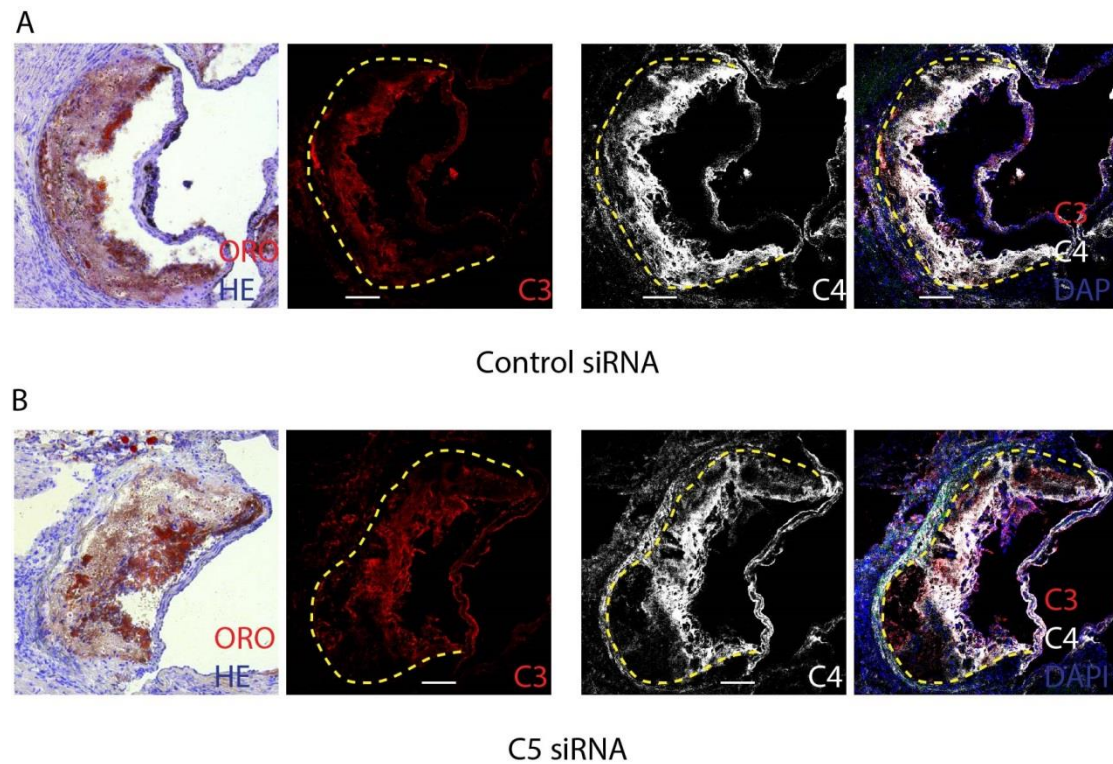


**Figure 3.35 C3 and C4 deposition in atherosclerotic plaque of the high-fat diet fed 32 weeks old ApoE<sup>-/-</sup> mice.** (A-B) Aortic root plaque from the high-fat diet fed 32 weeks old C5 siRNA and control siRNA-treated ApoE<sup>-/-</sup> mice. 10 μm fresh frozen sections of the aortic root were examined by C3 and C4 antibody immunofluorescence staining. Left pictures show the ORO/HE-stained sections next to the sections stained with C3 and C4 antibody. Scale bars: 100 μm. The green area in the pictures shows the



autofluorescence.

### 3.4.7 C5 siRNA does not affect atherosclerotic plaque burden in young ApoE<sup>-/-</sup> mice on a short-term high-fat diet

In order to explore whether the C5-mediated complement system only plays a role in early atherosclerosis, we selected 4 weeks high-fat diet during early atherosclerosis (Fig. 3.36).



**Figure 3.36 Experimental design.** 12 weeks old male ApoE<sup>-/-</sup> mice (liver-specific C5 siRNA treated mice: n=4; control siRNA treated mice: n=4), were treated with C5 or control siRNA every two weeks for 4 weeks and were given water and high-fat chow *ad libitum*.

After 4 weeks of siRNA treatment and a high-fat diet, the total aortas were analyzed with the *en-face* analysis (Fig. 3.37 A). The atherosclerotic plaques in these mice were much less than 16w long-term high-fat diet mice and as less as normal diet fed young mice. However, C5 siRNA still did not reduce early atherosclerosis during a period of four weeks of high-fat diet (Fig. 3.37 B).

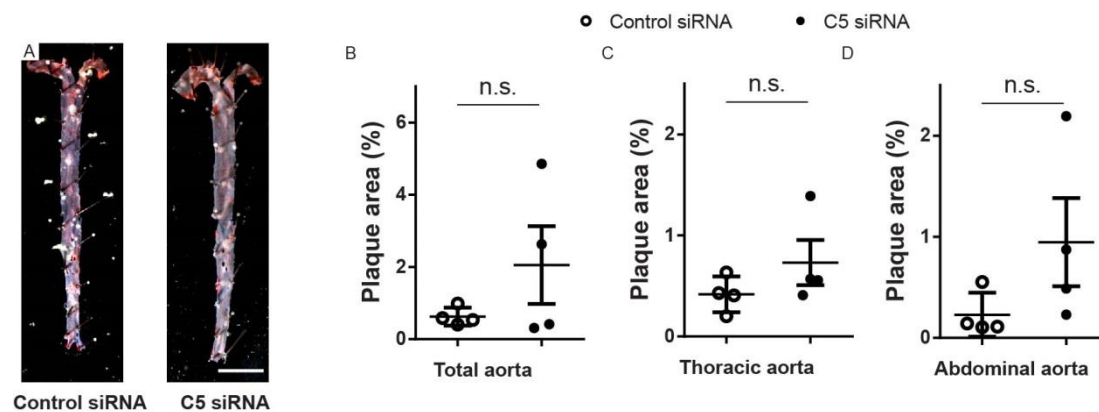


**Figure 3.37 Liver-specific C5 did not affect atherosclerotic lesion sizes in aortas of 12 weeks old**

**high-fat diet fed ApoE<sup>-/-</sup> mice. A. *en-face* Sudan IV staining.** Total aortas were pinned and stained with Sudan IV. Representative aortas from mice treated with control siRNA and liver-specific C5 siRNA; Scale bar: 500  $\mu$ m. **B.** The percent Sudan IV staining of the total aortic surface. **C.** The percent Sudan IV staining of the thoracic aorta. **D.** The percent Sudan IV staining of the abdominal aorta. Data represent means  $\pm$  SEM; Student's t-test, n.s.: no significant difference; C5 siRNA-treated mice: n=4; control siRNA-treated mice: n=4.

### 3.5. Classical complement cascade activation in human atherosclerosis

In human pathology, in 1962, Lachmann et al. observed complement protein (beta-1-C globulin) deposition in the vascular walls of malignant nephrosclerosis and in certain collagenous diseases. Atherosclerosis is viewed as the embodiment of chronic inflammatory disease now. The plaque progresses from the early stage of fatty streaks to a more complex advanced stage exemplified by a necrotic core. Complement protein deposition is a characteristic feature of human atherosclerotic lesions<sup>102-104</sup>. In order to explore whether the complement system is activated during human atherosclerosis progression, human atherosclerosis samples from carotid endarterectomy were classified into healthy arteries, early stage and advanced atherosclerotic plaques based on one of the American Heart Association classifications followed by quantification. Five healthy control arteries on autopsy (type 0-I), six early (type II-III) and nine advanced atherosclerotic plaques (type V-VII)<sup>105</sup> from carotid endarterectomy specimens were stained for CD68<sup>+</sup> macrophages/DCs, C1q, ApoE, and C5 (Fig. 3.38 A). These quantificational illustrations show CD68<sup>+</sup> macrophage infiltration, and C1q, ApoE, and C5 protein deposits increased in early and advanced plaques compared with control arteries (Fig. 3.38 B, C).

These data indicated that human atherosclerotic plaques are contained CD68<sup>+</sup> macrophages/DCs, and C1q, ApoE, and C5 protein deposition. Thus, the complement cascades are activated in human plaques. This section presented here was published<sup>95</sup>.

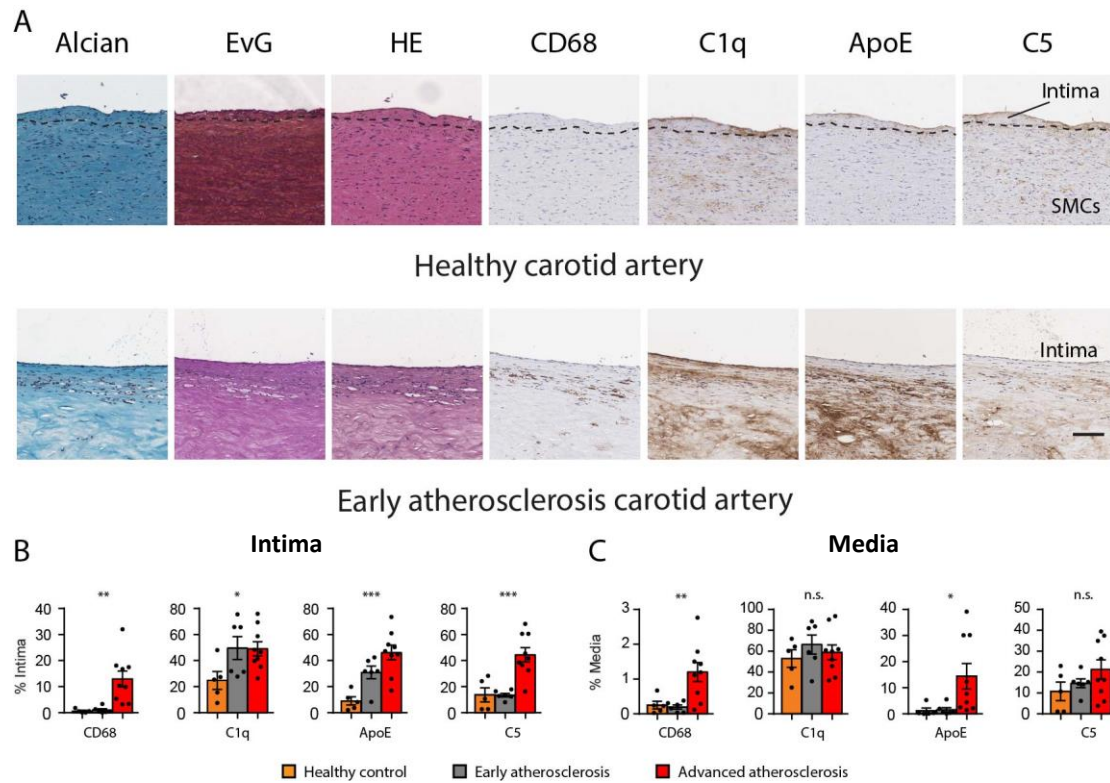


**Figure 3.38 Classical complement cascade activation in human atherosclerosis.** *A.* Human carotid artery sections were stained for Alcian, EvG, CD68, C1q, ApoE, and C5 by DAB and hematoxylin. Representative images from B and C. *B.* CD68, C1q, ApoE, and C5 signals in the intima were quantified. *C.* CD68, C1q, ApoE, and C5 signals in the media were quantified. CD68, C1q, ApoE, and C5 signals were quantified as described in Methods. Data represent means  $\pm$  SEM; one-way ANOVA, n.s.: no significant difference, \*  $p < 0.05$ , \*\*  $p < 0.01$ , \*\*\*:  $p < 0.005$ ; healthy control:  $n = 5$  (independent samples), early plaque:  $n = 6$ , advanced plaque:  $n = 9$ .

## 4. DISCUSSION

### 4.1 Discovery of an ApoE-complement C5 axis which controls atherosclerosis in mice

ApoE has traditionally been viewed as a lipid-binding glycoprotein whose major function is to clear remnants of chylomicrons and VLDL from the circulation. Previous studies had shown that ApoE<sup>-/-</sup> mice had five times normal plasma cholesterol and developed foam cell-rich depositions in their proximal aortas by the age of 3 months<sup>27</sup>. However, importantly, ApoE has also been recognized to be a multifunctional protein whose impact on tissue homeostasis extends beyond lipid transport. Thus, ApoE has been implicated in brain diseases as varied as Alzheimer's disease<sup>106</sup> and Parkinson's disease<sup>107</sup>. Moreover, the apolipoprotein has been implicated in affecting chronic inflammatory diseases, including several infectious diseases<sup>108</sup>. Its role in the regulation of immune responses has been discussed, but no molecular mechanism has been proposed. Yin et al.,<sup>95</sup> in our group recently demonstrated that ApoE forms a high-affinity complex with the complement-initiating molecule C1q and thereby dampens the activity of the CCC *in vitro* but - of particular interest - also *in vivo*. These studies were performed using a variety of mouse models to dissect the role of ApoE in tissue inflammation as varied as atherosclerosis (the current thesis) and choroid plexus inflammation and Alzheimer's disease. When these studies using translational studies into human atherosclerosis and diseased human brains are taken together with the data presented here, a major general and possibly ubiquitous role of ApoE in various unresolvable inflammatory diseases deserves attention.

The time window of liver-specific C5 siRNA treatment that I used to examine atherosclerosis in ApoE<sup>-/-</sup> mice (12 weeks to 32 weeks) covered the critical period during atherosclerosis initiation. A principal finding of my study is that the extent of total aortic atherosclerosis was markedly attenuated in aortas from normal chow-fed young C5 siRNA-treated mice.



A second important finding of the present study is that C5 siRNA not only attenuated the size of the atherosclerotic lesions but that it also affected the cellularity of the plaque. Thus, CD68<sup>+</sup> macrophages/DCs were reduced in lesions from experimental mice versus their control brethren. Moreover, CD3e<sup>+</sup> T cells were also reduced in C5 siRNA-treated mice. This finding implies that liver-derived C5 associated-complement activation promotes changes that are associated with an inflammatory response in the initiation of atherosclerotic plaques. Of note, complement protein C5 contributes to the progression of atherosclerosis by two distinctive ways: C5a is an activated biologically powerful anaphylatoxin generated by cleavage of the C5 protein by protease C5-convertase. However, C5b is another degradation product of C5 forming MAC, resulting in cell lysis. Our data cannot distinguish between the specific effects of these two C5 degradation products on atherosclerosis.

C5a acts as a powerful chemoattractant that can modulate the activity of the myeloid lineage, such as eosinophils, basophils and neutrophils, monocytes and most tissue macrophage subtypes, T cells and B cells<sup>47</sup>. Previous studies had shown that C5a promotes migration and adherence of neutrophils and monocytes to vessel walls, and initiates accumulation of complement and phagocytic cells at sites of infection<sup>109</sup>. In our chow-fed young mice, the reduction of the atherosclerotic lesion and the macrophage and T cell infiltration may, therefore, be caused by the absence of C5a in the treatment group rather than a reduction of MAC. MAC deposition is a typical feature of human plaques, however. The results of several studies suggested that MAC might also play an important role in the development of atherosclerosis<sup>110-112</sup>. Further studies are clearly needed to determine the distinctive contributions of the two C5 degradation products on atherosclerosis during the various stages of the disease, i.e., initiation, progression, and the late clinically significant stages.

In conclusion, we have demonstrated that the initiation of atherosclerosis in mice depends in part on the presence of liver-specific C5 mediated-complement activation. Our data indicate that the complement system needs to be considered when assessing the mechanisms of other inflammatory parameters related to atherosclerosis.

## 4.2 C5-targeted therapy aims to reduce atherosclerosis

We have demonstrated that C5 had the most prominent effects during the initiation of the lesion via increasing macrophage and T cell migration. Therefore, this study also suggested a causal role for liver-specific C5 in advanced atherosclerotic plaque in aged ApoE<sup>-/-</sup> mice. Normal chow-fed 58 weeks old ApoE<sup>-/-</sup> mice had already developed advanced plaques<sup>27</sup>. After 18 weeks liver-specific C5 siRNA treatment, however, neither the plaque size nor the macrophage content were changed.

The used siRNA has a GalNAc adduct, which specifically binds to and is taken up by the ASGPR, which is selectively and strongly expressed on hepatocytes. In the circulation, the majority of C5 protein is synthesized by the liver, though to a lesser degree it is also produced by tissue macrophages, blood monocytes<sup>113</sup>, and epithelial cells of the lung, the genitourinary system, and the intestine<sup>114</sup>. Advanced plaques contain macrophages. We hypothesize that C5 protein might be produced by macrophages locally which is consistent with our observation that C5 staining in aortic root sections showed that C5 was expressed in plaques in both the C5 treatment and control groups.

C5a is a powerful chemoattractant and is also involved in recruiting inflammatory cells via CD88. CD88 (the canonical C5a receptor) is expressed by most of the cell types observed in human atherosclerotic plaque, i.e. macrophages, ECs, SMCs<sup>115</sup>, and T cells. In our aged animals, the majority of C5 was reduced by liver-specific C5 siRNA. However, the expression of CD88 might be up-regulated by a compensatory reaction. Previous studies showed that in the inflamed human central nervous system, reactive astrocytes, microglia cells, and ECs expressed more CD88<sup>116</sup>. This would further explain why inhibition of C5 in aged ApoE<sup>-/-</sup> mice had no effect on macrophage infiltration. Further studies are needed to uncover the age-dependent effects of our treatment. A combination of C5 siRNA and inhibition of CD88 may clarify some of these open issues.

Atherosclerosis is strongly associated with aging<sup>117</sup>, as atherosclerotic plaques show

evidence of cellular senescence described by reduced vascular SMC proliferation, increased collagen deposition and decrease in arterial elastin content<sup>118</sup>, which promote vascular stiffness<sup>119</sup> and hypertension<sup>120</sup>; irreversible growth arrest and apoptosis occur in ECs, vascular SMCs and macrophages<sup>121</sup>, DNA damage, epigenetic modifications, and telomere shortening, and dysfunction observed in plaque vascular SMCs<sup>122</sup> and ECs<sup>123</sup>. Growing evidence further showed that cellular senescence promotes atherosclerosis<sup>124-126</sup>.

Mechanisms of the lack of impact of liver-specific C5 inhibition on atherosclerosis in aged ApoE<sup>-/-</sup> mice remains to be clearly defined. Several possibilities exist. a) Different stages of atherosclerotic plaques: In young ApoE<sup>-/-</sup> mice on chow diet, the C5 siRNA treatment was started at 12 weeks, and the mice did not develop visible plaques in the aorta at this point in time. There was no pre-existing inflammation in the aorta when we started the C5 siRNA treatment. After 20 weeks of treatment, C5 siRNA strongly reduced atherosclerotic plaque size and inflammation. These data support the conclusion that a presumed lipid-complement-inflammation axis promotes early atherosclerosis development. In aged ApoE<sup>-/-</sup> mice, the C5 siRNA treatment was started at 58 weeks when the mice had already developed atherosclerotic plaques. In advanced plaques, other pre-existing inflammatory triggers, i.e., crystal, macrophage-form cells or necrotic cores may trigger other pro-inflammatory pathways including inflammasome<sup>127</sup>. The immunofluorescence staining confirmed that those complement proteins were deposited in advanced plaques, while C5 siRNA treatment indeed reduced C5 deposited in advanced plaques in aged ApoE<sup>-/-</sup> mice fed with chow diet (Figure 3.23 -3.24). But the plaque size was not significantly reduced after C5 siRNA treatment in advanced plaques analyzed by en-face staining. Further studies are required to examine whether C5 siRNA treatment altered plaque stabilization; (b) C5 siRNA targeted liver-produced C5, but not locally produced C5. In aged ApoE<sup>-/-</sup> mice fed with chow diet, locally produced C5 by infiltrated T cells and monocytes may compensate C5 siRNA treatment which silenced serum C5; (c) the time period needed for C5 siRNA in the present study in aged mice may have been too short to yield

statistically significant data; (d) different age windows and consequently variability in plaque sizes may require larger mouse cohorts to proof an effect of complement inhibition in advanced atherosclerosis; (e) C5 may not be involved in advanced plaque progression. These two different models may represent early and advanced stages of atherosclerotic plaques in human diseases. However, cautions are required when interpreting murine data in view of a possible relevance for human diseases. Nevertheless, we confirmed that complement proteins and inflammation is present in human atherosclerotic plaques. In addition, our murine data strongly suggest that atherosclerotic plaques in young and aged ApoE<sup>-/-</sup> mice are suitable models to study the impact of complement activation in atherosclerosis.

### **4.3 Possible effect of high-fat diet on C5-dependent atherosclerosis**

Why C5 inhibition reduces plaque size and alters the cellular composition of plaques in ApoE<sup>-/-</sup> mice on a normal diet but not on a high-fat diet remains an important unresolved question. Our data show that 20 weeks of C5 siRNA treatment reduced atherosclerosis in 32 weeks old ApoE<sup>-/-</sup> mice on chow diet, while, 20 weeks of C5 siRNA treatment did not reduce atherosclerosis in 32 weeks old ApoE<sup>-/-</sup> mice on 16 weeks high-fat diet. In both mouse models, we used liver-specific C5 siRNA. It is possible that 16 weeks high-fat diet leads to a higher CD68 macrophage content in atherosclerotic plaques, which produced higher local concentrations of C5 to compensate for the lack of serum C5. However, we cannot exclude other possibilities, for example, that high-fat diet triggered the reprogramming of myeloid blood cells, which may enter the plaque independent of complement activation, as evidenced by our finding that C5 siRNA treatment or C5 knockout<sup>63</sup> does not reduce plaque size in ApoE<sup>-/-</sup> mice on high-fat diet.

Hence, we propose that there may be two mechanisms to initiate atherosclerotic plaque inflammation: (i) complement C5-dependent initiation of atherosclerosis; (ii) complement C5-independent initiation of atherosclerosis. Further studies are clearly required to address this important unresolved question in the future. These data indicated that atherosclerosis might respond to anti-complement therapeutic approaches

depending on the diet whereby the extreme levels of hyperlipidemia in high-fat diet fed mice may overwhelm the innate immune system, which, in turn, becomes dysfunctional. We have pointed out previously that the immune system may be dysfunctional when lipid levels reach unphysiological extreme levels in ApoE<sup>-/-</sup> mice<sup>8</sup>.

Indeed, the observation that high-fat diet versus normal chow diet leads to two different outcomes in murine complement inhibition studies suggests that complement activation-dependent atherosclerosis in normal chow diet versus complement activation-independent atherosclerosis in high-fat diet are mechanistically distinct. The impact of high-fat diet on the immune system has been studied by several groups: (a) Hedrick CC et al. reported that the high-fat diet might create intensive oxidative stress and alter apolipoproteins in the circulation, which may evoke immunologic responses when compared to mice on chow diet<sup>128</sup>; (b) Dansky et al. studied the role of the recombinaase activating gene 1 (Rag-1) gene (important for T and B cell development) in ApoE<sup>-/-</sup> mice on a chow diet versus high-fat diet. Rag-1<sup>-/-</sup>ApoE<sup>-/-</sup> mice showed a significant decrease in atherosclerotic plaque size compared to ApoE<sup>-/-</sup> mice under chow diet at 16 weeks of age, while there was no significant difference in plaque size when the mice were of high-fat diet. These data support the hypothesis that high fat diet triggers atherosclerosis independent of T and B cells<sup>129</sup>; (c) Murphy et al. reported that high-fat diet induced myeloid cell proliferation in the bone marrow of ApoE<sup>-/-</sup> mice, compared to chow diet-treated ApoE<sup>-/-</sup> mice<sup>130</sup>; (d) Christ et al. reported that high-fat diet triggers inflammasome activation, transcriptomic, and epigenomic reprogramming of myeloid progenitor cells, which leads to more pro-inflammatory cytokine expression by myeloid cells<sup>131</sup>.

#### **4.4 Is the C5-dependent effect on atherosclerosis only the tip of an iceberg of a broader and possibly ubiquitous role of C5 and ApoE in unresolvable inflammation?**

The present data, together with those of Yin et al.<sup>95</sup>, show that two other and very

distinct types of unresolvable inflammation, i.e., in choroid plexus inflammation and Alzheimer's disease, are linked to ApoE. Moreover, the translational work in Yin et al. suggest that the experimental mouse data may be applicable to the respective human diseases. In view of the discovery of the ApoE-C1q complex and its presence in distinct diseased tissues, we propose that other diseases including chronic inflammatory diseases caused by persistent bacterial and other infections as well as inflammatory types of cancer should be studied to examine a broader role of the complex in chronic inflammation.

#### **4.5 Liver-derived complement component C5 vs. local produced C5 in atherosclerosis**

Complement mRNAs, i.e. C1q, C2, C3, C4 and C5 have been reported in human atherosclerotic plaques as analyzed by PCR<sup>55,56,132</sup>. These data revealed that some complement proteins are transcribed locally rather than being derived from the liver. Complement C5 protein localized with macrophages indicating that macrophages may produce C5 protein locally. Whaley et al. and Hetland et al. detected complement C3, factor B (fB), factor D (fD), C2, C4 and C5 mRNA expression from human blood monocyte-derived macrophages or macrophages in vitro indicating that the mRNAs of these complement components are derived from immune cells, i.e. macrophages, in atherosclerotic plaques<sup>113,133,134</sup>. Meanwhile, C5 mRNA (but not that of C1q or C3) was below the detection threshold by microarray in atherosclerotic plaque indicating that the great majority of C5 is serum-derived and is recruited into inflammatory sites; this finding made it possible to target liver-specific C5 (which is shown in the present work to decrease serum C5 by >95%) without compromising locally produced C5. Our data, therefore, provide the first evidence that liver-produced C5 promote atherosclerosis development in young ApoE<sup>-/-</sup> mice. Whether macrophage-derived C5 plays the same role in atherosclerosis, however, is still unclear.

Moreover, recent research has shown that complement can influence the adaptive immune response by modulating DC function and thus regulating antigen-specific T

cell responses. In addition, local production and activation of complement have been suggested to be critical for DC development<sup>135,136</sup>.

## **4.6 Complement studies in other atherosclerotic mouse models**

### **4.6.1 Complement component C5 in atherosclerosis**

Patel S et al. 2001 knocked out the C5 gene in ApoE<sup>-/-</sup> mice, then maintained the mice on a high-fat diet for 18 weeks. There was no significant difference in atherosclerotic plaque size in the aortic root when compared to ApoE<sup>-/-</sup> control. The content of macrophage-derived foam cells in atherosclerotic plaque was also not different<sup>63</sup>. This study of global C5 knockout is inconclusive, however, as it does not distinguish between liver- versus local complement expression and because it does rely on unphysiologically high cholesterol concentrations which are known to be little affected by immune cells. Manthey H et al. 2011 blocked the C5a receptor CD88 by injecting the CD88 antagonist - PMX53 - in ApoE<sup>-/-</sup> mice maintained on a normal chow diet for 25 weeks. PMX53 treatment significantly reduced atherosclerotic plaque size in the brachiocephalic artery at the age of 30 weeks<sup>48</sup>. CD88 expression has been shown to be expressed by endothelial cells, smooth muscle cells and macrophages in plaques, suggesting that PMX53 treatment blocked the binding of C5a to CD88 in plaques. These data support a detrimental role of activated complement cascades in atherosclerosis. The apparent contradictory observations between Patel S et al. 2001 and Manthey H et al. 2011 may due to several reasons: knockout C5 versus C5a receptors; high-fat diet versus normal chow diet; advanced atherosclerosis plaques in ApoE<sup>-/-</sup> mice fed with 18 weeks high-fat diet versus early atherosclerotic plaques in 30 weeks old ApoE<sup>-/-</sup> mice maintained on a chow diet. In the present work, liver-specific C5 siRNA was used to treat 4 experimental groups of mice, in particular (i) 76 weeks old ApoE<sup>-/-</sup> mice on normal chow diet; (ii) 32 weeks old ApoE<sup>-/-</sup> mice fed with normal chow diet; (iii) 32 weeks old ApoE<sup>-/-</sup> mice fed with 16 weeks high-fat diet; (iv) 16 weeks old ApoE<sup>-/-</sup> mice fed with 4 weeks high-fat diet. Therefore, a broad strategy was used

to clarify important unresolved issues regarding the role of C5 in atherogenesis. We conclude that C5 inhibition did not reduce atherosclerosis in ApoE<sup>-/-</sup> mice on a high-fat diet (group iii). Thus, my data provide evidence that different diet conditions are critical to understanding atherosclerosis inflammation as related to C5.

#### 4.6.2 Complement activation studies on atherosclerosis in ApoE<sup>-/-</sup> mice

In mouse atherosclerosis, the roles of complement pathways in atherosclerosis are not fully understood as several complement components, i.e. C1q and C3, are not only involved in complement activation but also involved in the control of other forms of tissue homeostasis<sup>137</sup>. However, blocking the complement activation products, i.e. C3a and C5a receptors, prevents atherosclerosis (Table 4.1).

#### 4.6.3 Complement activation on atherosclerosis in LDLr<sup>-/-</sup> mice

Several previous studies have suggested a role of complement cascade activation in the pathogenesis of atherosclerosis using the LDLr<sup>-/-</sup> mouse model. LDLr<sup>-/-</sup> mice fed a high-fat diet showed a significant increase in the mRNA expression of complement C3, factor D and properdin in the liver compared to LDLr<sup>-/-</sup> mice on normal chow, suggesting that complement pathway activation may be important in LDLr<sup>-/-</sup> mice<sup>138</sup>. LDLr<sup>-/-</sup> mice deficient in C1qa on a normal diet were shown to develop threefold larger aortic root lesions than C1qa-sufficient animals, but no differences were observed when mice were maintained on a high-fat diet<sup>61</sup>. In addition, increased *en-face* atherosclerotic lesion size was reported in C3<sup>-/-</sup>LDLr<sup>-/-</sup> mice compared to LDLr<sup>-/-</sup> controls on high-fat diet<sup>139</sup>. These data may reflect the protective role of complement cascade activation in the atherogenesis of LDLr<sup>-/-</sup> mice.

However, experiments on the decay-accelerating factor (Daf), CD55, which prevents the formation of the C3 convertases, and on another inhibitor, i.e. CD59, which regulate the formation of TCC, showed both that Daf<sup>-/-</sup>LDLr<sup>-/-</sup> mice<sup>142</sup> and aCD59<sup>-/-</sup>LDLr<sup>-/-</sup> mice<sup>143</sup> developed more extensive *en-face* lesions of the aorta than LDLr<sup>-/-</sup> mice on both low- and high-fat diet. Bf<sup>-/-</sup>LDLr<sup>-/-</sup> mice also had significantly decreased cross-sectional



aortic root lesion fraction areas and reduced lesion complexity compared with LDLr<sup>-/-</sup> mice after a 12-week period of high-fat diet<sup>140</sup>. These data indicate the disparate effects of upstream and terminal complement components; the deficiency of the complement system may protect the development of atherosclerosis in LDLr<sup>-/-</sup> mice (Table 4.1).

**Table 4.1 Complement proteins in experimental atherosclerosis models**

Increased atherosclerosis			
<i>Animal model</i>	<i>Diet</i>	<i>Effect on atherosclerotic plaque size</i>	<i>Reference</i>
C1q <sup>-/-</sup> LDLr <sup>-/-</sup> mice	Normal chow	Increased aortic root plaque size.	61
C3 <sup>-/-</sup> ApoE <sup>-/-</sup> LDLr <sup>-/-</sup> mice	Normal chow	Increased aortic <i>en-face</i> plaque size.	62
C3 <sup>-/-</sup> LDLr <sup>-/-</sup> mice	High-fat diet	Increased aortic <i>en-face</i> and aortic arch plaque size.	139
Decreased atherosclerosis			
<i>Animal model</i>	<i>Diet</i>	<i>Effect on atherosclerotic plaque size</i>	<i>Reference</i>
Factor B <sup>-/-</sup> LDLr <sup>-/-</sup> mice	High-fat diet	Decreased aortic root plaque size	140
C3aR <sup>-/-</sup> ApoE <sup>-/-</sup> mice	Normal chow	Decreased aortic root plaque size in females but not in males	141
Anti C5 antibody treat mCd59ab <sup>-/-</sup> ApoE <sup>-/-</sup> mice	High-fat diet	Reduced aortic <i>en-face</i> and aortic arch plaque size	112
C5aR antagonist on ApoE <sup>-/-</sup> mice	Normal chow	Reduced brachiocephalic arteries plaque burden	48
C6 <sup>-/-</sup> ApoE <sup>-/-</sup> mice	High-fat diet	Decreased brachiocephalic artery plaque size	60
Daf <sup>-/-</sup> LDLr <sup>-/-</sup> mice	High-fat diet	Increased aortic <i>en-face</i> stained lesion size	142
	Low-fat diet	Increased aortic <i>en-face</i> stained lesion size; Increased aortic root size and complexity	
aCD59 <sup>-/-</sup> LDLr <sup>-/-</sup> mice	High-fat diet	Increased aortic <i>en-face</i> stained lesion size	143
	Low-fat diet	Increased aortic <i>en-face</i> stained lesion size; Increased aortic root size and complexity	
No difference on atherosclerosis			
<i>Animal model</i>	<i>Diet</i>	<i>Effect on atherosclerotic plaque size</i>	<i>Reference</i>
C1q <sup>-/-</sup> LDLr <sup>-/-</sup> mice	High-fat diet	No difference in aortic root plaque size	61
Factor B <sup>-/-</sup> LDLr <sup>-/-</sup> mice	Normal chow	No difference in aortic root plaque size	140
Factor B <sup>-/-</sup> ApoE <sup>-/-</sup> LDLr <sup>-/-</sup> mice	Normal chow	No differences in aortic <i>en-face</i> and aortic root plaque size	62
C5 <sup>-/-</sup> ApoE <sup>-/-</sup> mice	High-fat diet	No differences in aortic root plaque size	63
Daf <sup>-/-</sup> LDLr <sup>-/-</sup> mice	High-fat diet	No differences in aortic root lesion size	142
aCD59 <sup>-/-</sup> LDLr <sup>-/-</sup> mice	High-fat diet	No differences in aortic root lesion size	143

The LDLr<sup>-/-</sup> mice are different from the ApoE<sup>-/-</sup> mouse model, which were used in our atherosclerosis study. In LDLr<sup>-/-</sup> mice, atherosclerotic lesions do not develop spontaneously as in ApoE<sup>-/-</sup> animals, but are inducible under high-fat diet.

#### **4.7 Can C5-dependent atherogenesis in mice be translated to human atherosclerosis?**

Human atherosclerosis is a chronic and complex disease of large and medium-sized arteries<sup>3</sup>. It takes decades to form atherosclerotic plaques in human arteries, and it is an age-dependent disease<sup>3</sup>. Human atherosclerotic plaques are heterogeneous containing multiple pathologies. Wild type mice do not develop atherosclerosis on a chow diet and only minimally on high-fat diet<sup>144</sup>. Several murine models have been used to mimic human atherosclerotic pathologies<sup>145,146</sup>. In mice, atherosclerotic plaques develop within a few weeks to few months, and the pathological features in murine models reproduce features of human atherosclerotic plaques. Yet, caution is warranted when data obtained in mice are translated to humans. I reported that lipid deposits in atherosclerosis plaque activated the complement cascades, which in turn triggered chronic inflammation in ApoE<sup>-/-</sup> mice. We reported that ApoE acts as endogenous complement inhibitor<sup>95</sup>, which may provide mechanistic insight for this observation. In order to validate whether lipid-complement-inflammation axis contributes to human atherosclerosis, we decided to stain complement C1q, ApoE, and C5 and CD68 using different stages of atherosclerotic plaques (Fig. 3.38). My data supported the conclusion that complement activation may indeed contribute to atherosclerosis inflammation in human atherosclerosis. However, complement-independent inflammation also contributes to atherosclerosis development in mice (ApoE<sup>-/-</sup> mice on high-fat diet). I hypothesize that human atherosclerotic plaques consist of both complement-triggered inflammation and complement-independent inflammation. Thus, more studies are required to clarify whether patients with cardiovascular diseases will benefit from complement C5 siRNA treatment. Based on these data, we believe that diets did not affect the efficiency of C5 siRNA in vivo. Moreover, in a phase 1/2 clinical

study, N-acetylgalactosamine-conjugated C5 siRNA (target human C5 mRNA, ALN-CC5, Alnylam® Pharmaceuticals) showed safety in healthy adult volunteers and patients with paroxysmal nocturnal hemoglobinuria (PNH) (clinicaltrials.gov; NCT02352493), and several clinical trials to treat complement-mediated diseases are ongoing (clinicaltrials.gov; NCT03841448, NCT03999840). These data support the concept that our approach in mice may be translatable to human patients with complement-mediated diseases including atherosclerosis.

#### **4.8 Young and aged ApoE<sup>-/-</sup> mice are suitable murine models to study of the roles of complement cascades in atherosclerosis**

Young ApoE<sup>-/-</sup> mice and aged ApoE<sup>-/-</sup> mice were used to study the different stages of atherosclerotic plaques. In young ApoE<sup>-/-</sup> mice on chow diet, the C5 siRNA treatment was started from the age of 12 weeks, when the mice had not yet developed visible plaques. After 20 weeks of treatment, C5 siRNA strongly reduced atherosclerotic plaque size and inflammation, supporting the conclusion that a presumed lipid-complement-inflammation axis promotes early atherosclerosis development. In aged ApoE<sup>-/-</sup> mice, the C5 siRNA treatment was started at the age of 58 weeks, when the mice had already developed atherosclerotic plaques. In advanced plaques, other pre-existing inflammatory triggers, i.e., cholesterol crystal, macrophage-foam cells or necrotic cores may trigger other pro-inflammatory pathways including inflammasomes<sup>127</sup>. We also performed immunofluorescence staining to confirm that those complement proteins are deposited in advanced plaques, and C5 siRNA treatment indeed reduced C5 deposited in advanced plaques in aged ApoE<sup>-/-</sup> mice fed with chow diet (Figures 3.23-3.24). However, the plaque size was not significantly reduced after C5 siRNA treatment in advanced plaques by *en-face* staining. Further studies are required to examine whether C5 siRNA treatment altered plaque stability.

As discussed above, C5 siRNA targeted liver-produced C5, but not locally produced C5. In aged ApoE<sup>-/-</sup> mice on chow diet, locally produced C5 by infiltrated T cells and monocytes may compensate C5 siRNA treatment which silenced serum C5 selectively.

These two different models may be regarded to represent early and advanced stages of atherosclerotic plaques in human diseases, respectively, and caution is required before translating murine data to human diseases. Complement proteins and inflammation have been observed in human atherosclerotic plaques, supporting those atherosclerotic plaques in young and aged ApoE<sup>-/-</sup> mice are adequate murine models to study the impact the roles of complement activation in atherosclerosis.

## 5. SUMMARY

Atherosclerosis can be viewed as an age-dependent chronic inflammatory disease of arteries which constitutes the leading cause of deaths worldwide. Complement cascades are major constituents of innate immunity and also significantly contribute to adaptive immune responses. Complement components have been found in human atherosclerotic plaques, but their roles in disease progression have been found to yield often contradictory outcomes. In the current study, the roles of liver-derived complement C5 during different stages of atherosclerosis using ApoE-deficient mice at various ages as experimental models for human age-related chronic inflammatory diseases were explored. C5 constitutes a final protein product of all three complement cascades which undergoes a final cleavage reaction to yield highly active molecules in innate immunity. Under normal chow, we chose to study atherosclerosis in young versus aged mice, which represent early and advanced stages of atherosclerosis, respectively. When we challenged ApoE<sup>-/-</sup> mice with a high-fat diet, the development of atherosclerotic plaque was exacerbated under conditions of extreme hyperlipidemia. Our data are consistent with the possibility that there are two distinct mechanisms underlying the progression of atherosclerosis depending on the dietary condition: One which is dependent on complement and the other which is independent on complement C5 under extreme hyperlipidemia. Moreover, our observation of a strict age-dependency of the effect of C5 siRNA on disease outcome uncovers the involvement of C5 in early but not advanced atherosclerosis. When taken together, the current study allows studying the roles of complement inhibition during different stages and different types of dietary conditions. These data are likely to encourage future studies into the molecular mechanisms of complement-sensitive pro-atherosclerotic events, which in turn may lead to new therapeutic approaches to treat and/or prevent atherosclerosis.

## 6. ZUSAMMENFASSUNG

Atherosklerose kann als eine altersabhängige chronische Entzündung der Arterienwand angesehen werden, die als Ursache für die weltweit führende Todesursache gilt. Komplementkaskaden sind wesentlich an angeborenen Immunreaktionen beteiligt und spielen auch wichtige Rollen an den Schnittstellen zwischen angeborenen und adaptiven Immunreaktionen. Ihre Proproteine und aktive Konstituenten wurden bereits früher in atherosklerotischen Plaques beobachtet. Allerdings haben Untersuchungen ihrer Funktion kontroverse Ergebnisse gezeigt. In dieser Promotionsarbeit wurde die Rolle des in der Leber synthetisierten Komplementproteins C5 in murinen Modellen der Atherosklerose untersucht, d.h. der ApoE-defizienten Maus. C5 wird vor allem in der Leber produziert und stellt ein Proprotein am Ende aller drei Komplementkaskaden dar. Unter normalen Diätbedingungen (normales Mausfutter) konnte gezeigt werden, dass die Inhibition der C5 Transkription durch ein Leber-spezifisches C5 siRNA Molekül zu einer signifikanten Reduktion der Progression der Atherosclerose in jungen ApoE-defizienten Mäusen führt, während die Effekte des gleichen Moleküls in alten Mäusen nicht zu beobachten waren. C5 siRNA hatte ebenfalls keine Effekte auf die Ausprägung der Erkrankung in Untersuchungen von ApoE-defizienten Mäusen, die einer hochkalorischen Nahrung mit einem hohen Fettgehalt (der Western Diät) unterzogen wurden. Diese Ergebnisse deuten an, dass es zwei distinkte altersabhängige Formen der Atherosklerose gibt: Eine frühe Form, die auf eine Therapie mit C5 Therapeutika anspricht und einer fortgeschrittenen Form, die resistent gegen diese Therapeutika ist. Die Daten zeigen auch, dass die klassische Komplementkaskade eine Rolle unter Bedingungen der moderaten nicht aber der extremen Hyperlipidämie, wie sie durch eine hochkalorische Diät mit einem hohen Fettgehalt erreicht wird, spielt. Diese Ergebnisse können als Grundlage dienen, die molekularen Mechanismen des C5 Proteins in einer prototypischen chronisch entzündlichen Erkrankung, der Atherosklerose, aufzudecken, um neue Therapiestrategien dieser kausal nicht therapierbaren Erkrankung zu entwickeln.

## 7. REFERENCES

- 1 Buttar, H. S., Li, T. & Ravi, N. Prevention of cardiovascular diseases: Role of exercise, dietary interventions, obesity and smoking cessation. *Exp Clin Cardiol* **10**, 229-249, (2005).
- 2 Glass, C. K. & Witztum, J. L. Atherosclerosis. the road ahead. *Cell* **104**, 503-516, (2001).
- 3 Ross, R. Atherosclerosis--an inflammatory disease. *N Engl J Med* **340**, 115-126, (1999).
- 4 Hansson, G. K. & Hermansson, A. The immune system in atherosclerosis. *Nat Immunol* **12**, 204-212, (2011).
- 5 Libby, P. Inflammation in atherosclerosis. *Arterioscler Thromb Vasc Biol* **32**, 2045-2051, (2012).
- 6 Liu, L. *et al.* Imaging the subcellular structure of human coronary atherosclerosis using micro-optical coherence tomography. *Nat Med* **17**, 1010-1014, (2011).
- 7 Ashley, E. A. & Niebauer, J. in *Cardiology Explained* (2004).
- 8 Mohanta, S. K. *et al.* Artery tertiary lymphoid organs contribute to innate and adaptive immune responses in advanced mouse atherosclerosis. *Circ Res* **114**, 1772-1787, (2014).
- 9 Weber, C. & Noels, H. Atherosclerosis: current pathogenesis and therapeutic options. *Nat Med* **17**, 1410-1422, (2011).
- 10 Libby, P. Inflammation in atherosclerosis. *Nature* **420**, 868-874, (2002).
- 11 Raines, E. W. The extracellular matrix can regulate vascular cell migration, proliferation, and survival: relationships to vascular disease. *Int J Exp Pathol* **81**, 173-182, (2000).
- 12 Lusis, A. J. Atherosclerosis. *Nature* **407**, 233-241, (2000).
- 13 Bobryshev, Y. V. & Lord, R. S. S-100 positive cells in human arterial intima and in atherosclerotic lesions. *Cardiovasc Res* **29**, 689-696, (1995).

- 14 Jonasson, L., Holm, J., Skalli, O., Bondjers, G. & Hansson, G. K. Regional accumulations of T cells, macrophages, and smooth muscle cells in the human atherosclerotic plaque. *Arteriosclerosis* **6**, 131-138, (1986).
- 15 Carpentier, J. L. *et al.* Binding and internalization of <sup>125</sup>I-LDL in normal and mutant human fibroblasts. A quantitative autoradiographic study. *Exp Cell Res* **121**, 135-142, (1979).
- 16 Steinman, R. M. Decisions about dendritic cells: past, present, and future. *Annu Rev Immunol* **30**, 1-22, (2012).
- 17 Subramanian, M., Thorp, E., Hansson, G. K. & Tabas, I. Treg-mediated suppression of atherosclerosis requires MYD88 signaling in DCs. *J Clin Invest* **123**, 179-188, (2013).
- 18 Koltsova, E. K. & Ley, K. How dendritic cells shape atherosclerosis. *Trends Immunol* **32**, 540-547, (2011).
- 19 Xu, Q. B., Oberhuber, G., Gruschwitz, M. & Wick, G. Immunology of atherosclerosis: cellular composition and major histocompatibility complex class II antigen expression in aortic intima, fatty streaks, and atherosclerotic plaques in young and aged human specimens. *Clin Immunol Immunopathol* **56**, 344-359, (1990).
- 20 van der Wal, A. C., Das, P. K., Bentz van de Berg, D., van der Loos, C. M. & Becker, A. E. Atherosclerotic lesions in humans. In situ immunophenotypic analysis suggesting an immune mediated response. *Lab Invest* **61**, 166-170, (1989).
- 21 Kleindienst, R. *et al.* Immunology of atherosclerosis. Demonstration of heat shock protein 60 expression and T lymphocytes bearing alpha/beta or gamma/delta receptor in human atherosclerotic lesions. *Am J Pathol* **142**, 1927-1937, (1993).
- 22 Hayday, A. C. [gamma][delta] cells: a right time and a right place for a conserved third way of protection. *Annu Rev Immunol* **18**, 975-1026, (2000).
- 23 Jackson, C. L. Is there life after plaque rupture? *Biochem Soc Trans* **35**, 887-889, (2007).
- 24 Kinderlerer, A. R. *et al.* Statin-induced expression of CD59 on vascular endothelium in hypoxia: a potential mechanism for the anti-inflammatory actions of statins in rheumatoid arthritis. *Arthritis Res Ther* **8**, R130, (2006).



- 
- 25 Mason, J. C. *et al.* Statin-induced expression of decay-accelerating factor protects vascular endothelium against complement-mediated injury. *Circ Res* **91**, 696-703, (2002).
- 26 Nakamura, K. *et al.* Statin prevents plaque disruption in apoE-knockout mouse model through pleiotropic effect on acute inflammation. *Atherosclerosis* **206**, 355-361, (2009).
- 27 Zhang, S. H., Reddick, R. L., Piedrahita, J. A. & Maeda, N. Spontaneous hypercholesterolemia and arterial lesions in mice lacking apolipoprotein E. *Science* **258**, 468-471, (1992).
- 28 Plump, A. S. *et al.* Severe hypercholesterolemia and atherosclerosis in apolipoprotein E-deficient mice created by homologous recombination in ES cells. *Cell* **71**, 343-353, (1992).
- 29 Jawien, J., Nastalek, P. & Korbut, R. Mouse models of experimental atherosclerosis. *J Physiol Pharmacol* **55**, 503-517, (2004).
- 30 Nakashima, Y., Plump, A. S., Raines, E. W., Breslow, J. L. & Ross, R. ApoE-deficient mice develop lesions of all phases of atherosclerosis throughout the arterial tree. *Arterioscler Thromb* **14**, 133-140, (1994).
- 31 Ishibashi, S. *et al.* Hypercholesterolemia in low density lipoprotein receptor knockout mice and its reversal by adenovirus-mediated gene delivery. *J Clin Invest* **92**, 883-893, (1993).
- 32 Joven, J. *et al.* The results in rodent models of atherosclerosis are not interchangeable: the influence of diet and strain. *Atherosclerosis* **195**, e85-92, (2007).
- 33 Rosenfeld, M. E. *et al.* Advanced atherosclerotic lesions in the innominate artery of the ApoE knockout mouse. *Arterioscler Thromb Vasc Biol* **20**, 2587-2592, (2000).
- 34 Johnson, J. L. & Jackson, C. L. Atherosclerotic plaque rupture in the apolipoprotein E knockout mouse. *Atherosclerosis* **154**, 399-406, (2001).
- 35 Rosenfeld, M. E., Averill, M. M., Bennett, B. J. & Schwartz, S. M. Progression and disruption of advanced atherosclerotic plaques in murine models. *Curr Drug Targets* **9**, 210-216, (2008).
- 36 van Ree, J. H. *et al.* Diet-induced hypercholesterolemia and atherosclerosis in heterozygous apolipoprotein E-deficient mice. *Atherosclerosis* **111**, 25-37, (1994).

- 37 Reddick, R. L., Zhang, S. H. & Maeda, N. Atherosclerosis in mice lacking apo E. Evaluation of lesional development and progression. *Arteriosclerosis and Thrombosis: A Journal of Vascular Biology* **14**, 141-147, (1994).
- 38 Nesargikar, P. N., Spiller, B. & Chavez, R. The complement system: history, pathways, cascade and inhibitors. *Eur J Microbiol Immunol (Bp)* **2**, 103-111, (2012).
- 39 Chaplin, H., Jr. Review: the burgeoning history of the complement system 1888-2005. *Immunohematology* **21**, 85-93, (2005).
- 40 Walport, M. J. Complement. Second of two parts. *N Engl J Med* **344**, 1140-1144, (2001).
- 41 Daly, N. L., Scanlon, M. J., Djordjevic, J. T., Kroon, P. A. & Smith, R. Three-dimensional structure of a cysteine-rich repeat from the low-density lipoprotein receptor. *Proc Natl Acad Sci U S A* **92**, 6334-6338, (1995).
- 42 Walport, M. J. Complement. First of two parts. *N Engl J Med* **344**, 1058-1066, (2001).
- 43 Qin, X. & Gao, B. The complement system in liver diseases. *Cell Mol Immunol* **3**, 333-340, (2006).
- 44 Zhou, Z., Xu, M. J. & Gao, B. Hepatocytes: a key cell type for innate immunity. *Cell Mol Immunol* **13**, 301-315, (2016).
- 45 Esser, A. F. The membrane attack complex of complement. Assembly, structure and cytotoxic activity. *Toxicology* **87**, 229-247, (1994).
- 46 Zipfel, P. F. & Skerka, C. Complement regulators and inhibitory proteins. *Nat Rev Immunol* **9**, 729-740, (2009).
- 47 Monk, P. N., Scola, A. M., Madala, P. & Fairlie, D. P. Function, structure and therapeutic potential of complement C5a receptors. *Br J Pharmacol* **152**, 429-448, (2007).
- 48 Manthey, H. D. *et al.* Complement C5a inhibition reduces atherosclerosis in ApoE<sup>-/-</sup> mice. *FASEB J* **25**, 2447-2455, (2011).
- 49 Hivroz, C., Fischer, E., Kazatchkine, M. D. & Grillot-Courvalin, C. Differential effects of the stimulation of complement receptors CR1 (CD35) and CR2 (CD21) on cell proliferation and intracellular Ca<sup>2+</sup> mobilization of chronic lymphocytic leukemia B cells. *J Immunol* **146**, 1766-1772, (1991).

- 50 Subramanian, V. B., Clemenza, L., Krych, M. & Atkinson, J. P. Substitution of two amino acids confers C3b binding to the C4b binding site of CR1 (CD35). Analysis based on ligand binding by chimpanzee erythrocyte complement receptor. *J Immunol* **157**, 1242-1247, (1996).
- 51 Hebell, T., Ahearn, J. M. & Fearon, D. T. Suppression of the immune response by a soluble complement receptor of B lymphocytes. *Science* **254**, 102-105, (1991).
- 52 Pekalski, M. L. *et al.* Neonatal and adult recent thymic emigrants produce IL-8 and express complement receptors CR1 and CR2. *JCI Insight* **2**, (2017).
- 53 Wagner, C. *et al.* The complement receptor 3, CR3 (CD11b/CD18), on T lymphocytes: activation-dependent up-regulation and regulatory function. *Eur J Immunol* **31**, 1173-1180, (2001).
- 54 Ben Nasr, A. *et al.* Critical role for serum opsonins and complement receptors CR3 (CD11b/CD18) and CR4 (CD11c/CD18) in phagocytosis of *Francisella tularensis* by human dendritic cells (DC): uptake of *Francisella* leads to activation of immature DC and intracellular survival of the bacteria. *J Leukoc Biol* **80**, 774-786, (2006).
- 55 Niculescu, F., Rus, H., Cristea, A. & Vlaicu, R. Localization of the terminal C5b-9 complement complex in the human aortic atherosclerotic wall. *Immunol Lett* **10**, 109-114, (1985).
- 56 Vlaicu, R., Niculescu, F., Rus, H. G. & Cristea, A. Immunohistochemical localization of the terminal C5b-9 complement complex in human aortic fibrous plaque. *Atherosclerosis* **57**, 163-177, (1985).
- 57 Niculescu, F., Rus, H. G. & Vlaicu, R. Decay-accelerating factor regulates complement-mediated damage in the human atherosclerotic wall. *Immunol Lett* **26**, 17-23, (1990).
- 58 Seifert, P. S. & Hansson, G. K. Complement receptors and regulatory proteins in human atherosclerotic lesions. *Arteriosclerosis* **9**, 802-811, (1989).
- 59 Yasojima, K., Schwab, C., McGeer, E. G. & McGeer, P. L. Complement components, but not complement inhibitors, are upregulated in atherosclerotic plaques. *Arterioscler Thromb Vasc Biol* **21**, 1214-1219, (2001).

- 60 Lewis, R. D., Jackson, C. L., Morgan, B. P. & Hughes, T. R. The membrane attack complex of complement drives the progression of atherosclerosis in apolipoprotein E knockout mice. *Mol Immunol* **47**, 1098-1105, (2010).
- 61 Bhatia, V. K. *et al.* Complement C1q reduces early atherosclerosis in low-density lipoprotein receptor-deficient mice. *Am J Pathol* **170**, 416-426, (2007).
- 62 Persson, L. *et al.* Lack of complement factor C3, but not factor B, increases hyperlipidemia and atherosclerosis in apolipoprotein E<sup>-/-</sup> low-density lipoprotein receptor<sup>-/-</sup> mice. *Arterioscler Thromb Vasc Biol* **24**, 1062-1067, (2004).
- 63 Patel, S. *et al.* ApoE<sup>(-/-)</sup> mice develop atherosclerosis in the absence of complement component C5. *Biochem Biophys Res Commun* **286**, 164-170, (2001).
- 64 Ricklin, D. & Lambris, J. D. Complement in immune and inflammatory disorders: therapeutic interventions. *J Immunol* **190**, 3839-3847, (2013).
- 65 Gasque, P. *et al.* Roles of the complement system in human neurodegenerative disorders: pro-inflammatory and tissue remodeling activities. *Mol Neurobiol* **25**, 1-17, (2002).
- 66 Hajishengallis, G. & Lambris, J. D. Complement-targeted therapeutics in periodontitis. *Adv Exp Med Biol* **735**, 197-206, (2013).
- 67 Parra, S. *et al.* Complement system and small HDL particles are associated with subclinical atherosclerosis in SLE patients. *Atherosclerosis* **225**, 224-230, (2012).
- 68 Kolev, M. V., Ruseva, M. M., Harris, C. L., Morgan, B. P. & Donev, R. M. Implication of complement system and its regulators in Alzheimer's disease. *Curr Neuropharmacol* **7**, 1-8, (2009).
- 69 Zipfel, P. F., Lauer, N. & Skerka, C. The role of complement in AMD. *Adv Exp Med Biol* **703**, 9-24, (2010).
- 70 Zipfel, P. F. & Skerka, C. Complement dysfunction in hemolytic uremic syndrome. *Curr Opin Rheumatol* **18**, 548-555, (2006).
- 71 Marti-Carvajal, A. J., Anand, V., Cardona, A. F. & Sola, I. Eculizumab for treating patients with paroxysmal nocturnal hemoglobinuria. *Cochrane Database Syst Rev*, CD010340, (2014).

- 72 Hollan, I. *et al.* Cardiovascular disease in autoimmune rheumatic diseases. *Autoimmun Rev* **12**, 1004-1015, (2013).
- 73 Kusner, L. L. *et al.* Investigational RNAi Therapeutic Targeting C5 Is Efficacious in Pre-clinical Models of Myasthenia Gravis. *Mol Ther Methods Clin Dev* **13**, 484-492, (2019).
- 74 Parker, C. *et al.* Diagnosis and management of paroxysmal nocturnal hemoglobinuria. *Blood* **106**, 3699-3709, (2005).
- 75 Schroder-Braunstein, J. & Kirschfink, M. Complement deficiencies and dysregulation: Pathophysiological consequences, modern analysis, and clinical management. *Mol Immunol* **114**, 299-311, (2019).
- 76 Nozaki, M. *et al.* Drusen complement components C3a and C5a promote choroidal neovascularization. *Proc Natl Acad Sci U S A* **103**, 2328-2333, (2006).
- 77 Davidson, A. What is damaging the kidney in lupus nephritis? *Nat Rev Rheumatol* **12**, 143-153, (2016).
- 78 Lintner, K. E. *et al.* Early Components of the Complement Classical Activation Pathway in Human Systemic Autoimmune Diseases. *Front Immunol* **7**, 36, (2016).
- 79 Sano, Y. *et al.* Hereditary deficiency of the third component of complement in two sisters with systemic lupus erythematosus-like symptoms. *Arthritis Rheum* **24**, 1255-1260, (1981).
- 80 Manzi, S. *et al.* Age-specific incidence rates of myocardial infarction and angina in women with systemic lupus erythematosus: comparison with the Framingham Study. *Am J Epidemiol* **145**, 408-415, (1997).
- 81 Manderson, A. P., Botto, M. & Walport, M. J. The role of complement in the development of systemic lupus erythematosus. *Annu Rev Immunol* **22**, 431-456, (2004).
- 82 Crowson, A. N. & Magro, C. M. Deposition of membrane attack complex in cutaneous lesions of lupus erythematosus. *J Am Acad Dermatol* **31**, 515-516, (1994).
- 83 Kim, J. S., Lee, J. W., Kim, B. K., Lee, J. H. & Chung, J. The use of the complement inhibitor eculizumab (Soliris(R)) for treating Korean patients with paroxysmal nocturnal hemoglobinuria. *Korean J Hematol* **45**, 269-274, (2010).

- 84 Yamada, Y., Abe, R., Okano, Y. & Miyakawa, Y. Long-term Eculizumab Treatment Contributes to Recovery from End-stage Renal Disease Caused by Atypical Hemolytic Uremic Syndrome. *Intern Med* **56**, 1085-1088, (2017).
- 85 Fleisig, A. J. & Verrier, E. D. Pexelizumab -- a C5 complement inhibitor for use in both acute myocardial infarction and cardiac surgery with cardiopulmonary bypass. *Expert Opin Biol Ther* **5**, 833-839, (2005).
- 86 Borodovsky, A. *et al.* ALN-CC5, an Investigational RNAi Therapeutic Targeting C5 for Complement Inhibition. (2014).
- 87 Huang, Y. Preclinical and Clinical Advances of GalNAc-Decorated Nucleic Acid Therapeutics. *Mol Ther Nucleic Acids* **6**, 116-132, (2017).
- 88 Mehta, G., Scheinman, R. I., Holers, V. M. & Banda, N. K. A New Approach for the Treatment of Arthritis in Mice with a Novel Conjugate of an Anti-C5aR1 Antibody and C5 Small Interfering RNA. *J Immunol* **194**, 5446-5454, (2015).
- 89 Wang, Y. *et al.* Amelioration of lupus-like autoimmune disease in NZB/WF1 mice after treatment with a blocking monoclonal antibody specific for complement component C5. *Proc Natl Acad Sci U S A* **93**, 8563-8568, (1996).
- 90 Weerth, S. H., Rus, H., Shin, M. L. & Raine, C. S. Complement C5 in experimental autoimmune encephalomyelitis (EAE) facilitates remyelination and prevents gliosis. *Am J Pathol* **163**, 1069-1080, (2003).
- 91 Xiao, H. *et al.* C5a receptor (CD88) blockade protects against MPO-ANCA GN. *J Am Soc Nephrol* **25**, 225-231, (2014).
- 92 Veillard, N. R., Steffens, S., Burger, F., Pelli, G. & Mach, F. Differential expression patterns of proinflammatory and antiinflammatory mediators during atherogenesis in mice. *Arterioscler Thromb Vasc Biol* **24**, 2339-2344, (2004).
- 93 Daugherty, A. & Rateri, D. L. Development of experimental designs for atherosclerosis studies in mice. *Methods* **36**, 129-138, (2005).
- 94 Bianchini, M. *et al.* PD-L1 expression on nonclassical monocytes reveals their origin and immunoregulatory function. *Sci Immunol* **4**, (2019).
- 95 Yin, C. *et al.* ApoE attenuates unresolvable inflammation by complex formation with activated C1q. *Nat Med*, (2019).

- 96 Yin, C. *et al.* Generation of Aorta Transcript Atlases of Wild-Type and Apolipoprotein E-null Mice by Laser Capture Microdissection-Based mRNA Expression Microarrays. *Methods Mol Biol* **1339**, 297-308, (2015).
- 97 Grabner, R. *et al.* Lymphotoxin beta receptor signaling promotes tertiary lymphoid organogenesis in the aorta adventitia of aged ApoE<sup>-/-</sup> mice. *J Exp Med* **206**, 233-248, (2009).
- 98 Arlaud, G. J., Biro, A. & Ling, W. L. Enzymatically modified low-density lipoprotein is recognized by c1q and activates the classical complement pathway. *J Lipids* **2011**, 376092, (2011).
- 99 Colten, H. R., Ooi, Y. M. & Edelson, P. J. Synthesis and secretion of complement proteins by macrophages. *Ann N Y Acad Sci* **332**, 482-490, (1979).
- 100 Ottonello, L. *et al.* rC5a directs the in vitro migration of human memory and naive tonsillar B lymphocytes: implications for B cell trafficking in secondary lymphoid tissues. *J Immunol* **162**, 6510-6517, (1999).
- 101 Mohanta, S., Yin, C., Weber, C., Hu, D. & Habenicht, A. J. Aorta Atherosclerosis Lesion Analysis in Hyperlipidemic Mice. *Bio Protoc* **6**, (2016).
- 102 Niculescu, F., Rus, H. G. & Vlaicu, R. Activation of the human terminal complement pathway in atherosclerosis. *Clin Immunol Immunopathol* **45**, 147-155, (1987).
- 103 Niculescu, F. & Rus, H. Complement activation and atherosclerosis. *Mol Immunol* **36**, 949-955, (1999).
- 104 Seifert, P. S. & Kazatchkine, M. D. The complement system in atherosclerosis. *Atherosclerosis* **73**, 91-104, (1988).
- 105 Tsipis, A., Athanassiadou, A. M., Petrou, E. & Iakovou, I. Novel oral anticoagulants in peripheral arterial and coronary artery disease. *Cardiovasc Hematol Agents Med Chem* **12**, 21-25, (2014).
- 106 Roda, A. R., Montoliu-Gaya, L. & Villegas, S. The Role of Apolipoprotein E Isoforms in Alzheimer's Disease. *J Alzheimers Dis*, (2019).
- 107 Emamzadeh, F. N., Aojula, H., McHugh, P. C. & Allsop, D. Effects of different isoforms of apoE on aggregation of the alpha-synuclein protein implicated in Parkinson's disease. *Neurosci Lett* **618**, 146-151, (2016).

- 108 Mahley, R. W., Weisgraber, K. H. & Huang, Y. Apolipoprotein E: structure determines function, from atherosclerosis to Alzheimer's disease to AIDS. *J Lipid Res* **50 Suppl**, S183-188, (2009).
- 109 Manthey, H. D., Woodruff, T. M., Taylor, S. M. & Monk, P. N. Complement component 5a (C5a). *Int J Biochem Cell Biol* **41**, 2114-2117, (2009).
- 110 Li, B. *et al.* Molecular mechanism of inhibitory effects of CD59 gene on atherosclerosis in ApoE (-/-) mice. *Immunol Lett* **156**, 68-81, (2013).
- 111 An, G. *et al.* CD59 but not DAF deficiency accelerates atherosclerosis in female ApoE knockout mice. *Mol Immunol* **46**, 1702-1709, (2009).
- 112 Wu, G. *et al.* Complement regulator CD59 protects against atherosclerosis by restricting the formation of complement membrane attack complex. *Circ Res* **104**, 550-558, (2009).
- 113 Whaley, K. Biosynthesis of the complement components and the regulatory proteins of the alternative complement pathway by human peripheral blood monocytes. *J Exp Med* **151**, 501-516, (1980).
- 114 Ezkurdia, I. *et al.* Multiple evidence strands suggest that there may be as few as 19,000 human protein-coding genes. *Hum Mol Genet* **23**, 5866-5878, (2014).
- 115 Oksjoki, R. *et al.* Receptors for the anaphylatoxins C3a and C5a are expressed in human atherosclerotic coronary plaques. *Atherosclerosis* **195**, 90-99, (2007).
- 116 Gasque, P., Singhrao, S. K., Neal, J. W., Gotze, O. & Morgan, B. P. Expression of the receptor for complement C5a (CD88) is up-regulated on reactive astrocytes, microglia, and endothelial cells in the inflamed human central nervous system. *Am J Pathol* **150**, 31-41, (1997).
- 117 Wang, J. C. & Bennett, M. Aging and atherosclerosis: mechanisms, functional consequences, and potential therapeutics for cellular senescence. *Circ Res* **111**, 245-259, (2012).
- 118 Ziemann, S. & Kass, D. Advanced glycation end product cross-linking: pathophysiologic role and therapeutic target in cardiovascular disease. *Congest Heart Fail* **10**, 144-149; quiz 150-141, (2004).



- 119 Astrand, H. *et al.* In vivo estimation of the contribution of elastin and collagen to the mechanical properties in the human abdominal aorta: effect of age and sex. *J Appl Physiol (1985)* **110**, 176-187, (2011).
- 120 Franklin, S. S. *et al.* Hemodynamic patterns of age-related changes in blood pressure. The Framingham Heart Study. *Circulation* **96**, 308-315, (1997).
- 121 Lutgens, E. *et al.* Biphasic pattern of cell turnover characterizes the progression from fatty streaks to ruptured human atherosclerotic plaques. *Cardiovasc Res* **41**, 473-479, (1999).
- 122 Matthews, C. *et al.* Vascular smooth muscle cells undergo telomere-based senescence in human atherosclerosis: effects of telomerase and oxidative stress. *Circ Res* **99**, 156-164, (2006).
- 123 Ogami, M. *et al.* Telomere shortening in human coronary artery diseases. *Arterioscler Thromb Vasc Biol* **24**, 546-550, (2004).
- 124 Calvert, P. A. *et al.* Leukocyte telomere length is associated with high-risk plaques on virtual histology intravascular ultrasound and increased proinflammatory activity. *Arterioscler Thromb Vasc Biol* **31**, 2157-2164, (2011).
- 125 Zhou, X., Perez, F., Han, K. & Jurivich, D. A. Clonal senescence alters endothelial ICAM-1 function. *Mech Ageing Dev* **127**, 779-785, (2006).
- 126 Song, Y. *et al.* Aging enhances the basal production of IL-6 and CCL2 in vascular smooth muscle cells. *Arterioscler Thromb Vasc Biol* **32**, 103-109, (2012).
- 127 Duewell, P. *et al.* NLRP3 inflammasomes are required for atherogenesis and activated by cholesterol crystals. *Nature* **464**, 1357-1361, (2010).
- 128 Hedrick, C. C. *et al.* Short-term feeding of atherogenic diet to mice results in reduction of HDL and paraoxonase that may be mediated by an immune mechanism. *Arterioscler Thromb Vasc Biol* **20**, 1946-1952, (2000).
- 129 Dansky, H. M., Charlton, S. A., Harper, M. M. & Smith, J. D. T and B lymphocytes play a minor role in atherosclerotic plaque formation in the apolipoprotein E-deficient mouse. *Proc Natl Acad Sci U S A* **94**, 4642-4646, (1997).

- 130 Murphy, A. J. *et al.* ApoE regulates hematopoietic stem cell proliferation, monocytosis, and monocyte accumulation in atherosclerotic lesions in mice. *J Clin Invest* **121**, 4138-4149, (2011).
- 131 Christ, A. *et al.* Western Diet Triggers NLRP3-Dependent Innate Immune Reprogramming. *Cell* **172**, 162-175 e114, (2018).
- 132 Vlaicu, R., Rus, H. G., Niculescu, F. & Cristea, A. Immunoglobulins and complement components in human aortic atherosclerotic intima. *Atherosclerosis* **55**, 35-50, (1985).
- 133 Hetland, G., Johnson, E. & Aasebo, U. Human alveolar macrophages synthesize the functional alternative pathway of complement and active C5 and C9 in vitro. *Scand J Immunol* **24**, 603-608, (1986).
- 134 Hetland, G., Johnson, E., Falk, R. J. & Eskeland, T. Synthesis of complement components C5, C6, C7, C8 and C9 in vitro by human monocytes and assembly of the terminal complement complex. *Scand J Immunol* **24**, 421-428, (1986).
- 135 Peng, Q., Li, K., Patel, H., Sacks, S. H. & Zhou, W. Dendritic cell synthesis of C3 is required for full T cell activation and development of a Th1 phenotype. *J Immunol* **176**, 3330-3341, (2006).
- 136 Peng, Q. *et al.* Local production and activation of complement up-regulates the allostimulatory function of dendritic cells through C3a-C3aR interaction. *Blood* **111**, 2452-2461, (2008).
- 137 Kolev, M., Le Friec, G. & Kemper, C. Complement--tapping into new sites and effector systems. *Nat Rev Immunol* **14**, 811-820, (2014).
- 138 Recinos, A., 3rd *et al.* Liver gene expression associated with diet and lesion development in atherosclerosis-prone mice: induction of components of alternative complement pathway. *Physiol Genomics* **19**, 131-142, (2004).
- 139 Buono, C. *et al.* Influence of C3 deficiency on atherosclerosis. *Circulation* **105**, 3025-3031, (2002).
- 140 Malik, T. H. *et al.* The alternative pathway is critical for pathogenic complement activation in endotoxin- and diet-induced atherosclerosis in low-density lipoprotein receptor-deficient mice. *Circulation* **122**, 1948-1956, (2010).

- 141 Yang, X. *et al.* Identification and validation of genes affecting aortic lesions in mice. *J Clin Invest* **120**, 2414-2422, (2010).
- 142 Leung, V. W. *et al.* Decay-accelerating factor suppresses complement C3 activation and retards atherosclerosis in low-density lipoprotein receptor-deficient mice. *Am J Pathol* **175**, 1757-1767, (2009).
- 143 Yun, S., Leung, V. W., Botto, M., Boyle, J. J. & Haskard, D. O. Brief report: accelerated atherosclerosis in low-density lipoprotein receptor-deficient mice lacking the membrane-bound complement regulator CD59. *Arterioscler Thromb Vasc Biol* **28**, 1714-1716, (2008).
- 144 Paigen, B. Genetics of responsiveness to high-fat and high-cholesterol diets in the mouse. *Am J Clin Nutr* **62**, 458S-462S, (1995).
- 145 Getz, G. S. & Reardon, C. A. Diet and murine atherosclerosis. *Arterioscler Thromb Vasc Biol* **26**, 242-249, (2006).
- 146 Getz, G. S. & Reardon, C. A. Diet, Microbes, and Murine Atherosclerosis. *Arterioscler Thromb Vasc Biol* **38**, 2269-2271, (2018).

## 8. ACKNOWLEDGEMENTS

I would like to express my special thanks of gratitude to my supervisors Univ.-Prof. Dr. rer. nat. Sabine Steffens who gave me the opportunity to do this wonderful project. Without her close supervision, constant encouragement, advice and constructive criticism, my Ph.D. work would never have been possible.

I would like to give my warmest thanks to Prof. Dr. med. Andreas JR Habenicht for all the suggestions, supports and generous help.

It was a great pleasure to work with a cheerful and friendly group of colleagues, and I would like to thank them for their help. During my past few years, I have been advised and aided intensively by Dr. Chuangjun Yin, an experienced and enthusiastic researcher, whose supervision, contributions, and suggestions during my training and research work have enabled me to produce this work. I would also like to acknowledge Dr. Sarajo Mohanta for his crucial comments, encouragement, and suggestions during generous help. I am very thankful to Dr. Desheng Hu for his help with FACS work. I would like to give thanks to Dr. Xavier Blanchet for his support and training regarding ELISA.

I would like to take this opportunity to express my immense gratitude to all the past and present members of the Habenicht lab who have given their invaluable support and assistance. Additionally, I will like to thank the China Scholarship Council (CSC) for the funding during my Doctoral studies.

I would like to extend my thanks to my family and friends for their trust, care, and support. Finally, I would like to express my deepest gratitude to my beloved husband, Yuanfang Li, for his love, encouragement, support, patience, and understanding throughout my Ph.D.

## 9. SUPPLEMENT

**Table S1. Probe sets of total aortas up and down-regulated transcripts in Wt and ApoE<sup>-/-</sup> mice during aging.**

Differential expression of probe sets was determined as described in Material and Methods for different complement system related Gene Ontology terms: **A.** innate immune response (GO: 0045087), **B.** classical complement pathway (GO: 0006958), **C.** alternative complement pathway (GO: 0006957), **D.** regulation of complement activation (GO: 0030449). **E.** Leukocyte migration (GO: 0050900), meloid leukocyte migration (GO: 0097529), **F.** Phagocytosis (GO: 0006909), **G.** Cellular response to lipid (GO: 0071396). Further data are displayed as heat maps in Fig. 3.1 and Fig. 3.2. Probe sets are ordered according to fold change between aorta from 78 weeks old ApoE<sup>-/-</sup> mice versus 6 weeks. Columns of the mean value for each gene show signal intensity without normalization.

### A. Innate immune response (GO: 0045087)

Affymetrix Probe set ID	Gene symbol	Gene name	Entrez Gene ID	Mean Wt aorta 6 weeks	Mean Wt aorta 32 weeks	Mean Wt aorta 78 weeks	Mean ApoE <sup>-/-</sup> aorta 6 weeks	Mean ApoE <sup>-/-</sup> aorta 32 weeks	Mean ApoE <sup>-/-</sup> aorta 78 weeks	Fold change ApoE <sup>-/-</sup> aorta 78 weeks vs. 6 weeks	p ANOVA
1421792_s_at	Trem2	triggering receptor expressed on myeloid cells 2	83433	22	25	27	22	707	1816	83.52	2.00E-07
1424305_at	Igj	immunoglobulin joining	16069	117	207	664	206	314	13650	66.11	6.00E-05
1427747_a_at	Lcn2	lipocalin 2	16819	70	98	145	66	3505	3726	56.51	5.00E-07
1460188_at	Ptpn6	protein tyrosine phosphatase, non-receptor type 6	15170	37	51	198	46	567	1324	28.96	6.00E-06
1449858_at	Cd86	CD86 antigen	12524	15	8	21	11	107	296	25.86	0.001
1426808_at	Lgals3	lectin, galactose binding, soluble 3	16854	652	822	1038	693	9961	13992	20.2	2.00E-08

SUPPLEMENT

Affymetrix Probe set ID	Gene symbol	Gene name	Entrez Gene ID	Mean <i>Wt</i> aorta 6 weeks	Mean <i>Wt</i> aorta 32 weeks	Mean <i>Wt</i> aorta 78 weeks	Mean <i>Apoe</i> <sup>-/-</sup> aorta 6 weeks	Mean <i>Apoe</i> <sup>-/-</sup> aorta 32 weeks	Mean <i>Apoe</i> <sup>-/-</sup> aorta 78 weeks	Fold change <i>Apoe</i> <sup>-/-</sup> aorta 78 weeks vs. 6 weeks	p ANOVA
1420699_at	Clec7a	C-type lectin domain family 7, member a	56644	238	388	461	273	3319	5253	19.26	9.00E-08
1418126_at	Ccl5	chemokine (C-C motif)	20304	24	73	420	67	406	1222	18.28	0.009
1438858_x_at	H2-Aa	histocompatibility 2, class II	14960	523	1020	1766	544	4473	9321	17.13	5.00E-06
1443783_x_at	H2-Aa	histocompatibility 2, class II antigen A, alpha	14960	94	219	391	111	942	1563	14.02	8.00E-06
1460204_at	Tec	tec protein tyrosine kinase	21682	98	34	200	64	335	874	13.74	1.00E-04
1429947_a_at	Zbp1	Z-DNA binding protein 1	58203	36	66	40	41	160	565	13.67	7.00E-05
1425477_x_at	H2-Ab1	histocompatibility 2, class II antigen A, beta 1	14961	279	361	491	263	1416	3555	13.53	8.00E-06
1429525_s_at	Myo1f	myosin IF	17916	84	146	152	73	486	990	13.51	5.00E-06
1452279_at	Cfp	complement factor properdin	18636	232	130	281	112	733	1502	13.42	0.008
1449195_s_at	Cxcl16	chemokine (C-X-C motif) ligand 16	66102	190	164	238	146	1008	1929	13.18	7.00E-07
1420804_s_at	Clec4d	C-type lectin domain family 4, member d	17474	153	166	152	142	716	1741	12.23	5.00E-06
1436778_at	Cybb	cytochrome b-245, beta polypeptide	13058	329	376	637	312	1584	3259	10.45	6.00E-07
1452431_s_at	H2-Aa	histocompatibility 2, class II antigen A, alpha	14960	612	862	1303	606	2998	6322	10.42	2.00E-05
1416871_at	Adam8	a disintegrin and metallopeptidase domain 8	11501	195	215	174	181	1113	1881	10.42	9.00E-07
1451721_a_at	H2-Ab1	histocompatibility 2, class II antigen A, beta 1	14961	457	616	941	514	2144	5102	9.93	1.00E-06
1420380_at	Ccl2	chemokine (C-C motif) ligand 2	20296	99	49	126	95	414	915	9.65	1.00E-04
1429524_at	Myo1f	myosin IF	17916	79	145	184	115	491	1106	9.65	4.00E-06

SUPPLEMENT

Affymetrix Probe set ID	Gene symbol	Gene name	Entrez Gene ID	Mean <i>Wt</i> aorta 6 weeks	Mean <i>Wt</i> aorta 32 weeks	Mean <i>Wt</i> aorta 78 weeks	Mean <i>Apoe</i> <sup>-/-</sup> aorta 6 weeks	Mean <i>Apoe</i> <sup>-/-</sup> aorta 32 weeks	Mean <i>Apoe</i> <sup>-/-</sup> aorta 78 weeks	Fold change <i>Apoe</i> <sup>-/-</sup> aorta 78 weeks vs. 6 weeks	p ANOVA
1422932_a_at	Vav1	vav 1 oncogene	22324	31	68	22	46	230	431	9.41	4.00E-04
1435226_at	Rnf19b	ring finger protein 19B	75234	339	398	397	55	367	509	9.3	0.003
1422903_at	Ly86	lymphocyte antigen 86	17084	417	477	693	421	1743	3863	9.18	2.00E-06
1449049_at	Tlr1	toll-like receptor 1	21897	78	97	100	84	339	711	8.45	3.00E-05
1450648_s_at	H2-Ab1	histocompatibility 2, class II antigen A, beta 1	14961	780	1005	1459	782	2234	6399	8.19	1.00E-05
1425951_a_at	Clec4n	C-type lectin domain family 4, member n	56620	37	106	112	65	311	510	7.81	0.002
1418718_at	Cxcl16	chemokine (C-X-C motif) ligand 16	66102	462	481	623	437	1456	3219	7.36	8.00E-07
1417063_at	C1qb	complement component 1, q subcomponent, beta polypeptide	12260	1347	1154	1506	1169	5621	8251	7.06	5.00E-07
1417876_at	Fcgr1	Fc receptor, IgG, high affinity I	14129	156	174	234	153	627	1066	6.96	2.00E-06
1417025_at	H2-Eb1	histocompatibility 2, class II antigen E beta	14969	1013	1729	2610	1222	4520	8317	6.8	3.00E-06
1419627_s_at	Clec4n	C-type lectin domain family 4, member n	56620	142	179	272	152	559	1027	6.77	6.00E-05
1451987_at	Arrb2	arrestin, beta 2	216869	170	188	174	147	568	986	6.71	2.00E-05
1447621_s_at	Tmem173	transmembrane protein 173	72512	111	120	160	83	332	552	6.67	4.00E-05
1420715_a_at	Pparg	peroxisome proliferator activated receptor gamma	19016	29	476	171	60	375	400	6.65	0.002
1418261_at	Syk	spleen tyrosine kinase	20963	311	375	517	281	875	1860	6.63	7.00E-06
1436779_at	Cybb	cytochrome b-245, beta polypeptide	13058	262	334	357	246	864	1603	6.52	2.00E-06

SUPPLEMENT

Affymetrix Probe set ID	Gene symbol	Gene name	Entrez Gene ID	Mean <i>Wt</i> aorta 6 weeks	Mean <i>Wt</i> aorta 32 weeks	Mean <i>Wt</i> aorta 78 weeks	Mean <i>Apoe</i> <sup>-/-</sup> aorta 6 weeks	Mean <i>Apoe</i> <sup>-/-</sup> aorta 32 weeks	Mean <i>Apoe</i> <sup>-/-</sup> aorta 78 weeks	Fold change <i>Apoe</i> <sup>-/-</sup> aorta 78 weeks vs. 6 weeks	p ANOVA
1425519_a_at	Cd74	CD74 antigen (invariant polypeptide of major histocompatibility complex, class II antigen-associated)	16149	1634	2699	4537	1955	7675	11699	5.98	4.00E-06
1449401_at	C1qc	complement component 1, q subcomponent, C chain	12262	1942	1677	2435	1819	8204	10753	5.91	7.00E-07
1427368_x_at	Fes	feline sarcoma oncogene	14159	74	198	187	117	320	671	5.76	2.00E-05
1457753_at	Tlr13	toll-like receptor 13	279572	136	153	141	136	496	758	5.59	1.00E-07
1423166_at	Cd36	CD36 antigen	12491	794	3237	1578	835	4019	4649	5.57	8.00E-06
1418776_at	Gbp8	guanylate-binding protein 8	76074	23	75	100	46	122	258	5.54	8.00E-04
1417346_at	Pycard	PYD and CARD domain containing	66824	399	333	506	335	802	1825	5.44	7.00E-06
1452948_at	Tnfaip8l2	tumor necrosis factor, alpha-induced protein 8-like 2	69769	173	135	45	99	360	533	5.39	6.00E-05
1434815_a_at	Mapkapk3	mitogen-activated protein kinase-activated protein kinase 3	102626	119	228	235	87	267	468	5.35	9.00E-04
1421525_a_at	Naip5	NLR family, apoptosis inhibitory protein 5	17951	99	123	146	113	349	594	5.26	1.00E-05
1434653_at	Ptk2b	PTK2 protein tyrosine kinase 2 beta	19229	261	463	424	263	748	1346	5.12	1.00E-06
1452410_a_at	Fes	feline sarcoma oncogene	14159	138	141	164	118	341	597	5.07	2.00E-05
1418262_at	Syk	spleen tyrosine kinase	20963	149	133	185	133	404	664	4.98	2.00E-05
1420499_at	Gch1	GTP cyclohydrolase 1	14528	108	102	176	97	271	475	4.9	8.00E-05
1419609_at	Ccr1	chemokine (C-C motif) receptor 1	12768	92	149	166	125	365	604	4.85	7.00E-05



SUPPLEMENT

Affymetrix Probe set ID	Gene symbol	Gene name	Entrez Gene ID	Mean <i>Wt</i> aorta 6 weeks	Mean <i>Wt</i> aorta 32 weeks	Mean <i>Wt</i> aorta 78 weeks	Mean <i>Apoe</i> <sup>-/-</sup> aorta 6 weeks	Mean <i>Apoe</i> <sup>-/-</sup> aorta 32 weeks	Mean <i>Apoe</i> <sup>-/-</sup> aorta 78 weeks	Fold change <i>Apoe</i> <sup>-/-</sup> aorta 78 weeks vs. 6 weeks	p ANOVA
1435290_x_at	H2-Aa	histocompatibility 2, class II	14960	2113	4191	5680	2340	8604	11007	4.7	7.00E-06
1427691_a_at	Ifnar2	interferon (alpha and beta)	15976	77	175	47	93	296	435	4.69	0.005
1423768_at	Unc93b1	unc-93 homolog B1 (C.	54445	629	694	766	561	1301	2623	4.67	2.00E-06
1417268_at	Cd14	CD14 antigen	12475	577	649	838	605	1254	2776	4.59	2.00E-06
1437726_x_at	C1qb	complement component 1, q	12260	1568	1745	1897	1774	7646	8089	4.56	7.00E-07
1451174_at	Nrros	negative regulator of reactive oxygen species	224109	263	327	389	293	744	1334	4.56	7.00E-06
1417381_at	C1qa	complement component 1, q	12259	1952	1766	1881	1925	6761	8373	4.35	1.00E-07
1422978_at	Cybb	cytochrome b-245, beta polypeptide	13058	193	211	199	204	619	883	4.33	7.00E-06
1424560_at	Pstpip1	proline-serine-threonine phosphatase-interacting protein 1	19200	160	92	120	158	365	681	4.31	5.00E-04
1417378_at	Cadml	cell adhesion molecule 1	54725	353	320	421	290	608	1230	4.24	9.00E-06
1423954_at	C3	complement component 3	12266	1929	4798	3722	2416	8194	10023	4.15	2.00E-06
1460231_at	Irf5	interferon regulatory factor 5	27056	176	214	293	189	462	764	4.04	5.00E-05
1460273_a_at	Naip2	NLR family, apoptosis inhibitory protein 2	17948	80	138	136	110	293	444	4.03	2.00E-05
1420361_at	Slc11a1	solute carrier family 11 (proton-coupled divalent metal ion transporters), member 1	18173	662	704	802	668	1645	2664	3.99	1.00E-06
1460245_at	Klrd1	killer cell lectin-like receptor, subfamily D, member 1	16643	121	156	170	139	230	541	3.89	1.00E-04

SUPPLEMENT

Affymetrix Probe set ID	Gene symbol	Gene name	Entrez Gene ID	Mean <i>Wt</i> aorta 6 weeks	Mean <i>Wt</i> aorta 32 weeks	Mean <i>Wt</i> aorta 78 weeks	Mean <i>Apoe</i> <sup>-/-</sup> aorta 6 weeks	Mean <i>Apoe</i> <sup>-/-</sup> aorta 32 weeks	Mean <i>Apoe</i> <sup>-/-</sup> aorta 78 weeks	Fold change <i>Apoe</i> <sup>-/-</sup> aorta 78 weeks vs. 6 weeks	p ANOVA
1450883_a_at	Cd36	CD36 antigen	12491	1224	4327	1699	1492	5328	5773	3.87	1.00E-05
1429527_a_at	Plscr1	phospholipid scramblase 1	22038	113	162	147	112	346	430	3.85	1.00E-05
1426239_s_at	Arrb2	arrestin, beta 2	216869	426	477	568	505	857	1941	3.84	1.00E-05
1449455_at	Hck	hemopoietic cell kinase	15162	304	332	451	317	658	1215	3.84	9.00E-06
1429831_at	Pik3ap1	phosphoinositide-3-kinase adaptor protein 1	83490	194	184	278	161	299	614	3.82	3.00E-06
1420653_at	Tgfb1	transforming growth factor, beta 1	21803	516	538	551	440	1292	1670	3.79	8.00E-07
1425902_a_at	Nfkb2	nuclear factor of kappa light polypeptide gene enhancer in B cells 2, p49/p100	18034	188	112	258	129	204	487	3.78	8.00E-04
1425396_a_at	Lck	lymphocyte protein tyrosine kinase	16818	126	176	244	168	188	623	3.71	3.00E-04
1421366_at	Clec5a	C-type lectin domain family 5, member a	23845	52	70	96	79	168	281	3.58	0.001
1424254_at	Ifitm1	interferon induced transmembrane protein 1	68713	148	284	244	202	369	723	3.58	3.00E-04
1437176_at	Nlrc5	NLR family, CARD domain containing 5	434341	168	236	265	207	314	737	3.56	2.00E-04
1454268_a_at	Cyba	cytochrome b-245, alpha polypeptide	13057	2532	2330	3388	2574	5556	9049	3.52	2.00E-06
1447927_at	Gbp6	guanylate binding protein 6	100702	244	375	398	190	524	667	3.52	0.004
1422013_at	Clec4a2	C-type lectin domain family 4, member a2	26888	197	248	276	169	397	592	3.49	2.00E-05
1417470_at	Apobec3	apolipoprotein B mRNA editing enzyme, catalytic polypeptide 3	80287	207	217	330	299	496	1023	3.42	2.00E-04

## SUPPLEMENT

Affymetrix Probe set ID	Gene symbol	Gene name	Entrez Gene ID	Mean <i>Wt</i> aorta 6 weeks	Mean <i>Wt</i> aorta 32 weeks	Mean <i>Wt</i> aorta 78 weeks	Mean <i>Apoe</i> <sup>-/-</sup> aorta 6 weeks	Mean <i>Apoe</i> <sup>-/-</sup> aorta 32 weeks	Mean <i>Apoe</i> <sup>-/-</sup> aorta 78 weeks	Fold change <i>Apoe</i> <sup>-/-</sup> aorta 78 weeks vs. 6 weeks	p ANOVA
1419879_s_at	Trim25	tripartite motif-containing 25	217069	403	462	645	407	917	1377	3.38	3.00E-06
1419873_s_at	Csflr	colony stimulating factor 1 receptor	12978	1231	1391	1675	1179	3013	3981	3.38	3.00E-05
1419526_at	Fgr	Gardner-Rasheed feline sarcoma viral (Fgr) oncogene homolog	14191	184	254	418	227	569	763	3.37	1.00E-04
1425289_a_at	Cr2	complement receptor 2	12902	132	161	241	118	135	396	3.35	0.02
1417376_a_at	Cadml	cell adhesion molecule 1	54725	233	253	273	241	443	802	3.33	4.00E-05
1453181_x_at	Plscr1	phospholipid scramblase 1	22038	120	158	169	132	314	439	3.32	1.00E-05
1419569_a_at	Isg20	interferon-stimulated protein	57444	257	340	589	270	311	883	3.27	0.01
1434366_x_at	C1qb	complement component 1, q subcomponent, beta polypeptide	12260	1499	1543	1546	1518	5822	4861	3.2	1.00E-05
1417377_at	Cadml	cell adhesion molecule 1	54725	70	106	76	97	176	303	3.13	0.03
1435040_at	Irak3	interleukin-1 receptor-associated kinase 3	73914	131	212	264	133	427	394	2.97	8.00E-05
1419394_s_at	S100a8	S100 calcium binding protein A8 (calgranulin A)	20201	140	528	792	402	628	1182	2.94	0.007
1456694_x_at	Ptpn6	protein tyrosine phosphatase, non-receptor type 6	15170	449	549	568	367	660	1075	2.93	0.001
1419132_at	Tlr2	toll-like receptor 2	24088	329	398	499	378	713	1099	2.91	1.00E-05
1421358_at	H2-M3	histocompatibility 2, M region locus 3	14991	727	816	1169	671	1076	1924	2.87	3.00E-05
1420404_at	Cd86	CD86 antigen	12524	160	152	167	141	232	402	2.85	6.00E-04
1421547_at	Cd180	CD180 antigen	17079	223	279	274	219	599	621	2.84	5.00E-05

## SUPPLEMENT

Affymetrix Probe set ID	Gene symbol	Gene name	Entrez Gene ID	Mean <i>Wt</i> aorta 6 weeks	Mean <i>Wt</i> aorta 32 weeks	Mean <i>Wt</i> aorta 78 weeks	Mean <i>Apoe</i> <sup>-/-</sup> aorta 6 weeks	Mean <i>Apoe</i> <sup>-/-</sup> aorta 32 weeks	Mean <i>Apoe</i> <sup>-/-</sup> aorta 78 weeks	Fold change <i>Apoe</i> <sup>-/-</sup> aorta 78 weeks vs. 6 weeks	p ANOVA
1450783_at	Ifit1	interferon-induced protein with tetratricopeptide repeats 1	15957	148	201	310	181	427	504	2.78	3.00E-05
1434438_at	Samhd1	SAM domain and HD domain, 1	56045	689	971	1146	696	1035	1897	2.73	0.002
1440481_at	Stat1	signal transducer and activator of transcription 1	20846	104	104	103	117	165	316	2.71	0.002
1453281_at	Pik3cd	phosphatidylinositol 3- kinase catalytic delta polypeptide	18707	228	201	252	235	350	630	2.69	5.00E-04
1426415_a_at	Trim25	tripartite motif-containing 25	217069	107	105	62	112	231	299	2.67	2.00E-04
1436625_at	Fcgr1	Fc receptor, IgG, high affinity I	14129	150	172	282	182	348	484	2.65	0.001
1440169_x_at	Ifnar2	interferon (alpha and beta) receptor 2	15976	356	463	580	456	915	1196	2.62	2.00E-04
1428696_at	Rftn1	raftlin lipid raft linker 1	76438	760	731	1117	982	1315	2457	2.5	7.00E-06
1420915_at	Stat1	signal transducer and activator of transcription 1	20846	300	422	402	313	628	778	2.49	2.00E-05
1448756_at	S100a9	S100 calcium binding protein A9 (calgranulin B)	20202	109	442	600	261	459	648	2.48	0.01
1418240_at	Gbp2	guanylate binding protein 2	14469	721	912	1200	778	1313	1913	2.46	3.00E-04
1419042_at	Iigp1	interferon inducible GTPase 1	60440	366	623	582	414	855	1011	2.44	0.006
1435906_x_at	Gbp2	guanylate binding protein 2	14469	713	996	1131	750	1395	1828	2.44	2.00E-04
1450884_at	Cd36	CD36 antigen	12491	147	624	269	200	508	484	2.42	4.00E-05
1417244_a_at	Irf7	interferon regulatory factor 7	54123	253	302	393	266	425	633	2.38	4.00E-04

SUPPLEMENT

Affymetrix Probe set ID	Gene symbol	Gene name	Entrez Gene ID	Mean <i>Wt</i> aorta 6 weeks	Mean <i>Wt</i> aorta 32 weeks	Mean <i>Wt</i> aorta 78 weeks	Mean <i>Apoe</i> <sup>-/-</sup> aorta 6 weeks	Mean <i>Apoe</i> <sup>-/-</sup> aorta 32 weeks	Mean <i>Apoe</i> <sup>-/-</sup> aorta 78 weeks	Fold change <i>Apoe</i> <sup>-/-</sup> aorta 78 weeks vs. 6 weeks	p ANOVA
1436199_at	Trim14	tripartite motif-containing 14	74735	134	164	226	172	273	406	2.36	7.00E-05
1453196_a_at	Oas12	2'-5' oligoadenylate synthetase-like 2	23962	303	274	360	232	554	547	2.35	3.00E-04
1416118_at	Trim59	tripartite motif-containing 59	66949	173	92	126	143	137	331	2.31	3.00E-04
1429692_s_at	Gch1	GTP cyclohydrolase 1	14528	140	136	136	123	199	282	2.29	0.001
1448550_at	Lbp	lipopolysaccharide binding protein	16803	931	1284	1276	998	1934	2268	2.27	5.00E-05
1425065_at	Oas2	2'-5' oligoadenylate synthetase 2	246728	142	109	185	145	232	330	2.27	0.05
1433699_at	Tnfaip3	tumor necrosis factor, alpha-induced protein 3	21929	569	683	845	643	1032	1441	2.24	1.00E-04
1434903_s_at	Il1rl2	interleukin 1 receptor-like 2	107527	148	148	142	125	200	278	2.23	0.001
1449130_at	Cd1d1	CD1d1 antigen	12479	257	983	341	225	818	497	2.21	5.00E-05
1432478_a_at	Rnf19b	ring finger protein 19B	75234	233	245	168	224	329	485	2.16	0.001
1418392_a_at	Gbp3	guanylate binding protein 3	55932	365	502	404	348	716	747	2.15	0.001
1450033_a_at	Stat1	signal transducer and activator of transcription 1	20846	462	539	381	447	740	951	2.12	8.00E-04
1442804_at	Fgr	Gardner-Rasheed feline sarcoma viral (Fgr) oncogene homolog	14191	207	237	399	263	407	559	2.12	0.001
1425974_a_at	Trim25	tripartite motif-containing 25	217069	543	468	535	456	737	952	2.09	8.00E-05
1449874_at	Ly96	lymphocyte antigen 96	17087	393	259	353	296	403	617	2.08	8.00E-04
1417856_at	Relb	avian reticuloendotheliosis viral (v-rel) oncogene related B	19698	178	192	280	178	219	370	2.08	0.007

SUPPLEMENT

Affymetrix Probe set ID	Gene symbol	Gene name	Entrez Gene ID	Mean <i>Wt</i> aorta 6 weeks	Mean <i>Wt</i> aorta 32 weeks	Mean <i>Wt</i> aorta 78 weeks	Mean <i>Apoe</i> <sup>-/-</sup> aorta 6 weeks	Mean <i>Apoe</i> <sup>-/-</sup> aorta 32 weeks	Mean <i>Apoe</i> <sup>-/-</sup> aorta 78 weeks	Fold change <i>Apoe</i> <sup>-/-</sup> aorta 78 weeks vs. 6 weeks	p ANOVA
1426276_at	Ifih1	interferon induced with helicase C domain 1	71586	463	477	581	444	747	919	2.07	1.00E-05
1433803_at	Jak1	Janus kinase 1	16451	755	904	1113	847	1208	1745	2.06	1.00E-04
1423518_at	Csk	c-src tyrosine kinase	12988	492	500	676	473	535	962	2.03	5.00E-04
1453913_a_at	Tap2	transporter 2, ATP-binding cassette, sub-family B (MDR/TAP)	21355	242	429	486	285	458	565	1.98	5.00E-05
1450829_at	Tnfaip3	tumor necrosis factor, alpha-induced protein 3	21929	50	77	119	133	144	239	1.8	0.01
1422781_at	Tlr3	toll-like receptor 3	142980	221	279	223	184	459	325	1.77	0.02
1449131_s_at	Cd1d1	CD1d1 antigen	12479	536	1490	801	531	1176	930	1.75	7.00E-05
1438676_at	Gbp6	guanylate binding protein 6	100702	129	273	180	166	316	265	1.6	5.00E-04
1457664_x_at	C2	complement component 2 (within H-2S)	12263	357	255	619	365	420	573	1.57	0.002
1418666_at	Ptx3	pentraxin related gene	19288	137	133	104	152	277	239	1.57	0.02
1427911_at	Tmem173	transmembrane protein 173	72512	415	434	241	527	773	820	1.55	0.001
1449935_a_at	Dnaja3	DnaJ (Hsp40) homolog, subfamily A, member 3	83945	472	955	505	470	812	707	1.5	9.00E-04
1423285_at	Coch	coagulation factor C homolog (Limulus polyphemus)	12810	313	356	613	213	274	272	1.28	0.004
1439364_a_at	Mmp2	matrix metalloproteinase 2	17390	3914	2827	2177	3996	3443	4990	1.25	2.00E-04
1416136_at	Mmp2	matrix metalloproteinase 2	17390	5328	3177	2750	5567	4910	6603	1.19	7.00E-06
1423153_x_at	Cfh	complement component factor h	12628	4181	6155	3959	4945	8564	4094	-1.21	6.00E-04

SUPPLEMENT

Affymetrix Probe set ID	Gene symbol	Gene name	Entrez Gene ID	Mean <i>Wt</i> aorta 6 weeks	Mean <i>Wt</i> aorta 32 weeks	Mean <i>Wt</i> aorta 78 weeks	Mean <i>Apoe</i> <sup>-/-</sup> aorta 6 weeks	Mean <i>Apoe</i> <sup>-/-</sup> aorta 32 weeks	Mean <i>Apoe</i> <sup>-/-</sup> aorta 78 weeks	Fold change <i>Apoe</i> <sup>-/-</sup> aorta 78 weeks vs. 6 weeks	p ANOVA
1442511_at	Ipo7	importin 7	233726	188	95	145	203	94	150	-1.35	0.001
1433804_at	Jak1	Janus kinase 1	16451	260	134	123	299	225	196	-1.52	0.001
1421907_at	Med1	mediator complex subunit 1	19014	1092	681	497	1138	844	722	-1.58	0.05
1455095_at	Hist2h2b e	histone cluster 2, H2be	319190	579	844	496	591	693	343	-1.72	1.00E-04
1452961_at	Tril	TLR4 interactor with leucine-rich repeats	66873	277	404	319	316	414	179	-1.77	0.03
1450743_s_at	Syncrip	synaptotagmin binding, cytoplasmic RNA interacting protein	56403	483	180	73	423	266	228	-1.85	0.007
1422102_a_at	Stat5b	signal transducer and activator of transcription 5B	20851	326	292	265	404	190	213	-1.89	0.002
1422769_at	Syncrip	synaptotagmin binding, cytoplasmic RNA interacting protein	56403	511	226	172	442	313	227	-1.95	1.00E-05
1447854_s_at	Hist2h2b e	histone cluster 2, H2be	319190	813	854	735	929	749	448	-2.08	0.001
1422216_at	Mid2	midline 2	23947	633	452	474	585	412	275	-2.13	3.00E-04
1451773_s_at	Polr3f	polymerase (RNA) III (DNA directed) polypeptide F	70408	262	148	113	203	194	93	-2.19	0.002
1442827_at	Tlr4	toll-like receptor 4	21898	413	183	137	320	208	142	-2.26	9.00E-04
1437673_at	Wnt5a	wingless-type MMTV integration site family, member 5A	22418	246	284	183	201	226	85	-2.37	0.003
1427646_a_at	Arhgef2	rho/rac guanine nucleotide exchange factor (GEF) 2	16800	707	443	469	802	425	336	-2.39	0.01

SUPPLEMENT

Affymetrix Probe set ID	Gene symbol	Gene name	Entrez Gene ID	Mean <i>Wt</i> aorta 6 weeks	Mean <i>Wt</i> aorta 32 weeks	Mean <i>Wt</i> aorta 78 weeks	Mean <i>Apoe</i> <sup>-/-</sup> aorta 6 weeks	Mean <i>Apoe</i> <sup>-/-</sup> aorta 32 weeks	Mean <i>Apoe</i> <sup>-/-</sup> aorta 78 weeks	Fold change <i>Apoe</i> <sup>-/-</sup> aorta 78 weeks vs. 6 weeks	p ANOVA
1421042_at	Arhgef2	rho/rac guanine nucleotide exchange factor (GEF) 2	16800	1304	849	791	1487	796	594	-2.5	7.00E-04
1436791_at	Wnt5a	wingless-type MMTV integration site family, member 5A	22418	706	850	713	786	717	241	-3.26	2.00E-05
1448152_at	Igf2	insulin-like growth factor 2	16002	648	786	721	668	582	195	-3.43	0.004
1448818_at	Wnt5a	wingless-type MMTV integration site family, member 5A	22418	653	606	253	721	519	140	-5.14	8.00E-06

**B. Classical complement pathway (GO: 0006958)**

Affymetrix Probe set ID	Gene symbol	Gene name	Entrez Gene ID	Mean <i>Wt</i> aorta 6 weeks	Mean <i>Wt</i> aorta 32 weeks	Mean <i>Wt</i> aorta 78 weeks	Mean <i>Apoe</i> <sup>-/-</sup> aorta 6 weeks	Mean <i>Apoe</i> <sup>-/-</sup> aorta 32 weeks	Mean <i>Apoe</i> <sup>-/-</sup> aorta 78 weeks	Fold change <i>Apoe</i> <sup>-/-</sup> aorta 78 weeks vs. 6 weeks	p ANOVA
1417063_at	C1qb	complement component 1, q subcomponent, beta polypeptide	12260	1347	1154	1506	1169	5621	8251	7.06	5.00E-07
1449401_at	C1qc	complement component 1, q subcomponent, C chain	12262	1942	1677	2435	1819	8204	10753	5.91	7.00E-07
1437726_x_at	C1qb	complement component 1, q subcomponent, beta polypeptide	12260	1568	1745	1897	1774	7646	8089	4.56	7.00E-07
1417381_at	C1qa	complement component 1, q subcomponent, alpha polypeptide	12259	1952	1766	1881	1925	6761	8373	4.35	1.00E-07



SUPPLEMENT

Affymetrix Probe set ID	Gene symbol	Gene name	Entrez Gene ID	Mean <i>Wt</i> aorta 6 weeks	Mean <i>Wt</i> aorta 32 weeks	Mean <i>Wt</i> aorta 78 weeks	Mean <i>Apoe</i> <sup>-/-</sup> aorta 6 weeks	Mean <i>Apoe</i> <sup>-/-</sup> aorta 32 weeks	Mean <i>Apoe</i> <sup>-/-</sup> aorta 78 weeks	Fold change <i>Apoe</i> <sup>-/-</sup> aorta 78 weeks vs. 6 weeks	p ANOVA
1423954_at	C3	complement component 3	12266	1929	4798	3722	2416	8194	10023	4.15	2.00E-06
1425289_a_at	Cr2	complement receptor 2	12902	132	161	241	118	135	396	3.35	0.02
1434366_x_at	C1qb	complement component 1, q subcomponent, beta polypeptide	12260	1499	1543	1546	1518	5822	4861	3.2	1.00E-05
1457664_x_at	C2	complement component 2 (within H-2S)	12263	357	255	619	365	420	573	1.57	0.002

**C. Alternative complement pathway (GO: 0006957)**

Affymetrix Probe set ID	Gene symbol	Gene name	Entrez Gene ID	Mean <i>Wt</i> aorta 6 weeks	Mean <i>Wt</i> aorta 32 weeks	Mean <i>Wt</i> aorta 78 weeks	Mean <i>Apoe</i> <sup>-/-</sup> aorta 6 weeks	Mean <i>Apoe</i> <sup>-/-</sup> aorta 32 weeks	Mean <i>Apoe</i> <sup>-/-</sup> aorta 78 weeks	Fold change <i>Apoe</i> <sup>-/-</sup> aorta 78 weeks vs. 6 weeks	p ANOVA
1452279_at	Cfp	complement factor properdin	18636	232	130	281	112	733	1502	13.42	0.008
1423954_at	C3	complement component 3	12266	1929	4798	3722	2416	8194	10023	4.15	2.00E-06
1423153_x_at	Cfh	complement component factor h	12628	4181	6155	3959	4945	8564	4094	-1.21	6.00E-04

**D. Regulation of complement activation (GO: 0030449)**

Affymetrix Probe set ID	Gene symbol	Gene name	Entrez Gene ID	Mean <i>Wt</i> aorta 6 weeks	Mean <i>Wt</i> aorta 32 weeks	Mean <i>Wt</i> aorta 78 weeks	Mean <i>Apoe</i> <sup>-/-</sup> aorta 6 weeks	Mean <i>Apoe</i> <sup>-/-</sup> aorta 32 weeks	Mean <i>Apoe</i> <sup>-/-</sup> aorta 78 weeks	Fold change <i>Apoe</i> <sup>-/-</sup> aorta 78 weeks vs. 6 weeks	p ANOVA
1423954_at	C3	complement component 3	12266	1929	4798	3722	2416	8194	10023	4.15	2.00E-06
1423153_x_at	Cfh	complement component factor h	12628	4181	6155	3959	4945	8564	4094	-1.21	6.00E-04

**E. Leukocyte migration (GO: 0050900)**

Affymetrix Probe set ID	Gene symbol	Gene name	Entrez Gene ID	Mean <i>Wt</i> aorta 6 weeks	Mean <i>Wt</i> aorta 32 weeks	Mean <i>Wt</i> aorta 78 weeks	Mean <i>Apoe</i> <sup>-/-</sup> aorta 6 weeks	Mean <i>Apoe</i> <sup>-/-</sup> aorta 32 weeks	Mean <i>Apoe</i> <sup>-/-</sup> aorta 78 weeks	Fold change <i>Apoe</i> <sup>-/-</sup> aorta 78 weeks vs. 6 weeks	p ANOVA
1449254_at	Spp1	secreted phosphoprotein 1	20750	46	93	326	76	13398	13789	180.67	3.00E-05
1418457_at	Cxcl14	chemokine (C-X-C motif) ligand 14	57266	5	4	3	5	48	299	63.89	3.00E-05
1419561_at	Ccl3	chemokine (C-C motif) ligand 3	20302	6	18	9	12	212	597	48.71	5.00E-06
1419282_at	Ccl12	chemokine (C-C motif) ligand 12	20293	83	27	134	23	374	926	40.66	4.00E-05
1418652_at	Cxcl9	chemokine (C-X-C motif) ligand 9	17329	15	65	42	20	72	601	30.5	2.00E-04
1417851_at	Cxcl13	chemokine (C-X-C motif) ligand 13	55985	79	91	272	83	330	1980	23.92	2.00E-06
1426808_at	Lgals3	lectin, galactose binding, soluble 3	16854	652	822	1038	693	9961	13992	20.2	2.00E-08

## SUPPLEMENT

Affymetrix Probe set ID	Gene symbol	Gene name	Entrez Gene ID	Mean <i>Wt</i> aorta 6 weeks	Mean <i>Wt</i> aorta 32 weeks	Mean <i>Wt</i> aorta 78 weeks	Mean <i>Apoe</i> <sup>-/-</sup> aorta 6 weeks	Mean <i>Apoe</i> <sup>-/-</sup> aorta 32 weeks	Mean <i>Apoe</i> <sup>-/-</sup> aorta 78 weeks	Fold change <i>Apoe</i> <sup>-/-</sup> aorta 78 weeks vs. 6 weeks	p ANOVA
1442082_at	C3ar1	complement component 3a receptor 1	12267	162	203	280	175	2019	3522	20.11	6.00E-08
1418126_at	Ccl5	chemokine (C-C motif) ligand 5	20304	24	73	420	67	406	1222	18.28	0.009
1450678_at	Itgb2	integrin beta 2	16414	274	540	582	384	2879	6211	16.19	7.00E-07
1418340_at	Fcer1g	Fc receptor, IgE, high affinity I, gamma polypeptide	14127	507	690	889	382	2708	5707	14.95	2.00E-05
1419483_at	C3ar1	complement component 3a receptor 1	12267	342	353	423	332	2266	4841	14.58	5.00E-07
1419209_at	Cxcl1	chemokine (C-X-C motif) ligand 1	14825	110	172	157	103	1157	1394	13.59	6.00E-06
1442082_at	C3ar1	complement component 3a receptor 1	12267	162	203	280	175	2019	3522	20.11	6.00E-08
1418126_at	Ccl5	chemokine (C-C motif) ligand 5	20304	24	73	420	67	406	1222	18.28	0.009
1450678_at	Itgb2	integrin beta 2	16414	274	540	582	384	2879	6211	16.19	7.00E-07
1418340_at	Fcer1g	Fc receptor, IgE, high affinity I, gamma polypeptide	14127	507	690	889	382	2708	5707	14.95	2.00E-05
1419483_at	C3ar1	complement component 3a receptor 1	12267	342	353	423	332	2266	4841	14.58	5.00E-07
1419209_at	Cxcl1	chemokine (C-X-C motif) ligand 1	14825	110	172	157	103	1157	1394	13.59	6.00E-06
1449195_s_at	Cxcl16	chemokine (C-X-C motif) ligand 16	66102	190	164	238	146	1008	1929	13.18	7.00E-07
1436003_at	Vcam1	vascular cell adhesion molecule 1	22329	158	178	297	146	1348	1865	12.8	1.00E-07

SUPPLEMENT

Affymetrix Probe set ID	Gene symbol	Gene name	Entrez Gene ID	Mean <i>Wt</i> aorta 6 weeks	Mean <i>Wt</i> aorta 32 weeks	Mean <i>Wt</i> aorta 78 weeks	Mean <i>Apoe</i> <sup>-/-</sup> aorta 6 weeks	Mean <i>Apoe</i> <sup>-/-</sup> aorta 32 weeks	Mean <i>Apoe</i> <sup>-/-</sup> aorta 78 weeks	Fold change <i>Apoe</i> <sup>-/-</sup> aorta 78 weeks vs. 6 weeks	p ANOVA
1430700_a_at	Pla2g7	phospholipase A2, group VII (platelet-activating factor acetylhydrolase, plasma)	27226	219	238	169	164	1438	2061	12.53	2.00E-04
1455269_a_at	Coro1a	coronin, actin binding protein 1A	12721	169	336	625	275	1527	3332	12.12	1.00E-05
1419482_at	C3ar1	complement component 3a receptor 1	12267	235	228	335	252	1530	2963	11.78	1.00E-06
1416246_a_at	Coro1a	coronin, actin binding protein 1A	12721	334	325	498	336	1586	3943	11.75	1.00E-05
1421712_at	Sele	selectin, endothelial cell	20339	20	48	83	34	184	362	10.78	7.00E-04
1416871_at	Adam8	a disintegrin and metallopeptidase domain 8	11501	195	215	174	181	1113	1881	10.42	9.00E-07
1428787_at	Nckap1l	NCK associated protein 1 like	105855	130	86	249	159	779	1589	10	7.00E-05
1420380_at	Ccl2	chemokine (C-C motif) ligand 2	20296	99	49	126	95	414	915	9.65	1.00E-04
1448620_at	Fcgr3	Fc receptor, IgG, low affinity III	14131	324	357	399	369	1881	3536	9.58	3.00E-06
1422932_a_at	Vav1	vav 1 oncogene	22324	31	68	22	46	230	431	9.41	4.00E-04
1422445_at	Itga6	integrin alpha 6	16403	356	738	578	308	1476	2682	8.7	1.00E-04
1418930_at	Cxcl10	chemokine (C-X-C motif) ligand 10	15945	84	92	98	48	185	403	8.33	5.00E-04
1418204_s_at	Aif1	allograft inflammatory factor 1	11629	166	234	394	191	676	1456	7.63	8.00E-07
1418718_at	Cxcl16	chemokine (C-X-C motif) ligand 16	66102	462	481	623	437	1456	3219	7.36	8.00E-07

SUPPLEMENT

Affymetrix Probe set ID	Gene symbol	Gene name	Entrez Gene ID	Mean Wt aorta 6 weeks	Mean Wt aorta 32 weeks	Mean Wt aorta 78 weeks	Mean <i>Apoe</i> <sup>-/-</sup> aorta 6 weeks	Mean <i>Apoe</i> <sup>-/-</sup> aorta 32 weeks	Mean <i>Apoe</i> <sup>-/-</sup> aorta 78 weeks	Fold change <i>Apoe</i> <sup>-/-</sup> aorta 78 weeks vs. 6 weeks	p ANOVA
1435903_at	Cd300a	CD300A antigen	217303	214	236	244	184	720	1349	7.35	1.00E-06
1421186_at	Ccr2	chemokine (C-C motif) receptor 2	12772	154	154	132	130	619	939	7.21	3.00E-05
1418261_at	Syk	spleen tyrosine kinase	20963	311	375	517	281	875	1860	6.63	7.00E-06
1448162_at	Vcam1	vascular cell adhesion molecule 1	22329	1927	2139	2776	1455	7397	8838	6.07	1.00E-07
1425519_a_at	Cd74	CD74 antigen (invariant polypeptide of major histocompatibility complex, class II antigen-associated)	16149	1634	2699	4537	1955	7675	11699	5.98	4.00E-06
1428786_at	Nckap1l	NCK associated protein 1 like	105855	283	375	583	364	896	2157	5.92	2.00E-06
1451314_a_at	Vcam1	vascular cell adhesion molecule 1	22329	902	949	1671	857	3474	5052	5.89	1.00E-06
1417346_at	Pycard	PYD and CARD domain containing	66824	399	333	506	335	802	1825	5.44	7.00E-06
1449127_at	Selplg	selectin, platelet (p- selectin) ligand	20345	254	336	457	279	728	1495	5.36	5.00E-05
1415803_at	Cx3cl1	chemokine (C-X3-C motif) ligand 1	20312	262	349	622	278	772	1458	5.24	1.00E-06
1434653_at	Ptk2b	PTK2 protein tyrosine kinase 2 beta	19229	261	463	424	263	748	1346	5.12	1.00E-06
1417620_at	Rac2	RAS-related C3 botulinum substrate 2	19354	366	467	503	475	1376	2369	4.99	3.00E-06
1418262_at	Syk	spleen tyrosine kinase	20963	149	133	185	133	404	664	4.98	2.00E-05
1451374_x_at	Cklf	chemokine-like factor	75458	152	119	140	75	198	365	4.85	7.00E-04
1419609_at	Ccr1	chemokine (C-C motif) receptor 1	12768	92	149	166	125	365	604	4.85	7.00E-05

SUPPLEMENT

Affymetrix Probe set ID	Gene symbol	Gene name	Entrez Gene ID	Mean <i>Wt</i> aorta 6 weeks	Mean <i>Wt</i> aorta 32 weeks	Mean <i>Wt</i> aorta 78 weeks	Mean <i>Apoe</i> <sup>-/-</sup> aorta 6 weeks	Mean <i>Apoe</i> <sup>-/-</sup> aorta 32 weeks	Mean <i>Apoe</i> <sup>-/-</sup> aorta 78 weeks	Fold change <i>Apoe</i> <sup>-/-</sup> aorta 78 weeks vs. 6 weeks	p ANOVA
1460302_at	Thbs1	thrombospondin 1	21825	1405	897	1318	1466	3249	7044	4.81	2.00E-06
1448859_at	Cxcl13	chemokine (C-X-C motif) ligand 13	55985	344	292	521	366	506	1742	4.76	3.00E-04
1422444_at	Itga6	integrin alpha 6	16403	140	214	185	130	501	611	4.71	0.005
1422046_at	Itgam	integrin alpha M	16409	128	116	120	118	435	542	4.6	4.00E-05
1448449_at	Ripk3	receptor-interacting serine- threonine kinase 3	56532	98	72	104	80	174	365	4.59	4.00E-05
1417574_at	Cxcl12	chemokine (C-X-C motif) ligand 12	20315	577	562	615	474	1216	2174	4.58	1.00E-05
1415989_at	Vcam1	vascular cell adhesion molecule 1	22329	1174	1182	1475	1035	3424	4723	4.56	4.00E-07
1422823_at	Eps8	epidermal growth factor receptor pathway substrate 8	13860	247	296	317	207	683	922	4.45	5.00E-05
1427892_at	Myo1g	myosin IG	246177	229	319	418	289	623	1236	4.28	7.00E-06
1421187_at	Ccr2	chemokine (C-C motif) receptor 2	12772	59	71	18	57	218	244	4.27	1.00E-04
1439902_at	C5ar1	complement component 5a receptor 1	12273	128	130	163	108	287	460	4.24	7.00E-05
1434069_at	Prex1	phosphatidylinositol-3,4,5- trisphosphate-dependent Rac exchange factor 1	277360	329	307	310	286	624	1159	4.06	1.00E-05
1449984_at	Cxcl2	chemokine (C-X-C motif) ligand 2	20310	67	97	113	78	179	306	3.94	1.00E-04
1419728_at	Cxcl5	chemokine (C-X-C motif) ligand 5	20311	36	46	74	36	200	136	3.73	7.00E-04
1417676_a_at	Ptpro	protein tyrosine	19277	240	281	311	226	530	822	3.64	7.00E-06

## SUPPLEMENT

Affymetrix Probe set ID	Gene symbol	Gene name	Entrez Gene ID	Mean <i>Wt</i> aorta 6 weeks	Mean <i>Wt</i> aorta 32 weeks	Mean <i>Wt</i> aorta 78 weeks	Mean <i>Apoe</i> <sup>-/-</sup> aorta 6 weeks	Mean <i>Apoe</i> <sup>-/-</sup> aorta 32 weeks	Mean <i>Apoe</i> <sup>-/-</sup> aorta 78 weeks	Fold change <i>Apoe</i> <sup>-/-</sup> aorta 78 weeks vs. 6 weeks	p ANOVA
1449925_at	Cxcr3	chemokine (C-X-C motif) receptor 3	12766	156	151	234	164	194	595	3.62	8.00E-05
1422824_s_at	Eps8	epidermal growth factor receptor pathway substrate 8	13860	281	335	416	234	637	846	3.61	2.00E-07
1450377_at	Thbs1	thrombospondin 1	21825	717	476	570	799	1329	2712	3.39	1.00E-06
1450414_at	Pdgfb	platelet derived growth factor, B polypeptide	18591	315	569	533	320	676	1084	3.38	9.00E-06
1417751_at	Stk10	serine/threonine kinase 10	20868	328	238	642	299	598	1006	3.37	0.01
1415804_at	Cx3cl1	chemokine (C-X3-C motif) ligand 1	20312	67	134	123	78	315	258	3.3	0.003
1425357_a_at	Grem1	gremlin 1	23892	130	147	161	112	178	358	3.21	4.00E-04
1424495_a_at	Cklf	chemokine-like factor	75458	249	241	266	185	347	584	3.16	7.00E-04
1424067_at	Icam1	intercellular adhesion molecule 1	15894	715	772	949	690	1677	2170	3.14	1.00E-06
1418806_at	Csf3r	colony stimulating factor 3 receptor (granulocyte)	12986	134	206	247	133	326	417	3.13	0.02
1452050_at	Camk1d	calcium/calmodulin- dependent protein kinase ID	227541	114	215	189	143	292	436	3.04	6.00E-05
1419394_s_at	S100a8	S100 calcium binding protein A8 (calgranulin A)	20201	140	528	792	402	628	1182	2.94	0.007
1419132_at	Tlr2	toll-like receptor 2	24088	329	398	499	378	713	1099	2.91	1.00E-05
1418252_at	Padi2	peptidyl arginine deiminase, type II	18600	126	178	252	166	226	482	2.9	5.00E-04
1421188_at	Ccr2	chemokine (C-C motif)	12772	167	187	236	166	349	465	2.81	2.00E-04
1419480_at	Sell	selectin, lymphocyte	20343	150	187	285	194	187	527	2.72	0.002
1422190_at	C5ar1	complement component 5a receptor 1	12273	195	215	240	175	354	473	2.71	0.003

SUPPLEMENT

Affymetrix Probe set ID	Gene symbol	Gene name	Entrez Gene ID	Mean Wt aorta 6 weeks	Mean Wt aorta 32 weeks	Mean Wt aorta 78 weeks	Mean <i>Apoe</i> <sup>-/-</sup> aorta 6 weeks	Mean <i>Apoe</i> <sup>-/-</sup> aorta 32 weeks	Mean <i>Apoe</i> <sup>-/-</sup> aorta 78 weeks	Fold change <i>Apoe</i> <sup>-/-</sup> aorta 78 weeks vs. 6 weeks	p ANOVA
1424208_at	Ptger4	prostaglandin E receptor 4 (subtype EP4)	19219	470	631	955	533	1065	1426	2.68	2.00E-04
1449399_a_at	Il1b	interleukin 1 beta	16176	154	248	277	264	306	701	2.66	9.00E-04
1425863_a_at	Ptpro	protein tyrosine phosphatase, receptor type, O	19277	102	107	114	87	203	218	2.52	9.00E-04
1417122_at	Vav3	vav 3 oncogene	57257	150	247	205	178	308	447	2.51	0.001
1448756_at	S100a9	S100 calcium binding protein A9 (calgranulin B)	20202	109	442	600	261	459	648	2.48	0.01
1420558_at	Selp	selectin, platelet	20344	1203	955	966	882	1883	2152	2.44	9.00E-05
1457644_s_at	Cxcl1	chemokine (C-X-C motif) ligand 1	14825	652	678	472	530	1301	1276	2.41	0.003
1421073_a_at	Ptger4	prostaglandin E receptor 4 (subtype EP4)	19219	112	115	133	96	219	228	2.37	7.00E-04
1450357_a_at	Ccr6	chemokine (C-C motif) receptor 6	12458	182	215	239	211	189	496	2.35	0.02
1421578_at	Ccl4	chemokine (C-C motif) ligand 4	20303	369	367	586	386	521	885	2.29	0.003
1448550_at	Lbp	lipopolysaccharide binding protein	16803	931	1284	1276	998	1934	2268	2.27	5.00E-05
1425860_x_at	Cklf	chemokine-like factor	75458	438	380	438	373	470	841	2.25	3.00E-04
1416371_at	Apod	apolipoprotein D	11815	474	1606	1672	607	1712	1358	2.24	2.00E-06
1419481_at	Sell	selectin, lymphocyte	20343	165	161	206	213	197	463	2.17	0.002
1448600_s_at	Vav3	vav 3 oncogene	57257	212	366	305	250	365	542	2.17	6.00E-04
1438643_at	Camk1d	calcium/calmodulin- dependent protein kinase ID	227541	145	174	133	160	282	340	2.12	0.009
1441855_x_at	Cxcl1	chemokine (C-X-C motif) ligand 1	14825	580	592	713	590	1086	1251	2.12	8.00E-04



## SUPPLEMENT

Affymetrix Probe set ID	Gene symbol	Gene name	Entrez Gene ID	Mean <i>Wt</i> aorta 6 weeks	Mean <i>Wt</i> aorta 32 weeks	Mean <i>Wt</i> aorta 78 weeks	Mean <i>Apoe</i> <sup>-/-</sup> aorta 6 weeks	Mean <i>Apoe</i> <sup>-/-</sup> aorta 32 weeks	Mean <i>Apoe</i> <sup>-/-</sup> aorta 78 weeks	Fold change <i>Apoe</i> <sup>-/-</sup> aorta 78 weeks vs. 6 weeks	p ANOVA
1425733_a_at	Eps8	epidermal growth factor receptor pathway substrate 8	13860	241	257	253	231	392	488	2.12	3.00E-05
1448823_at	Cxcl12	chemokine (C-X-C motif) ligand 12	20315	5885	5864	6394	5182	8384	10772	2.08	7.00E-06
1450020_at	Cx3cr1	chemokine (C-X3-C motif) receptor 1	13051	104	116	64	146	283	302	2.06	3.00E-04
1419300_at	Flt1	FMS-like tyrosine kinase 1	14254	228	351	441	267	371	540	2.03	7.00E-04
1435495_at	Adora1	adenosine A1 receptor	11539	149	258	96	89	185	158	1.77	0.004
1436037_at	Itga4	integrin alpha 4	16401	583	457	457	585	753	1018	1.74	0.002
1417789_at	Ccl11	chemokine (C-C motif) ligand 11	20292	246	801	630	296	713	495	1.67	3.00E-04
1437347_at	Ednrb	endothelin receptor type B	13618	604	655	708	488	1040	812	1.66	0.04
1418456_a_at	Cxcl14	chemokine (C-X-C motif) ligand 14	57266	253	309	174	279	395	454	1.63	2.00E-05
1449528_at	Figf	c-fos induced growth factor	14205	1234	2306	2562	1309	2829	2009	1.53	8.00E-04
1449906_at	Selp	selectin, platelet	20344	205	146	102	180	454	273	1.52	0.002
1422474_at	Pde4b	phosphodiesterase 4B, cAMP specific	18578	496	1257	1183	659	1373	860	1.3	4.00E-04
1451803_a_at	Vegfb	vascular endothelial growth factor B	22340	344	743	629	422	723	544	1.29	0.001
1421857_at	Adam17	a disintegrin and metallopeptidase domain 17	11491	849	443	318	746	452	556	-1.34	3.00E-04
1425587_a_at	Ptpnj	protein tyrosine phosphatase, receptor type, J	19271	246	175	106	214	226	156	-1.37	0.01

## SUPPLEMENT

Affymetrix Probe set ID	Gene symbol	Gene name	Entrez Gene ID	Mean <i>Wt</i> aorta 6 weeks	Mean <i>Wt</i> aorta 32 weeks	Mean <i>Wt</i> aorta 78 weeks	Mean <i>Apoe</i> <sup>-/-</sup> aorta 6 weeks	Mean <i>Apoe</i> <sup>-/-</sup> aorta 32 weeks	Mean <i>Apoe</i> <sup>-/-</sup> aorta 78 weeks	Fold change <i>Apoe</i> <sup>-/-</sup> aorta 78 weeks vs. 6 weeks	p ANOVA
1430630_at	Itgb1	integrin beta 1 (fibronectin receptor beta)	16412	196	165	96	169	160	108	-1.56	5.00E-04
1422102_a_at	Stat5b	signal transducer and activator of transcription 5B	20851	326	292	265	404	190	213	-1.89	0.002
1423503_at	Jam3	junction adhesion molecule 3	83964	1694	1509	1630	1718	1241	853	-2.01	2.00E-05
1425091_at	Rarres2	retinoic acid receptor responder (tazarotene induced) 2	71660	294	255	223	284	238	141	-2.02	2.00E-04
1423444_at	Rock1	Rho-associated coiled-coil containing protein kinase 1	19877	6804	4986	5060	6358	4734	3121	-2.04	2.00E-05
1423445_at	Rock1	Rho-associated coiled-coil containing protein kinase 1	19877	5911	5987	5146	6020	4999	2765	-2.18	5.00E-06
1454824_s_at	Mtus1	mitochondrial tumor suppressor 1	102103	2794	2882	2177	2573	2180	1131	-2.28	2.00E-05
1449396_at	Aoc3	amine oxidase, copper containing 3	11754	3675	3868	3401	4108	3563	1730	-2.37	8.00E-05
1437673_at	Wnt5a	wingless-type MMTV integration site family, member 5A	22418	246	284	183	201	226	85	-2.37	0.003
1436501_at	Mtus1	mitochondrial tumor suppressor 1	102103	2086	1613	1415	1767	1376	721	-2.45	3.00E-06
1436502_at	Mtus1	mitochondrial tumor suppressor 1	102103	923	579	442	654	443	240	-2.72	3.00E-04
1436791_at	Wnt5a	wingless-type MMTV integration site family, member 5A	22418	706	850	713	786	717	241	-3.26	2.00E-05

SUPPLEMENT

Affymetrix Probe set ID	Gene symbol	Gene name	Entrez Gene ID	Mean <i>Wt</i> aorta 6 weeks	Mean <i>Wt</i> aorta 32 weeks	Mean <i>Wt</i> aorta 78 weeks	Mean <i>Apoe</i> <sup>-/-</sup> aorta 6 weeks	Mean <i>Apoe</i> <sup>-/-</sup> aorta 32 weeks	Mean <i>Apoe</i> <sup>-/-</sup> aorta 78 weeks	Fold change <i>Apoe</i> <sup>-/-</sup> aorta 78 weeks vs. 6 weeks	p ANOVA
1431693_a_at	Il17b	interleukin 17B	56069	348	145	345	295	38	89	-3.32	0.002
1438533_at	Myo9b	myosin IXb	17925	240	99	60	204	114	58	-3.53	0.003
1415900_a_at	Kit	kit oncogene	16590	224	229	153	266	226	74	-3.58	0.03
1460729_at	Rock1	Rho-associated coiled-coil containing protein kinase 1	19877	1233	366	564	965	389	266	-3.63	2.00E-06
1450029_s_at	Itga9	integrin alpha 9	104099	1853	1428	1011	1932	1276	518	-3.73	1.00E-05
1439713_at	Itga1	integrin alpha 1	109700	410	304	118	425	278	92	-4.61	2.00E-04
1427771_x_at	Itgb1	integrin beta 1 (fibronectin receptor beta)	16412	1680	2297	732	2442	1692	505	-4.83	0.001
1460285_at	Itga9	integrin alpha 9	104099	3458	2214	1617	3486	1844	695	-5.01	2.00E-05
1448818_at	Wnt5a	wingless-type MMTV integration site family, member 5A	22418	653	606	253	721	519	140	-5.14	8.00E-06
1420860_at	Itga9	integrin alpha 9	104099	789	476	286	742	398	114	-6.49	3.00E-05

**F. Meloid leukocyte migration (GO: 0097529)**

Affymetrix Probe set ID	Gene symbol	Gene name	Entrez Gene ID	Mean <i>Wt</i> aorta 6 weeks	Mean <i>Wt</i> aorta 32 weeks	Mean <i>Wt</i> aorta 78 weeks	Mean <i>Apoe</i> <sup>-/-</sup> aorta 6 weeks	Mean <i>Apoe</i> <sup>-/-</sup> aorta 32 weeks	Mean <i>Apoe</i> <sup>-/-</sup> aorta 78 weeks	Fold change <i>Apoe</i> <sup>-/-</sup> aorta 78 weeks vs. 6 weeks	p ANOVA
1449254_at	Spp1	secreted phosphoprotein 1	20750	46	93	326	76	13398	13789	180.67	3.00E-05
1419561_at	Ccl3	chemokine (C-C motif) ligand 3	20302	6	18	9	12	212	597	48.71	5.00E-06
1419282_at	Ccl12	chemokine (C-C motif) ligand 12	20293	83	27	134	23	374	926	40.66	4.00E-05

## SUPPLEMENT

Affymetrix Probe set ID	Gene symbol	Gene name	Entrez Gene ID	Mean <i>Wt</i> aorta 6 weeks	Mean <i>Wt</i> aorta 32 weeks	Mean <i>Wt</i> aorta 78 weeks	Mean <i>ApoE</i> <sup>-/-</sup> aorta 6 weeks	Mean <i>ApoE</i> <sup>-/-</sup> aorta 32 weeks	Mean <i>ApoE</i> <sup>-/-</sup> aorta 78 weeks	Fold change <i>ApoE</i> <sup>-/-</sup> aorta 78 weeks vs. 6 weeks	p ANOVA
1426808_at	Lgals3	lectin, galactose binding, soluble 3	16854	652	822	1038	693	9961	13992	20.2	2.00E-08
1442082_at	C3ar1	complement component 3a receptor 1	12267	162	203	280	175	2019	3522	20.11	6.00E-08
1418126_at	Ccl5	chemokine (C-C motif) ligand 5	20304	24	73	420	67	406	1222	18.28	0.009
1450678_at	Itgb2	integrin beta 2	16414	274	540	582	384	2879	6211	16.19	7.00E-07
1418340_at	Fcgr1g	Fc receptor, IgE, high affinity I, gamma polypeptide	14127	507	690	889	382	2708	5707	14.95	2.00E-05
1419483_at	C3ar1	complement component 3a receptor 1	12267	342	353	423	332	2266	4841	14.58	5.00E-07
1419209_at	Cxcl1	chemokine (C-X-C motif) ligand 1	14825	110	172	157	103	1157	1394	13.59	6.00E-06
1430700_a_at	Pla2g7	phospholipase A2, group VII (platelet-activating factor acetylhydrolase, plasma)	27226	219	238	169	164	1438	2061	12.53	2.00E-04
1419482_at	C3ar1	complement component 3a receptor 1	12267	235	228	335	252	1530	2963	11.78	1.00E-06
1416871_at	Adam8	a disintegrin and metallopeptidase domain 8	11501	195	215	174	181	1113	1881	10.42	9.00E-07
1428787_at	Nckap1l	NCK associated protein 1 like	105855	130	86	249	159	779	1589	10	7.00E-05
1420380_at	Ccl2	chemokine (C-C motif) ligand 2	20296	99	49	126	95	414	915	9.65	1.00E-04
1448620_at	Fcgr3	Fc receptor, IgG, low affinity III	14131	324	357	399	369	1881	3536	9.58	3.00E-06

## SUPPLEMENT

Affymetrix Probe set ID	Gene symbol	Gene name	Entrez Gene ID	Mean Wt aorta 6 weeks	Mean Wt aorta 32 weeks	Mean Wt aorta 78 weeks	Mean <i>Apoe</i> <sup>-/-</sup> aorta 6 weeks	Mean <i>Apoe</i> <sup>-/-</sup> aorta 32 weeks	Mean <i>Apoe</i> <sup>-/-</sup> aorta 78 weeks	Fold change <i>Apoe</i> <sup>-/-</sup> aorta 78 weeks vs. 6 weeks	p ANOVA
1422932_a_at	Vav1	vav 1 oncogene	22324	31	68	22	46	230	431	9.41	4.00E-04
1418930_at	Cxcl10	chemokine (C-X-C motif) ligand 10	15945	84	92	98	48	185	403	8.33	5.00E-04
1418204_s_at	Aif1	allograft inflammatory factor 1	11629	166	234	394	191	676	1456	7.63	8.00E-07
1435903_at	Cd300a	CD300A antigen	217303	214	236	244	184	720	1349	7.35	1.00E-06
1421186_at	Ccr2	chemokine (C-C motif) receptor 2	12772	154	154	132	130	619	939	7.21	3.00E-05
1418261_at	Syk	spleen tyrosine kinase	20963	311	375	517	281	875	1860	6.63	7.00E-06
1425519_a_at	Cd74	CD74 antigen (invariant polypeptide of major histocompatibility complex, class II antigen-associated)	16149	1634	2699	4537	1955	7675	11699	5.98	4.00E-06
1428786_at	Nckap1l	NCK associated protein 1 like	105855	283	375	583	364	896	2157	5.92	2.00E-06
1415803_at	Cx3cl1	chemokine (C-X3-C motif) ligand 1	20312	262	349	622	278	772	1458	5.24	1.00E-06
1434653_at	Ptk2b	PTK2 protein tyrosine kinase 2 beta	19229	261	463	424	263	748	1346	5.12	1.00E-06
1417620_at	Rac2	RAS-related C3 botulinum substrate 2	19354	366	467	503	475	1376	2369	4.99	3.00E-06
1418262_at	Syk	spleen tyrosine kinase	20963	149	133	185	133	404	664	4.98	2.00E-05
1451374_x_at	Cklf	chemokine-like factor	75458	152	119	140	75	198	365	4.85	7.00E-04
1419609_at	Ccr1	chemokine (C-C motif) receptor 1	12768	92	149	166	125	365	604	4.85	7.00E-05
1460302_at	Thbs1	thrombospondin 1	21825	1405	897	1318	1466	3249	7044	4.81	2.00E-06
1422046_at	Itgam	integrin alpha M	16409	128	116	120	118	435	542	4.6	4.00E-05
1417574_at	Cxcl12	chemokine (C-X-C motif) ligand 12	20315	577	562	615	474	1216	2174	4.58	1.00E-05

## SUPPLEMENT

Affymetrix Probe set ID	Gene symbol	Gene name	Entrez Gene ID	Mean <i>Wt</i> aorta 6 weeks	Mean <i>Wt</i> aorta 32 weeks	Mean <i>Wt</i> aorta 78 weeks	Mean <i>Apoe</i> <sup>-/-</sup> aorta 6 weeks	Mean <i>Apoe</i> <sup>-/-</sup> aorta 32 weeks	Mean <i>Apoe</i> <sup>-/-</sup> aorta 78 weeks	Fold change <i>Apoe</i> <sup>-/-</sup> aorta 78 weeks vs. 6 weeks	p ANOVA
1419300_at	Flt1	FMS-like tyrosine kinase 1	14254	228	351	441	267	371	540	2.03	7.00E-04
1417789_at	Ccl11	chemokine (C-C motif) ligand 11	20292	246	801	630	296	713	495	1.67	3.00E-04
1437347_at	Ednrb	endothelin receptor type B	13618	604	655	708	488	1040	812	1.66	0.04
1449528_at	Figf	c-fos induced growth factor	14205	1234	2306	2562	1309	2829	2009	1.53	8.00E-04
1422474_at	Pde4b	phosphodiesterase 4B, cAMP specific	18578	496	1257	1183	659	1373	860	1.3	4.00E-04
1451803_a_at	Vegfb	vascular endothelial growth factor B	22340	344	743	629	422	723	544	1.29	0.001
1425587_a_at	Ptpn11	protein tyrosine phosphatase, receptor type, J	19271	246	175	106	214	226	156	-1.37	0.01
1422102_a_at	Stat5b	signal transducer and activator of transcription 5B	20851	326	292	265	404	190	213	-1.89	0.002
1423503_at	Jam3	junction adhesion molecule 3	83964	1694	1509	1630	1718	1241	853	-2.01	2.00E-05
1425091_at	Rarres2	retinoic acid receptor responder (tazarotene induced) 2	71660	294	255	223	284	238	141	-2.02	2.00E-04
1454824_s_at	Mtss1	mitochondrial tumor suppressor 1	102103	2794	2882	2177	2573	2180	1131	-2.28	2.00E-05
1436501_at	Mtss1	mitochondrial tumor suppressor 1	102103	2086	1613	1415	1767	1376	721	-2.45	3.00E-06
1436502_at	Mtss1	mitochondrial tumor suppressor 1	102103	923	579	442	654	443	240	-2.72	3.00E-04
1431693_a_at	Il17b	interleukin 17B	56069	348	145	345	295	38	89	-3.32	0.002
1438533_at	Myo9b	myosin IXb	17925	240	99	60	204	114	58	-3.53	0.003
1415900_a_at	Kit	kit oncogene	16590	224	229	153	266	226	74	-3.58	0.03

SUPPLEMENT

Affymetrix Probe set ID	Gene symbol	Gene name	Entrez Gene ID	Mean <i>Wt</i> aorta 6 weeks	Mean <i>Wt</i> aorta 32 weeks	Mean <i>Wt</i> aorta 78 weeks	Mean <i>Apoe</i> <sup>-/-</sup> aorta 6 weeks	Mean <i>Apoe</i> <sup>-/-</sup> aorta 32 weeks	Mean <i>Apoe</i> <sup>-/-</sup> aorta 78 weeks	Fold change <i>Apoe</i> <sup>-/-</sup> aorta 78 weeks vs. 6 weeks	p ANOVA
1450029_s_at	Itga9	integrin alpha 9	104099	1853	1428	1011	1932	1276	518	-3.73	1.00E-05
1439713_at	Itga1	integrin alpha 1	109700	410	304	118	425	278	92	-4.61	2.00E-04
1460285_at	Itga9	integrin alpha 9	104099	3458	2214	1617	3486	1844	695	-5.01	2.00E-05
1420860_at	Itga9	integrin alpha 9	104099	789	476	286	742	398	114	-6.49	3.00E-05

**G. Phagocytosis (GO: 0006909)**

Affymetrix Probe set ID	Gene symbol	Gene name	Entrez Gene ID	Mean <i>Wt</i> aorta 6 weeks	Mean <i>Wt</i> aorta 32 weeks	Mean <i>Wt</i> aorta 78 weeks	Mean <i>Apoe</i> <sup>-/-</sup> aorta 6 weeks	Mean <i>Apoe</i> <sup>-/-</sup> aorta 32 weeks	Mean <i>Apoe</i> <sup>-/-</sup> aorta 78 weeks	Fold change <i>Apoe</i> <sup>-/-</sup> aorta 78 weeks vs. 6 weeks	p ANOVA
1420699_at	Clec7a	C-type lectin domain family 7, member a	56644	238	388	461	273	3319	5253	19.26	9.00E-08
1438097_at	Rab20	RAB20, member RAS oncogene family	19332	8	7	46	12	77	184	15.09	5.00E-05
1418340_at	Fcgr1g	Fc receptor, IgE, high affinity I, gamma polypeptide	14127	507	690	889	382	2708	5707	14.95	2.00E-05
1455269_a_at	Coro1a	coronin, actin binding protein 1A	12721	169	336	625	275	1527	3332	12.12	1.00E-05
1416246_a_at	Coro1a	coronin, actin binding protein 1A	12721	334	325	498	336	1586	3943	11.75	1.00E-05
1422808_s_at	Dock2	dedicator of cyto-kinesis 2	94176	132	177	262	124	559	1417	11.48	1.00E-06
1428787_at	Nckap1l	NCK associated protein 1 like	105855	130	86	249	159	779	1589	10	7.00E-05
1420380_at	Ccl2	chemokine (C-C motif) ligand 2	20296	99	49	126	95	414	915	9.65	1.00E-04

## SUPPLEMENT

Affymetrix Probe set ID	Gene symbol	Gene name	Entrez Gene ID	Mean <i>Wt</i> aorta 6 weeks	Mean <i>Wt</i> aorta 32 weeks	Mean <i>Wt</i> aorta 78 weeks	Mean <i>Apoe</i> <sup>-/-</sup> aorta 6 weeks	Mean <i>Apoe</i> <sup>-/-</sup> aorta 32 weeks	Mean <i>Apoe</i> <sup>-/-</sup> aorta 78 weeks	Fold change <i>Apoe</i> <sup>-/-</sup> aorta 78 weeks vs. 6 weeks	p ANOVA
1448620_at	Fcgr3	Fc receptor, IgG, low affinity III	14131	324	357	399	369	1881	3536	9.58	3.00E-06
1422932_a_at	Vav1	vav 1 oncogene	22324	31	68	22	46	230	431	9.41	4.00E-04
1448452_at	Irf8	interferon regulatory factor 8	15900	80	70	93	86	464	726	8.46	3.00E-04
1418204_s_at	Aif1	allograft inflammatory factor 1	11629	166	234	394	191	676	1456	7.63	8.00E-07
1435903_at	Cd300a	CD300A antigen	217303	214	236	244	184	720	1349	7.35	1.00E-06
1416714_at	Irf8	interferon regulatory factor 8	15900	194	249	333	209	705	1523	7.3	7.00E-06
1421186_at	Ccr2	chemokine (C-C motif) receptor 2	12772	154	154	132	130	619	939	7.21	3.00E-05
1417876_at	Fcgr1	Fc receptor, IgG, high affinity I	14129	156	174	234	153	627	1066	6.96	2.00E-06
1420715_a_at	Pparg	peroxisome proliferator activated receptor gamma	19016	29	476	171	60	375	400	6.65	0.002
1418261_at	Syk	spleen tyrosine kinase	20963	311	375	517	281	875	1860	6.63	7.00E-06
1428786_at	Nckap1l	NCK associated protein 1 like	105855	283	375	583	364	896	2157	5.92	2.00E-06
1416985_at	Sirpa	signal-regulatory protein alpha	19261	927	971	1137	930	3410	5382	5.78	9.00E-07
1424987_at	5430435 G22Rik	RIKEN cDNA 5430435G22 gene	226421	313	302	408	330	886	1891	5.73	1.00E-06
1423166_at	Cd36	CD36 antigen	12491	794	3237	1578	835	4019	4649	5.57	8.00E-06
1435477_s_at	Fcgr2b	Fc receptor, IgG, low affinity IIb	14130	736	720	1048	705	2176	3922	5.56	4.00E-06



## SUPPLEMENT

Affymetrix Probe set ID	Gene symbol	Gene name	Entrez Gene ID	Mean <i>Wt</i> aorta 6 weeks	Mean <i>Wt</i> aorta 32 weeks	Mean <i>Wt</i> aorta 78 weeks	Mean <i>Apoe</i> <sup>-/-</sup> aorta 6 weeks	Mean <i>Apoe</i> <sup>-/-</sup> aorta 32 weeks	Mean <i>Apoe</i> <sup>-/-</sup> aorta 78 weeks	Fold change <i>Apoe</i> <sup>-/-</sup> aorta 78 weeks vs. 6 weeks	p ANOVA
1417346_at	Pycard	PYD and CARD domain containing	66824	399	333	506	335	802	1825	5.44	7.00E-06
1451941_a_at	Fcgr2b	Fc receptor, IgG, low affinity IIb	14130	549	458	690	506	1472	2594	5.13	1.00E-05
1435830_a_at	5430435 G22Rik	RIKEN cDNA 5430435G22 gene	226421	117	132	73	99	290	505	5.11	0.009
1418262_at	Syk	spleen tyrosine kinase	20963	149	133	185	133	404	664	4.98	2.00E-05
1460302_at	Thbs1	thrombospondin 1	21825	1405	897	1318	1466	3249	7044	4.81	2.00E-06
1455332_x_at	Fcgr2b	Fc receptor, IgG, low affinity IIb	14130	254	277	421	334	907	1444	4.32	3.00E-05
1427892_at	Myo1g	myosin IG	246177	229	319	418	289	623	1236	4.28	7.00E-06
1421187_at	Ccr2	chemokine (C-C motif) receptor 2	12772	59	71	18	57	218	244	4.27	1.00E-04
1423954_at	C3	complement component 3	12266	1929	4798	3722	2416	8194	10023	4.15	2.00E-06
1420361_at	Slc11a1	solute carrier family 11 (proton-coupled divalent metal ion transporters), member 1	18173	662	704	802	668	1645	2664	3.99	1.00E-06
1433678_at	Pld4	phospholipase D family, member 4	104759	284	345	354	270	714	1069	3.96	1.00E-05
1450883_a_at	Cd36	CD36 antigen	12491	1224	4327	1699	1492	5328	5773	3.87	1.00E-05
1449455_at	Hck	hemopoietic cell kinase	15162	304	332	451	317	658	1215	3.84	9.00E-06
1420653_at	Tgfb1	transforming growth factor, beta 1	21803	516	538	551	440	1292	1670	3.79	8.00E-07
1450377_at	Thbs1	thrombospondin 1	21825	717	476	570	799	1329	2712	3.39	1.00E-06
1419526_at	Fgr	Gardner-Rasheed feline sarcoma viral (Fgr) oncogene homolog	14191	184	254	418	227	569	763	3.37	1.00E-04

## SUPPLEMENT

Affymetrix Probe set ID	Gene symbol	Gene name	Entrez Gene ID	Mean <i>Wt</i> aorta 6 weeks	Mean <i>Wt</i> aorta 32 weeks	Mean <i>Wt</i> aorta 78 weeks	Mean <i>Apoe</i> <sup>-/-</sup> aorta 6 weeks	Mean <i>Apoe</i> <sup>-/-</sup> aorta 32 weeks	Mean <i>Apoe</i> <sup>-/-</sup> aorta 78 weeks	Fold change <i>Apoe</i> <sup>-/-</sup> aorta 78 weeks vs. 6 weeks	p ANOVA
1452050_at	Camk1d	calcium/calmodulin- dependent protein kinase ID	227541	114	215	189	143	292	436	3.04	6.00E-05
1421840_at	Abca1	ATP-binding cassette, sub- family A (ABC1), member 1	11303	1805	2970	2438	3039	7715	8828	2.9	8.00E-07
1421839_at	Abca1	ATP-binding cassette, sub- family A (ABC1), member 1	11303	406	422	385	673	1638	1913	2.84	5.00E-06
1448534_at	Sirpa	signal-regulatory protein alpha	19261	542	445	509	554	1153	1569	2.83	2.00E-05
1421188_at	Ccr2	chemokine (C-C motif) receptor 2	12772	167	187	236	166	349	465	2.81	2.00E-04
1421385_a_at	Myo7a	myosin VIIA	17921	228	269	272	241	408	673	2.79	3.00E-05
1416986_a_at	Sirpa	signal-regulatory protein alpha	19261	231	248	141	266	618	734	2.76	1.00E-05
1449399_a_at	Il1b	interleukin 1 beta	16176	154	248	277	264	306	701	2.66	9.00E-04
1436625_at	Fcgr1	Fc receptor, IgG, high affinity I	14129	150	172	282	182	348	484	2.65	0.001
1435220_s_at	Cdc42se 2	CDC42 small effector 2	72729	483	400	376	403	612	1057	2.63	4.00E-05
1439787_at	P2rx7	purinergic receptor P2X, ligand-gated ion channel, 7	18439	335	463	522	352	719	922	2.62	2.00E-06
1419238_at	Abca7	ATP-binding cassette, sub- family A (ABC1), member 7	27403	225	303	419	226	346	586	2.6	2.00E-04
1458683_at	Sirpb1a	signal-regulatory protein beta 1A	320832	160	87	154	170	200	440	2.59	0.02
1450884_at	Cd36	CD36 antigen	12491	147	624	269	200	508	484	2.42	4.00E-05
1419853_a_at	P2rx7	purinergic receptor P2X, ligand-gated ion channel, 7	18439	138	186	113	129	250	300	2.33	0.002

SUPPLEMENT

Affymetrix Probe set ID	Gene symbol	Gene name	Entrez Gene ID	Mean <i>Wt</i> aorta 6 weeks	Mean <i>Wt</i> aorta 32 weeks	Mean <i>Wt</i> aorta 78 weeks	Mean <i>Apoe</i> <sup>-/-</sup> aorta 6 weeks	Mean <i>Apoe</i> <sup>-/-</sup> aorta 32 weeks	Mean <i>Apoe</i> <sup>-/-</sup> aorta 78 weeks	Fold change <i>Apoe</i> <sup>-/-</sup> aorta 78 weeks vs. 6 weeks	p ANOVA
1448550_at	Lbp	lipopolysaccharide binding protein	16803	931	1284	1276	998	1934	2268	2.27	5.00E-05
1450392_at	Abca1	ATP-binding cassette, sub-family A (ABC1), member 1	11303	164	150	115	272	596	580	2.14	8.00E-06
1422651_at	Adipoq	adiponectin, C1Q and collagen domain containing	11450	2602	6562	3968	2524	5547	5362	2.12	0.001
1438643_at	Camk1d	calcium/calmodulin-dependent protein kinase ID	227541	145	174	133	160	282	340	2.12	0.009
1442804_at	Fgr	Gardner-Rasheed feline sarcoma viral (Fgr) oncogene homolog	14191	207	237	399	263	407	559	2.12	0.001
1423518_at	Csk	c-src tyrosine kinase	12988	492	500	676	473	535	962	2.03	5.00E-04
1457664_x_at	C2	complement component 2 (within H-2S)	12263	357	255	619	365	420	573	1.57	0.002
1418666_at	Ptx3	pentraxin related gene	19288	137	133	104	152	277	239	1.57	0.02
1441248_at	Clcn3	chloride channel 3	12725	133	79	240	167	115	249	1.49	0.005
1422553_at	Pten	phosphatase and tensin homolog	19211	1496	1011	617	1534	1229	973	-1.58	0.006
1428816_a_at	Gata2	GATA binding protein 2	14461	317	363	391	301	360	176	-1.71	0.007
1451939_a_at	Srpx	sushi-repeat-containing protein	51795	1194	526	566	1007	679	540	-1.87	6.00E-05
1432004_a_at	Dnm2	dynammin 2	13430	392	371	174	429	440	208	-2.07	8.00E-05
1421198_at	Itgav	integrin alpha V	16410	791	365	315	593	363	282	-2.1	4.00E-04
1453771_at	Gulp1	GULP, engulfment adaptor PTB domain containing 1	70676	1522	1384	1185	1500	1242	658	-2.28	1.00E-07
1420925_at	Tub	tubby candidate gene	22141	1457	1557	1616	1506	1087	433	-3.48	2.00E-04

## SUPPLEMENT

Affymetrix Probe set ID	Gene symbol	Gene name	Entrez Gene ID	Mean <i>Wt</i> aorta 6 weeks	Mean <i>Wt</i> aorta 32 weeks	Mean <i>Wt</i> aorta 78 weeks	Mean <i>Apoe</i> <sup>-/-</sup> aorta 6 weeks	Mean <i>Apoe</i> <sup>-/-</sup> aorta 32 weeks	Mean <i>Apoe</i> <sup>-/-</sup> aorta 78 weeks	Fold change <i>Apoe</i> <sup>-/-</sup> aorta 78 weeks vs. 6 weeks	p ANOVA
1417752_at	Coro1c	coronin, actin binding protein 1C	23790	1030	947	443	1219	818	334	-3.65	7.00E-06
1432092_a_at	Gulp1	GULP, engulfment adaptor PTB domain containing 1	70676	402	199	187	455	227	100	-4.53	0.03

**H. Cellular response to lipid (GO: 0071396)**

Affymetrix Probe set ID	Gene symbol	Gene name	Entrez Gene ID	Mean <i>Wt</i> aorta 6 weeks	Mean <i>Wt</i> aorta 32 weeks	Mean <i>Wt</i> aorta 78 weeks	Mean <i>Apoe</i> <sup>-/-</sup> aorta 6 weeks	Mean <i>Apoe</i> <sup>-/-</sup> aorta 32 weeks	Mean <i>Apoe</i> <sup>-/-</sup> aorta 78 weeks	Fold change <i>Apoe</i> <sup>-/-</sup> aorta 78 weeks vs. 6 weeks	p ANOVA
1421792_s_at	Trem2	triggering receptor expressed on myeloid cells 2	83433	22	25	27	22	707	1816	83.52	2.00E-07
1419282_at	Ccl12	chemokine (C-C motif) ligand 12	20293	83	27	134	23	374	926	40.66	4.00E-05
1450297_at	Il6	interleukin 6	16193	21	10	57	21	290	523	24.46	1.00E-04
1418126_at	Ccl5	chemokine (C-C motif) ligand 5	20304	24	73	420	67	406	1222	18.28	0.009
1449195_s_at	Cxcl16	chemokine (C-X-C motif) ligand 16	66102	190	164	238	146	1008	1929	13.18	7.00E-07
1420380_at	Ccl2	chemokine (C-C motif) ligand 2	20296	99	49	126	95	414	915	9.65	1.00E-04
1422903_at	Ly86	lymphocyte antigen 86	17084	417	477	693	421	1743	3863	9.18	2.00E-06
1445882_at	Cd300lb	CD300 antigen like family member B	217304	170	165	219	139	694	1201	8.67	1.00E-06
1448452_at	Irf8	interferon regulatory factor 8	15900	80	70	93	86	464	726	8.46	3.00E-04

## SUPPLEMENT

Affymetrix Probe set ID	Gene symbol	Gene name	Entrez Gene ID	Mean <i>Wt</i> aorta 6 weeks	Mean <i>Wt</i> aorta 32 weeks	Mean <i>Wt</i> aorta 78 weeks	Mean <i>Apoe</i> <sup>-/-</sup> aorta 6 weeks	Mean <i>Apoe</i> <sup>-/-</sup> aorta 32 weeks	Mean <i>Apoe</i> <sup>-/-</sup> aorta 78 weeks	Fold change <i>Apoe</i> <sup>-/-</sup> aorta 78 weeks vs. 6 weeks	p ANOVA
1418930_at	Cxcl10	chemokine (C-X-C motif) ligand 10	15945	84	92	98	48	185	403	8.33	5.00E-04
1418718_at	Cxcl16	chemokine (C-X-C motif) ligand 16	66102	462	481	623	437	1456	3219	7.36	8.00E-07
1416714_at	Irf8	interferon regulatory factor 8	15900	194	249	333	209	705	1523	7.3	7.00E-06
1420715_a_at	Pparg	peroxisome proliferator activated receptor gamma	19016	29	476	171	60	375	400	6.65	0.002
1425225_at	Fcgr4	Fc receptor, IgG, low affinity IV	246256	145	232	360	298	877	1955	6.56	2.00E-06
1426858_at	Inhbb	inhibin beta-B	16324	197	496	510	218	618	1219	5.6	1.00E-06
1423166_at	Cd36	CD36 antigen	12491	794	3237	1578	835	4019	4649	5.57	8.00E-06
1417346_at	Pycard	PYD and CARD domain containing	66824	399	333	506	335	802	1825	5.44	7.00E-06
1447643_x_at	Snai2	snail family zinc finger 2	20583	733	428	1253	398	856	2082	5.24	0.04
1434653_at	Ptk2b	PTK2 protein tyrosine kinase 2 beta	19229	261	463	424	263	748	1346	5.12	1.00E-06
1418099_at	Tnfrsf1b	tumor necrosis factor receptor superfamily, member 1b	21938	300	400	416	308	986	1555	5.05	6.00E-06
1417268_at	Cd14	CD14 antigen	12475	577	649	838	605	1254	2776	4.59	2.00E-06
1460273_a_at	Naip2	NLR family, apoptosis inhibitory protein 2	17948	80	138	136	110	293	444	4.03	2.00E-05
1449310_at	Ptger2	prostaglandin E receptor 2 (subtype EP2)	19217	60	77	87	65	151	255	3.95	1.00E-04
1450883_a_at	Cd36	CD36 antigen	12491	1224	4327	1699	1492	5328	5773	3.87	1.00E-05
1420653_at	Tgfb1	transforming growth factor, beta 1	21803	516	538	551	440	1292	1670	3.79	8.00E-07

## SUPPLEMENT

Affymetrix Probe set ID	Gene symbol	Gene name	Entrez Gene ID	Mean <i>Wt</i> aorta 6 weeks	Mean <i>Wt</i> aorta 32 weeks	Mean <i>Wt</i> aorta 78 weeks	Mean <i>ApoE</i> <sup>-/-</sup> aorta 6 weeks	Mean <i>ApoE</i> <sup>-/-</sup> aorta 32 weeks	Mean <i>ApoE</i> <sup>-/-</sup> aorta 78 weeks	Fold change <i>ApoE</i> <sup>-/-</sup> aorta 78 weeks vs. 6 weeks	p ANOVA
1447927_at	Gbp6	guanylate binding protein 6	100702	244	375	398	190	524	667	3.52	0.004
1420425_at	Prdm1	PR domain containing 1, with ZNF domain	12142	144	169	175	159	193	463	2.92	0.002
1421840_at	Abca1	ATP-binding cassette, sub- family A (ABC1), member 1	11303	1805	2970	2438	3039	7715	8828	2.9	8.00E-07
1421839_at	Abca1	ATP-binding cassette, sub- family A (ABC1), member 1	11303	406	422	385	673	1638	1913	2.84	5.00E-06
1421547_at	Cd180	CD180 antigen	17079	223	279	274	219	599	621	2.84	5.00E-05
1440481_at	Stat1	signal transducer and activator of transcription 1	20846	104	104	103	117	165	316	2.71	0.002
1449399_a_at	Il1b	interleukin 1 beta	16176	154	248	277	264	306	701	2.66	9.00E-04
1420992_at	Ankrd1	ankyrin repeat domain 1 (cardiac muscle)	107765	360	408	520	408	418	1054	2.58	0.001
1416303_at	Litaf	LPS-induced TN factor	56722	2048	1894	2430	2047	3700	5169	2.53	3.00E-06
1420915_at	Stat1	signal transducer and activator of transcription 1	20846	300	422	402	313	628	778	2.49	2.00E-05
1438091_a_at	H2afz	H2A histone family, member Z	51788	2221	2211	2803	1710	2651	4222	2.47	5.00E-05
1418240_at	Gbp2	guanylate binding protein 2	14469	721	912	1200	778	1313	1913	2.46	3.00E-04
1435906_x_at	Gbp2	guanylate binding protein 2	14469	713	996	1131	750	1395	1828	2.44	2.00E-04
1416304_at	Litaf	LPS-induced TN factor	56722	1054	720	953	1013	1704	2463	2.43	9.00E-05
1450884_at	Cd36	CD36 antigen	12491	147	624	269	200	508	484	2.42	4.00E-05
1448550_at	Lbp	lipopolysaccharide binding protein	16803	931	1284	1276	998	1934	2268	2.27	5.00E-05
1438092_x_at	H2afz	H2A histone family, member Z	51788	2062	2204	2383	1732	2584	3909	2.26	3.00E-05
1433699_at	Tnfaip3	tumor necrosis factor, alpha-induced protein 3	21929	569	683	845	643	1032	1441	2.24	1.00E-04

## SUPPLEMENT

Affymetrix Probe set ID	Gene symbol	Gene name	Entrez Gene ID	Mean <i>Wt</i> aorta 6 weeks	Mean <i>Wt</i> aorta 32 weeks	Mean <i>Wt</i> aorta 78 weeks	Mean <i>Apoe</i> <sup>-/-</sup> aorta 6 weeks	Mean <i>Apoe</i> <sup>-/-</sup> aorta 32 weeks	Mean <i>Apoe</i> <sup>-/-</sup> aorta 78 weeks	Fold change <i>Apoe</i> <sup>-/-</sup> aorta 78 weeks vs. 6 weeks	p ANOVA
1417932_at	Il18	interleukin 18	16173	266	241	362	270	475	594	2.2	0.004
1450392_at	Abca1	ATP-binding cassette, sub-family A (ABC1), member 1	11303	164	150	115	272	596	580	2.14	8.00E-06
1450033_a_at	Stat1	signal transducer and activator of transcription 1	20846	462	539	381	447	740	951	2.12	8.00E-04
1425214_at	P2ry6	pyrimidinergic receptor P2Y, G-protein coupled, 6	233571	646	940	826	828	1292	1737	2.1	4.00E-04
1449874_at	Ly96	lymphocyte antigen 96	17087	393	259	353	296	403	617	2.08	8.00E-04
1418744_s_at	Tesc	tescalcin	57816	177	572	509	152	403	316	2.07	0.001
1420991_at	Ankrd1	ankyrin repeat domain 1 (cardiac muscle)	107765	393	368	562	463	354	916	1.98	8.00E-04
1435458_at	Pim1	proviral integration site 1	18712	562	1097	507	694	950	1334	1.92	2.00E-05
1434185_at	Acaca	acetyl-Coenzyme A carboxylase alpha	107476	753	2742	1470	1006	2047	1815	1.8	0.004
1450829_at	Tnfaip3	tumor necrosis factor, alpha-induced protein 3	21929	50	77	119	133	144	239	1.8	0.01
1422678_at	Dgat2	diacylglycerol O-acyltransferase 2	67800	968	4122	2231	1527	3277	2664	1.74	3.00E-04
1424950_at	Sox9	SRY (sex determining region Y)-box 9	20682	72	134	46	113	313	192	1.71	8.00E-04
1438676_at	Gbp6	guanylate binding protein 6	100702	129	273	180	166	316	265	1.6	5.00E-04
1416958_at	Nr1d2	nuclear receptor subfamily 1, group D, member 2	353187	1849	4023	3301	1701	3317	2679	1.57	0.002
1416041_at	Sgk1	serum/glucocorticoid regulated kinase 1	20393	4259	2102	2122	2774	3162	4106	1.48	0.003
1423086_at	Npc1	Niemann-Pick type C1	18145	576	494	344	499	693	725	1.45	0.005

SUPPLEMENT

Affymetrix Probe set ID	Gene symbol	Gene name	Entrez Gene ID	Mean <i>Wt</i> aorta 6 weeks	Mean <i>Wt</i> aorta 32 weeks	Mean <i>Wt</i> aorta 78 weeks	Mean <i>Apoe</i> <sup>-/-</sup> aorta 6 weeks	Mean <i>Apoe</i> <sup>-/-</sup> aorta 32 weeks	Mean <i>Apoe</i> <sup>-/-</sup> aorta 78 weeks	Fold change <i>Apoe</i> <sup>-/-</sup> aorta 78 weeks vs. 6 weeks	p ANOVA
1431292_at	Twf2	twinfilin, actin-binding protein, homolog 2 (Drosophila)	23999	311	331	170	266	334	381	1.43	0.008
1418167_at	Tfap4	transcription factor AP4	83383	140	276	285	177	227	248	1.4	0.006
1422474_at	Pde4b	phosphodiesterase 4B, cAMP specific	18578	496	1257	1183	659	1373	860	1.3	4.00E-04
1439364_at	Mmp2	matrix metalloproteinase 2	17390	3914	2827	2177	3996	3443	4990	1.25	2.00E-04
1417273_at	Pdk4	pyruvate dehydrogenase kinase, isoenzyme 4	27273	1340	4010	1390	1020	2303	1252	1.23	1.00E-04
1422677_at	Dgat2	diacylglycerol O-acyltransferase 2	67800	735	2221	987	922	1797	1127	1.22	2.00E-04
1419415_at	Rarg	retinoic acid receptor, gamma	19411	736	1213	854	574	1209	698	1.22	0.004
1416136_at	Mmp2	matrix metalloproteinase 2	17390	5328	3177	2750	5567	4910	6603	1.19	7.00E-06
1436026_at	Zfp703	zinc finger protein 703	353310	674	1672	1251	1128	1541	1279	1.13	0.01
1426464_at	Nr1d1	nuclear receptor subfamily 1, group D, member 1	217166	503	1455	1219	638	1230	634	-1.01	0.004
1437064_at	Ar	androgen receptor	11835	496	815	1038	657	700	592	-1.11	0.001
1457721_at	Ppara	peroxisome proliferator activated receptor alpha	19013	152	433	210	182	313	141	-1.3	0.003
1436475_at	Nr2f2	nuclear receptor subfamily 2, group F, member 2	11819	457	720	910	552	624	421	-1.31	0.001
1448076_at	Ctr9	Ctr9, Paf1/RNA polymerase II complex component, homolog (S. cerevisiae)	22083	192	142	87	174	150	133	-1.31	0.009
1448395_at	Sfrp1	secreted frizzled-related protein 1	20377	1584	999	626	1162	1758	870	-1.33	3.00E-04



SUPPLEMENT

Affymetrix Probe set ID	Gene symbol	Gene name	Entrez Gene ID	Mean <i>Wt</i> aorta 6 weeks	Mean <i>Wt</i> aorta 32 weeks	Mean <i>Wt</i> aorta 78 weeks	Mean <i>Apoe</i> <sup>-/-</sup> aorta 6 weeks	Mean <i>Apoe</i> <sup>-/-</sup> aorta 32 weeks	Mean <i>Apoe</i> <sup>-/-</sup> aorta 78 weeks	Fold change <i>Apoe</i> <sup>-/-</sup> aorta 78 weeks vs. 6 weeks	p ANOVA
1421907_at	Med1	mediator complex subunit 1	19014	1092	681	497	1138	844	722	-1.58	0.05
1416594_at	Sfrp1	secreted frizzled-related protein 1	20377	476	46	81	379	384	230	-1.64	7.00E-06
1436326_at	Rora	RAR-related orphan receptor alpha	19883	1392	760	671	1244	696	699	-1.78	8.00E-06
1424034_at	Rora	RAR-related orphan receptor alpha	19883	2711	1328	1522	2238	1085	1240	-1.8	7.00E-06
1439107_a_at	Kmt2e	lysine (K)-specific methyltransferase 2E	69188	833	656	310	969	920	520	-1.87	0.006
1460647_a_at	Nr2f6	nuclear receptor subfamily 2, group F, member 6	13864	548	268	250	589	280	292	-2.01	6.00E-04
1425014_at	Nr2c2	nuclear receptor subfamily 2, group C, member 2	22026	240	193	131	236	205	117	-2.02	0.01
1426997_at	Thra	thyroid hormone receptor alpha	21833	943	1034	1176	1328	998	657	-2.02	0.005
1424035_at	Rora	RAR-related orphan receptor alpha	19883	289	153	146	329	133	156	-2.11	8.00E-04
1455165_at	Rora	RAR-related orphan receptor alpha	19883	1506	1025	992	1296	785	602	-2.15	3.00E-04
1425991_a_at	Kank2	KN motif and ankyrin repeat domains 2	235041	785	835	563	1050	866	483	-2.17	0.01
1420583_a_at	Rora	RAR-related orphan receptor alpha	19883	2192	981	1052	1729	829	794	-2.18	1.00E-05
1434766_at	Prkaa2	protein kinase, AMP- activated, alpha 2 catalytic subunit	108079	979	1180	867	982	830	448	-2.19	4.00E-05

## SUPPLEMENT

Affymetrix Probe set ID	Gene symbol	Gene name	Entrez Gene ID	Mean <i>Wt</i> aorta 6 weeks	Mean <i>Wt</i> aorta 32 weeks	Mean <i>Wt</i> aorta 78 weeks	Mean <i>Apoe</i> <sup>-/-</sup> aorta 6 weeks	Mean <i>Apoe</i> <sup>-/-</sup> aorta 32 weeks	Mean <i>Apoe</i> <sup>-/-</sup> aorta 78 weeks	Fold change <i>Apoe</i> <sup>-/-</sup> aorta 78 weeks vs. 6 weeks	p ANOVA
1442827_at	Tlr4	toll-like receptor 4	21898	413	183	137	320	208	142	-2.26	9.00E-04
1443823_s_at	Atp1a2	ATPase, Na <sup>+</sup> /K <sup>+</sup> transporting, alpha 2 polypeptide	98660	4204	4898	4399	4678	3867	2059	-2.27	0.002
1434893_at	Atp1a2	ATPase, Na <sup>+</sup> /K <sup>+</sup> transporting, alpha 2 polypeptide	98660	1696	2456	2107	2034	2020	882	-2.31	2.00E-04
1416487_a_at	Yap1	yes-associated protein 1	22601	502	332	207	413	267	174	-2.38	3.00E-04
1426057_a_at	Epha3	Eph receptor A3	13837	354	175	106	275	185	114	-2.41	2.00E-05
1421028_a_at	Mef2c	myocyte enhancer factor 2C	17260	1504	712	697	1362	767	561	-2.43	5.00E-05
1439527_at	Pgr	progesterone receptor	18667	1070	1270	1283	1023	564	415	-2.46	2.00E-04
1451927_a_at	Mapk14	mitogen-activated protein kinase 14	26416	266	222	119	287	224	113	-2.53	9.00E-05
1429463_at	Prkaa2	protein kinase, AMP- activated, alpha 2 catalytic subunit	108079	1407	1460	827	1475	1117	580	-2.54	5.00E-04
1425575_at	Epha3	Eph receptor A3	13837	1622	1172	800	1599	964	625	-2.56	1.00E-04
1427465_at	Atp1a2	ATPase, Na <sup>+</sup> /K <sup>+</sup> transporting, alpha 2 polypeptide	98660	1924	1820	1671	2017	1459	784	-2.57	6.00E-04
1429003_at	Snw1	SNW domain containing 1	66354	524	402	177	511	418	196	-2.61	1.00E-05
1421866_at	Nr3c1	nuclear receptor subfamily 3, group C, member 1	14815	726	301	383	682	476	257	-2.65	2.00E-04
1425574_at	Epha3	Eph receptor A3	13837	550	193	247	534	236	189	-2.82	4.00E-05
1458129_at	Rora	RAR-related orphan receptor alpha	19883	783	531	348	754	409	262	-2.87	7.00E-06
1422264_s_at	Klf9	Kruppel-like factor 9	16601	363	330	165	395	255	136	-2.91	0.003

SUPPLEMENT

Affymetrix Probe set ID	Gene symbol	Gene name	Entrez Gene ID	Mean <i>Wt</i> aorta 6 weeks	Mean <i>Wt</i> aorta 32 weeks	Mean <i>Wt</i> aorta 78 weeks	Mean <i>Apoe</i> <sup>-/-</sup> aorta 6 weeks	Mean <i>Apoe</i> <sup>-/-</sup> aorta 32 weeks	Mean <i>Apoe</i> <sup>-/-</sup> aorta 78 weeks	Fold change <i>Apoe</i> <sup>-/-</sup> aorta 78 weeks vs. 6 weeks	p ANOVA
1421027_a_at	Mef2c	myocyte enhancer factor 2C	17260	2673	1597	972	2514	1694	854	-2.94	2.00E-05
1451569_at	Nr2c2	nuclear receptor subfamily 2, group C, member 2	22026	346	153	121	331	233	104	-3.18	0.006
1451022_at	Lrp6	low density lipoprotein receptor-related protein 6	16974	207	120	45	199	131	58	-3.46	2.00E-04
1459372_at	Npas4	neuronal PAS domain protein 4	225872	320	122	62	200	51	45	-4.43	0.04
1453860_s_at	Nr3c1	nuclear receptor subfamily 3, group C, member 1	14815	227	81	46	174	103	20	-8.62	0.005
1449998_at	Nkx3-1	NK-3 transcription factor, locus 1 ( <i>Drosophila</i> )	18095	605	403	563	719	319	28	-26.12	1.00E-05